Paleo-ice sheet dynamics on the northwest Greenland continental shelf

Dissertation

zur Erlangung des akademischen Grades Dr. rer. nat.

vorgelegt dem Fachbereich Geowissenschaften

der Universität Bremen im Dezember 2017

von

Patricia Slabon

1. Gutachter: Prof. Dr. Wilfried Jokat

2. Gutachter: Prof. Dr. Gerhard Bohrmann

ALFRED-WEGENER-INSTITUT
HELMHOLTZ-ZENTRUM FÜR POLAR- UND MEERESFORSCHUNG

Universität Bremen

Erklärung

Hiermit versichere ich,

Patricia Slabon,

wohnhaft im Dunckersweg 43b, 22111 Hamburg,

dass ich

1. die Arbeit ohne unerlaubte fremde Hilfe angefertigt habe,
2. keine anderen als die von mir angegebenen Quellen und Hilfsmittel benutzt habe und
3. die den benutzten Werken wörtlich oder inhaltlich entnommenen Stellen als solche kenntlich gemacht habe.

Bremerhaven, den 05.04.2017

_____

Patricia Slabon

Die vorliegende Dissertation wurde am 06.04.2018 an der Universität Bremen verteidigt. Der Prüfungsausschuss bestand aus Prof. Dr. Wilfried Jokat (erster Gutachter), Prof. Dr. Gerhard Bohrmann (zweiter Gutachter), Prof. Dr. Tilo von Dobeneck, Prof. Dr. Marta Pérez Gussinyé, Dr. Miguel Andres-Martinez und Nicolas Stoll.

Summary

Increasing temperatures in the ocean and atmosphere result in the decline of the modern ice sheets in both hemispheres, causing global sea-level rise. Direct records on these ice-sheet dynamics are sparse as most observations were first initiated in the last century. Although ice-core analyses and satellite data from the polar regions increase our knowledge of modern ice flow and ice-sheet dynamics, the reconstruction and investigation of these dynamics during past glacial cycles is required to predict future scenarios for ice-sheet dynamics.

Erosional and depositional glacial landforms that developed under the paleo-ice sheet and at its margin are used to reconstruct past ice-sheet extends and dynamics. These glacial landforms indicate the flow direction of past ice-streams that drained the former ice-sheet. They indicate the maximum ice-sheet extent as well as ice-sheet stabilizations or re-advances during ice-sheet retreat.

This thesis focuses on the analysis of the Greenland ice-sheet dynamics since the last glacial maximum (LGM, 26.5-19 ka BP). The analysis is based on the identification and investigation of glacial landforms on the seabed of Melville Bay, on the northwest Greenland continental shelf. This region in northeast Baffin Bay hosts three large cross-shelf troughs. They were formed by ice-streams advancing to the shelf edge during past glacial cycles. They are among the widest and deepest cross-shelf troughs of the continental shelf of Greenland. High-resolution bathymetry, which is necessary for identification of glacial landforms at the seabed in and adjacent to these troughs is limited in this remote region due to harsh sea-ice conditions. Thus, detailed reconstructions of LGM ice-sheet dynamics and their timing in Melville Bay are incomplete.

In this thesis, I present new high-resolution bathymetry data from the northeast Baffin Bay that I investigated for submarine glacial landforms. The data have been recorded in 2010 with *RV Polarstern* and in 2015 with *RV Maria S. Merian*. This study aims to reconstruct the Greenland Ice Sheet dynamics since the LGM by inferring glacial processes and their relative chronology from the distribution and configuration of glacial landforms. The presented results show that the ice streams extended to the shelf edge and subsequent retreat of the ice streams varied between the glacial cross-shelf troughs in Melville Bay. Local ice domes on the shallow banks between the cross-shelf troughs are inferred from the distribution of glacial landforms.

A newly discovered trough network on the inner continental shelf extends from the large cross-shelf troughs towards the fjords under the modern ice sheet. It was likely formed by a former ice sheet. Steep ridges in the north of Melville Bay are likely related to Proterozoic volcanic dyke swarms that to some extent confined former meltwater and ice-stream pathways. The results of this thesis improve our understanding of the northwest Greenland ice-sheet dynamics during past glacials and indicate that at least some glacial processes are related to underlying bedrock morphology.

Zusammenfassung

Im Zuge des Klimawandels stiegen in den letzten Dekaden die Temperaturen der Ozeane und der Atmosphäre und führen hierdurch zu einem Rückzug der Eisschilde, der wiederum zum globalen Meeresspiegelanstieg beiträgt. Langfristige Nachweise der Eisschildentwicklung sind rar, da direkte Beobachtungen erst seit maximal Anfang des letzten Jahrhunderts zu Verfügung stehen. Obwohl Eisuntersuchungen in den Polarregionen, als auch satellitengestützte Methoden, die Kenntnis über den modernen Eisfluss weit vorangebracht haben, ermöglichen diese direkten Beobachtungen nicht die Rekonstruktion von Eisschilddynamiken die länger zurück liegen, wie zum Beispiel während der vergangenen Eiszeiten. Diese werden jedoch dringend benötigt um die zukünftige Entwicklung der Eisschilde in einem sich wandelnden Klima besser zu prognostizieren.

Glazial geprägte Strukturen, die unter dem Paläo-Eisschild und an dessen Rand durch Erosion und Deposition entstehen, können zur Rekonstruktion genutzt werden. So können aus einigen dieser glazialen Strukturen die ehemalige Fließrichtung der Eisströme abgeleitet werden über die das Eisschild abfloß. Andere Strukturen wiederum können eine maximale Eisschildausdehnung oder auch Phasen der Stabilisierung sowie Rückvorstöße während des Rückzugs anzeigen.

Der Fokus dieser Arbeit liegt auf der Analyse der grönländischen Eisschilddynamiken seit des letzten glazialen Maximums (LGM, 26.5-19 ka BP). Diese Analyse basiert auf der Identifizierung und Untersuchung glazialer Strukturen auf dem Meeresgrund der Melville Bay, auf dem Nordwestgrönländischen kontinentalen Schelf. Diese Region ist durch drei große glaziale Tröge geprägt, die durch Eisströme geformt und während vergangener glazialer Zyklen die Schelfkante erreicht haben. Sie gehören zu den breitesten und tiefsten glazialen Trögen des kontinentalen Schelfs Gröndlands. Hochauflösende Bathymetrie ermöglicht die Identifikation weiterer glazialer Strukturen am Meeresgrund innerhalb und entlang dieser Tröge. Da es sich bei dieser Region um eine abgelegene und zudem durch Meereis beeinflusste Gegend handelt sind nur äußerst begrenzt solche Datensätze vorhanden. Dementsprechend gab es von der Melville Bay bis zu dieser Arbeit keine detaillierte Rekonstruktion der LGM Eisschilddynamik.

In meiner Arbeit untersuche ich neue hochauflösende bathymetrische Daten aus der nordöstlichen Baffin Bay, die in den Jahren 2010 mit *RV Polarstern* und 2015 mit *RV Maria S. Merian* aufgenommen wurden, nach glazialen Strukturen und rekonstruiere hieraus die

Eisschilddynamiken des Grönländischen Eisschilds seit dem LGM. Die aufgeführten Ergebnisse deuten darauf hin, dass die Eisströme sich zum LGM bis zur kontinentalen Schelfkante ausgedehnt haben. Die Geschwindigkeit ihres anschließenden Rückzugs war jedoch in den jeweiligen Trögen unterschiedlich. Die Verteilung der glazialen Strukturen legt nahe, dass lokale Eisdome auf den flachen Bänken zwischen den Trögen lagen.

Ein neu entdecktes Netzwerk aus Trögen auf dem inneren Kontinentalschelf verbinden die großen Tröge des äußeren Kontinentalschelfs mit Fjorden die bis unter das moderne Eisschild reichen. Dieses Netzwerk wurde vermutlich durch ein früheres Eisschild geprägt. Steile Rücken im Norden der Melville Bay stehen wahrscheinlich in Verbindung mit Schwärmen proterozoischer vulkanischer Gesteinsgänge (Dykes). Diese haben zu einem gewissen Anteil frühere Schmelzwasser und Eisstrom-Wege begrenzt. Die Ergebnisse dieser Arbeit führen zu einem verbesserten Verständnis der nordwestgrönländischen Eisschilddynamik während vergangener Eiszeiten und deuten darauf hin, dass zumindest einige glaziale Prozesse von der unterliegenden Festgesteinsmorphologie gesteuert werden.

Content

List of Tables

List of Figures

Abbreviations

AMS	Accelerator Mass Spectrometry
AW	Atlantic Water
AWI	Alfred Wegener Institute Helmholtz Centre for Polar and Marine Research
BP	before present
Cal yr	Calendar years
CST	Cross-shelf trough
CTD	Conductivity-Temperature-Depth sensor/probe
DEM	Digital elevation model
DFG	Deutsche Forschungsgemeinschaft (German Science Foundation)
DGPS	Differential GPS
GIMP	Greenland Ice Mapping Project
GIS	Greenland Ice Sheet
GNSS	Global Navigation Satellite System (like GPS)
GPS	Global Positioning System
GZW	Grounding-zone wedge
IBCAO	International Bathymetric Chart of the Arctic Ocean
IIS	Innuitian Ice Sheet
ITB	Inter-trough bank
ka	kilo ages (kilo years)
kHz	kilohertz
LGM	Last Glacial Maximum
LIS	Laurentide Ice Sheet
RV	Research Vessel
SBES	Single beam echosounder
SBP	Sub-bottom profiler
SVP	Sound-Velocity Probe or Profiler
Ma	million ages
MB	Melville Bay
MBES	Multibeam echosounder
MSM44	Maria S. Merian Cruise no. 44
MVB	Melville Bay
MVBT	Melville Bay Trough
nwGIS	northwest Greenland Ice Sheet
SVP	Sound-velocity profiler
TGS	TGS-NOPEC Geophysical Company ASA
TMF	Trough-mouth fan
TWT	Two-way travel time
WGC	West Greenland Current
WGS84	World Geodetic System from 1984
YD	Younger Dryas

1. Introduction and motivation

1.1. Glaciation of the northwest Greenland continental shelf

Presently, Greenland hosts the last ice sheet, the Greenland Ice Sheet (GIS), in the northern hemisphere covering ~80% of the Greenland mainland (Fig. 1.1). The GIS is reacting to global warming due to the climate change, and tends to decrease (IPCC, 2013). If the modern GIS was to melt completely, global sea-level may rise up to 7 m (IPCC, 2013). The released freshwater discharge may, furthermore, influence the thermohaline circulation of the West Greenland Current (WGC) as identified in the past (Knudsen et al., 2008; Lane et al., 2015), but could also reduce or shift the Gulf Stream (e.g. Lynch-Stieglitz et al., 1999; Moore, 2005; van Kreveld et al., 2000). The decline of the Laurentide and Innuitian Ice Sheets (Fig. 1.1) after the Last Glacial Maximum (LGM, ~26.5-19 ka BP) had a similar impact (Clark et al., 2009; Clark et al., 2002; Kaufman et al., 2004; Renssen et al., 2012). Therefore, it is essential to understand the past ice-sheet dynamics of Greenland to model, validate and predict future retreat scenarios (e.g. Bingham et al., 2010). Although internal and external factors influencing the paleo-ice sheet cannot yet be all reconstructed, past ice sheet development, its dynamics and extend can be inferred by glacial geomorphology (e.g. Kleman and Borgström, 1996). With regard to advances and retreat scenarios based on glacial landforms identified in high-resolution bathymetry, it is possible to infer streaming, stagnation or slow flow of the ice sheet (e.g. Dowdeswell et al., 2008; Ó Cofaigh et al., 2008). The arrangement and character of the individual landforms relate to external influences such as roughness of the bed, confined flow, or meltwater supply. As most parts of Greenland are covered by ice, it is necessary to survey the more accessible seafloor that is less eroded from modern ice-sheet advances and that may give an impression from the LGM ice sheet extend and development.

This thesis focuses on the Baffin Bay (Figs. 1.1), a basin encircled by Canada in the North and West, and Greenland in the East. Baffin Bay is one of the most remote Arctic regions covered by only limited bathymetric surveys (Jakobsson et al., 2012b). In particular, I focus on the glacial landforms in Melville Bay, also termed Melville Bugt (Figs. 1.1, 1.2). Melville Bay is the northeast part of Baffin Bay, located on the continental shelf of Northwest Greenland. Melville Bay hosts the largest cross-shelf troughs of the Greenland continental shelf. They are among the largest of the northern hemisphere (Batchelor and Dowdeswell, 2014) and accommodated large, fast moving ice streams that drained the GIS during past glacial cycles and also during the LGM (Fig. 1.1-1.3). The onset zones of

the troughs lie on the crystalline basement on the inner continental shelf, near the modern coastline.

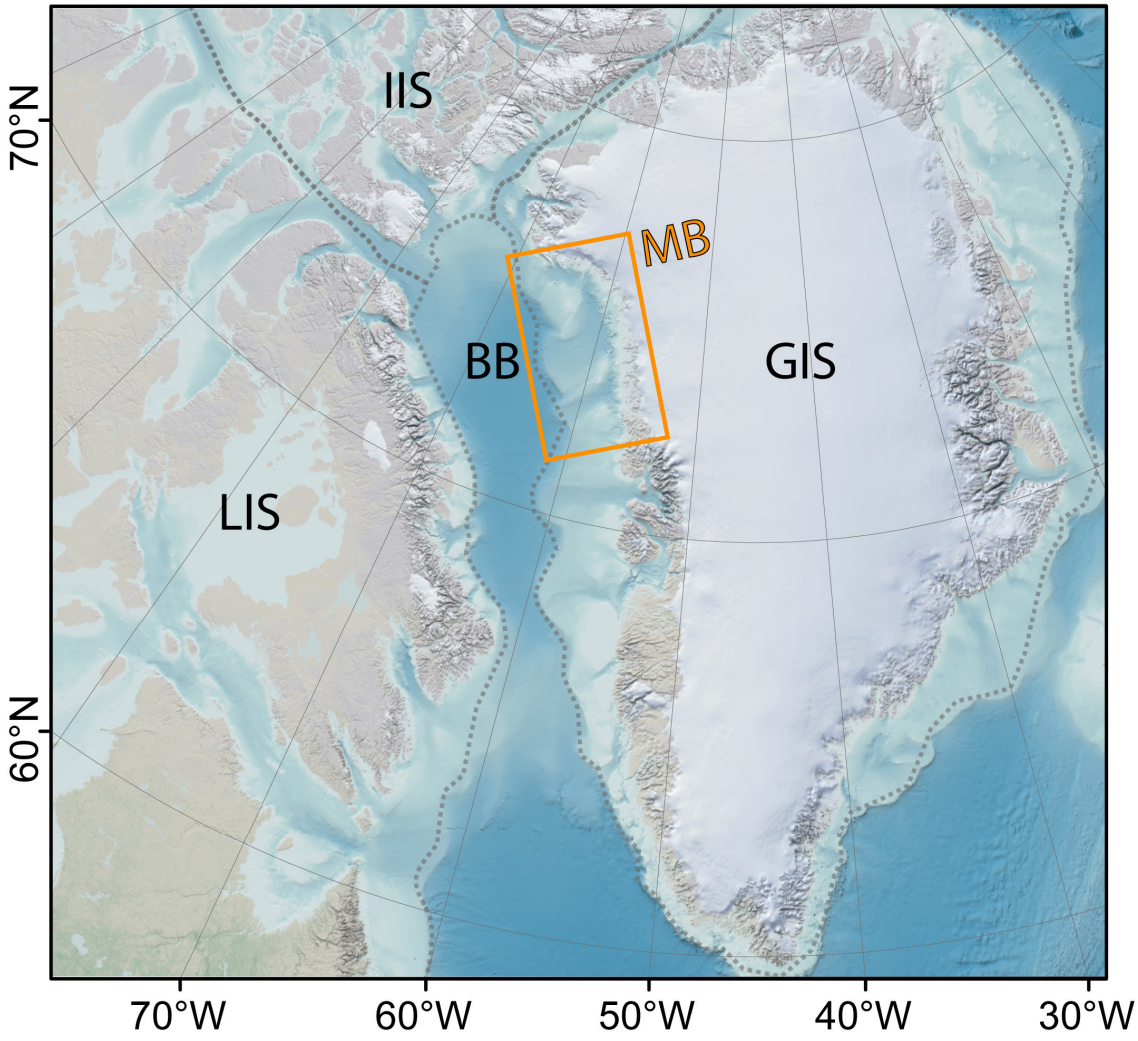

Figure 1.1: Overview of the study area of Melville Bay (orange box) on the continental shelf of northwest Greenland, based on the GEBCO_2014 grid (Weatherall et al., 2015), including IBCAO v.3.0 data (Jakobsson et al., 2012b). Note the modern Greenland Ice Sheet coverage in white. Dashed grey lines on the continental shelves indicate the outline of the former LGM ice-sheet extent modified from Batchelor and Dowdeswell (2014). BB: Baffin Bay; GIS: Greenland Ice Sheet; IIS: Innuitian Ice Sheet, LIS: Laurentide Ice Sheet; MB: Melville Bay.

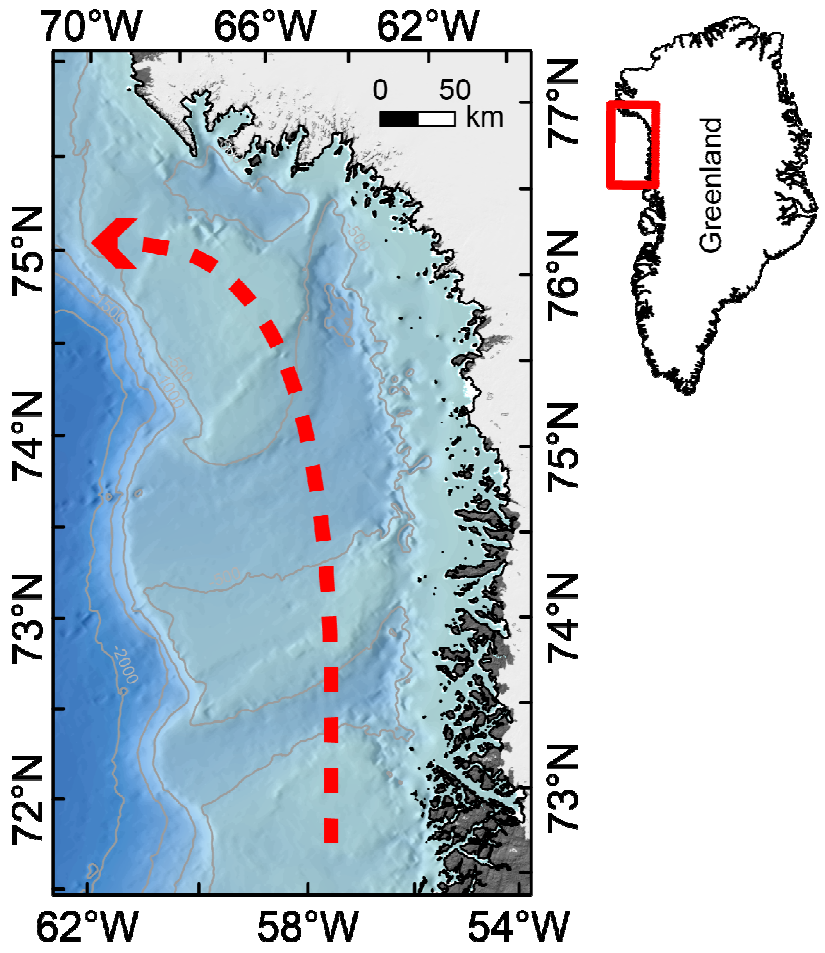

Figure 1.2: Overview of Melville Bay based on IBCAO v.3.0 data (Jakobsson et al., 2012b). Red dashed line indicates the warm West Greenland Current.

1.2. Bathymetric mapping of glacial landforms

More than 70% of the Earth's surface is covered by water, but only around 18% of the oceans are fully mapped with bathymetric data (Weatherall et al., 2015). The data coverage is even less in the remote and ice-covered regions of the Arctic. In 2012, only 11% of the Arctic ocean were mapped acoustically using high-resolution multibeam echosounders (Jakobsson et al., 2012b). The ocean topography used to fill the gaps in the high-resolution bathymetry data is often derived from coarse kilometre-scale satellite altimetry (e.g. Smith and Sandwell, 1997), contour lines from old digitized maps and appropriate interpolation algorithms between soundings.

As marine terminating glaciers and sea ice in the Arctic further retreat (e.g. IPCC, 2013, and references therein), they expose additional unmapped seafloor. High-resolution mapping of the seafloor in polar regions can reveal glacial landforms that are the

morphological imprints of former active ice sheets and ice-stream activities (e.g. Dowdeswell et al., 2008; Ó Cofaigh et al., 2008). Most recently preserved glacial landforms around Greenland were formed during the last glacial maximum (LGM) 26.500-19.000 yrs BP (Funder et al., 2011, and references therein) (Fig. 1.3). Those landforms are often too small to be identified or confidentially interpreted in ≥500 m resolution map products like e.g. the International Bathymetric Chart of the Arctic Ocean (IBCAO v.3.0) grid (Jakobsson et al., 2012b) (Fig. 1.1, 1.2).

Glacial landforms formed by the subglacial erosion of rock or by sub- and pro-glacial deposition of sediments indicate the presence of a former active ice sheet, generally accompanied by subglacial meltwater (Glasser and Bennett, 2004). Furthermore, these landforms can indicate the orientation of former ice-sheet drainage pathways as well as stabilizations of ice fronts during retreat phases of ice sheets (e.g. Dowdeswell et al., 2008; Ó Cofaigh et al., 2008). Radiocarbon dating on carboniferous shells and foraminifera within the associated marine sediment can be used to determine the age of the deposition (e.g. Bennike and Björck, 2002; Sheldon et al., 2016) and subsequently a minimum age since when the seafloor is free of the overlying ice cover. This remains, however, difficult for erosional glacial landforms that may have formed during several glacial cycles by erosion of rock (Krabbendam and Glasser, 2011). On this basis, prior investigations indicate an advance to the shelf edge of the northern hemisphere ice sheets during past glacials (e.g. Dyke et al., 2002; England et al., 2006; Funder et al., 2011; Jakobsson et al., 2014; Pieńkowski et al., 2013). Also the Greenland Ice Sheet advanced onto the continental shelf towards the shelf break e.g. during the LGM (e.g. Arndt et al., 2015; Dowdeswell et al., 2014; Funder et al., 2011; Hogan et al., 2016; Ó Cofaigh et al., 2013b; Sheldon et al., 2016) (Figs. 1.1, 1.3). Subsequent retreat was partly varying between individual ice sheets and small ice domes, and has not yet been fully identified on the entire West Greenland continental shelf (Funder et al., 2011). v

Melville Bay (Figs. 1.1-1.3) is one of these gaps where only conceptual LGM ice-sheet margins occur on the map of Funder et al. (2011). This remote and often sea-ice covered region is only sparsely covered with high-resolution bathymetry (Jakobsson et al., 2012b). In 2015, initial bathymetric surveys were conducted with the *RV Maria S. Merian* (Dorschel et al., 2016) to identify glacial landforms within the cross-shelf troughs of Melville Bay and to subsequently reconstruct the glacial history of the GIS in this region. During this expedition, systematic bathymetric surveys (Fig. 2.1) conducted along and across the axes of the major cross-shelf troughs cover potential glacial landforms. In addition, systematic surveys were performed with the aim to locally achieve almost full coverages of multibeam data e.g. on the channelized crystalline bedrock or at the transition from Mesozoic-Cenozoic sediment sequences to crystalline bedrock.

Bathymetry data from an expedition of *RV Polarstern* in 2010 (Damm, 2010) supplement the bathymetric datasets. Despite the newly available data, wide data gaps remain between the areas covered by multibeam soundings. To further increase the data coverage, for this study, additional data sets were acquired from different institutions and companies. The aforementioned new bathymetric datasets are part of the new compilation from Morlighem et al. (2017) that covers both, the sub-ice topography of Greenland as well as the adjacent waterways in 150 m resolution. This new compilation is included as background in the third manuscript (chapter 6).

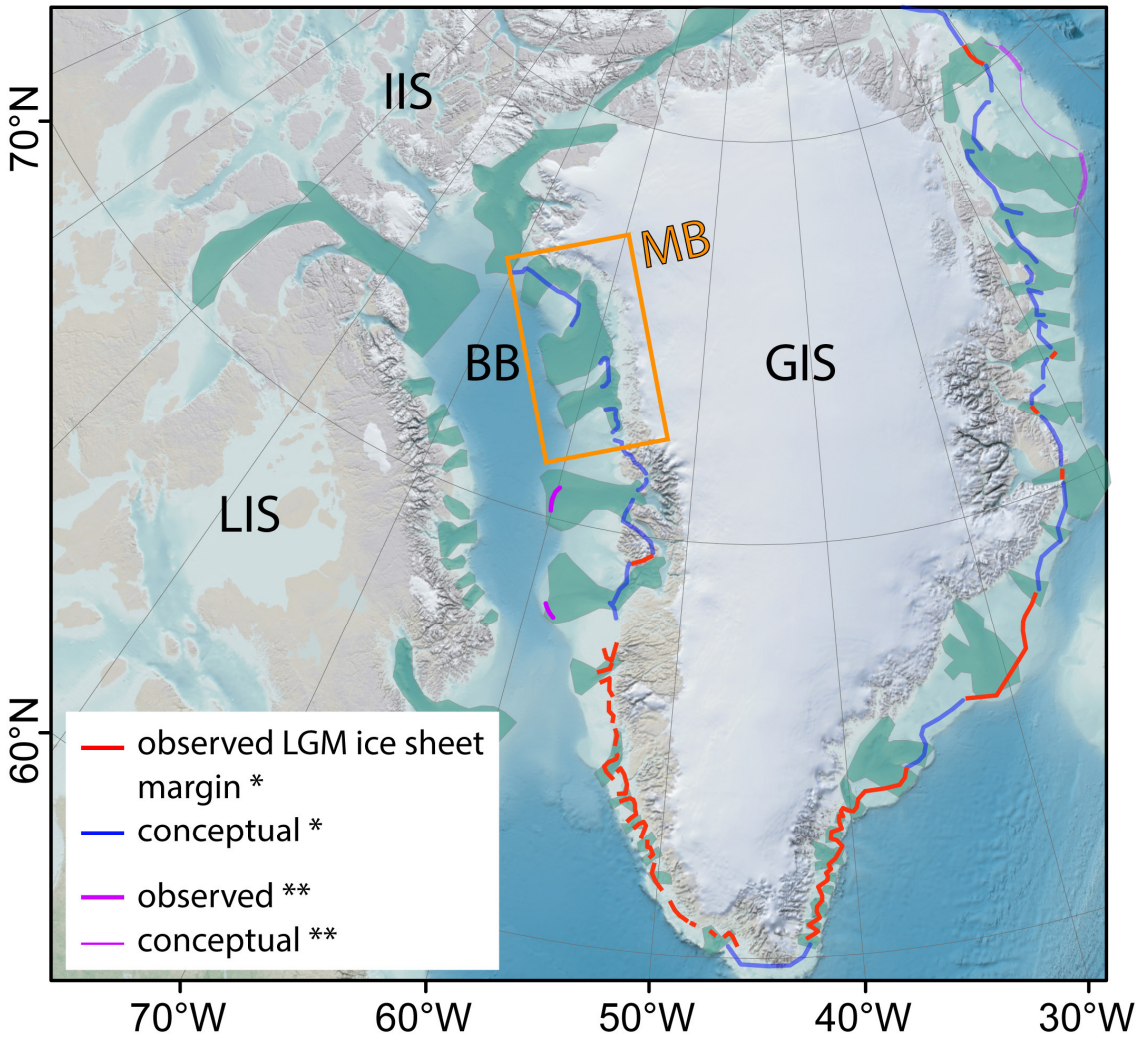

Figure 1.3: LGM Ice sheet margin modified from Funder et al. (2011) and complemented by recent observations (violet) at the shelf edge on the west and east Greenland continental shelf documenting the maximum extend **(Arndt et al., 2017; Dowdeswell et al., 2014; Hogan et al., 2016; Ó Cofaigh et al., 2013a; Ó Cofaigh et al., 2013b; Sheldon et al., 2016). Shapes of green coloured troughs are from Batchelor and Dowdeswell (2014).*

1.3. Research Questions

The central objectives and associated research questions of my thesis are presented below. The main materials, principles, and methods used during this thesis are presented in chapter 2. Three articles as first author were prepared for scientific peer-reviewed journals. They discuss the main objectives of this thesis. Chapter 3 gives an overview about the content of each publication and my contributions to them. The published and submitted articles form the chapters 4-6. A conclusion summarizing the results of this study with an outlook on potential upcoming research is given in chapters 7 and 8.

LGM ice-sheet dynamics in Melville Bay

The maximum extent of the GIS during the LGM is still uncharted for large parts on the Greenland continental shelf (Funder et al., 2011). Especially the remote and ice-covered North remains unexplored. Recent studies from central West Greenland complement previous results from southern Baffin Bay and offshore East Greenland (e.g. Arndt et al., 2015; Dowdeswell et al., 2014; Funder et al., 2011; Hogan et al., 2016; Ó Cofaigh et al., 2013b; Sheldon et al., 2016). Nevertheless, the paleo-ice sheet extent and the ice-sheet dynamics across large parts of the wide continental shelf, like the Melville Bay in northeast Baffin Bay, remains uncertain. Until recently, high-resolution bathymetry indicative of glacial landforms is limited to a relatively small area (~220 km²) in central Melville Bay (Freire et al., 2015; Gyllencreutz et al., 2016).

- ***What was the GIS extent during the LGM in Melville Bay, NE Baffin Bay?***
- ***Which glacial landforms characterize the paleo-ice stream pathways?***
- ***How was the associated ice-sheet retreat in the individual cross-shelf troughs characterized?***
- ***Where there ice domes on the inter-trough banks adjacent to the ice streams in the cross-shelf troughs?***
- ***When did the ice-sheet retreat?***

Pre-LGM ice-sheet dynamics

Ice sheets did not only cover the sedimentary parts of the continental shelf but also the crystalline bedrock close to the Greenland coast. On crystalline rock, glacial landforms are merely erosional and therefore different in appearance compared to depositional glacial landforms on sedimentary rock (e.g. Glasser and Bennett, 2004; Krabbendam and Glasser, 2011). They are often the product of several glaciations, and thus carry the signature of several ice sheet advances and retreats. Studies from Freire et al. (2015) and Gyllencreutz et al. (2016) from central Melville Bay infer the orientation of the ice-sheet streaming into the central cross-shelf trough from glacially overprinted bedrock.

- ***How is the bedrock morphology of eastern Melville Bay characterized?***
- ***Are there implications for former ice-sheet extents and dynamics across the bedrock?***
- ***Is there a relation between submarine bedrock morphology and modern ice sheets dynamics?***

Detailed investigation of the northern Melville Bay

The cross-shelf trough in northern Melville Bay is smaller, shallower, and less developed than the adjacent central and southern cross-shelf troughs. Erosional glacial landforms on the bedrock within and adjacent to this trough and at the transition to the central trough in northern Melville Bay may give further insight in the former ice-sheet dynamics of this region.

- ***How are glacial landforms in northern Melville Bay distributed?***
- ***Are there indications for changes in ice-sheet dynamics?***

2. Materials and methods

The hydro-acoustic datasets for this thesis were acquired during *RV Polarstern* expedition *ARK-XXV/3* in 2010 (Damm, 2010) and *RV Maria S. Merian* expedition *MSM44* in 2015 (Dorschel et al., 2016). They comprise multibeam echosounder data and sub-bottom profiler data. All data were recorded and processed by the bathymetry group of the Alfred Wegener Institute Helmholtz Centre for Polar and Marine Research (AWI). The datasets used in the respective papers have been complemented by bathymetric data from other sources (TGS NOPEC, NASA JPL, University of Sweden; see individual chapters 4, 5, and 6). The 500 m resolution IBCAO v.3.0 grid (Jakobsson et al., 2012b) was used for background bathymetric information of the first and second manuscript. Since September 2017, the 150 m resolution BedMachine v3 grid (Morlighem et al., 2017) is available that also includes data from this thesis and was used as background bathymetry within the third manuscript.

A general overview concerning hydro-acoustic principles and techniques is given below, describing the echosounder systems used during this thesis. Additional information on hydro-acoustics is given in the appropriate literature (e.g. de Jong et al., 2002; Lurton, 2004).

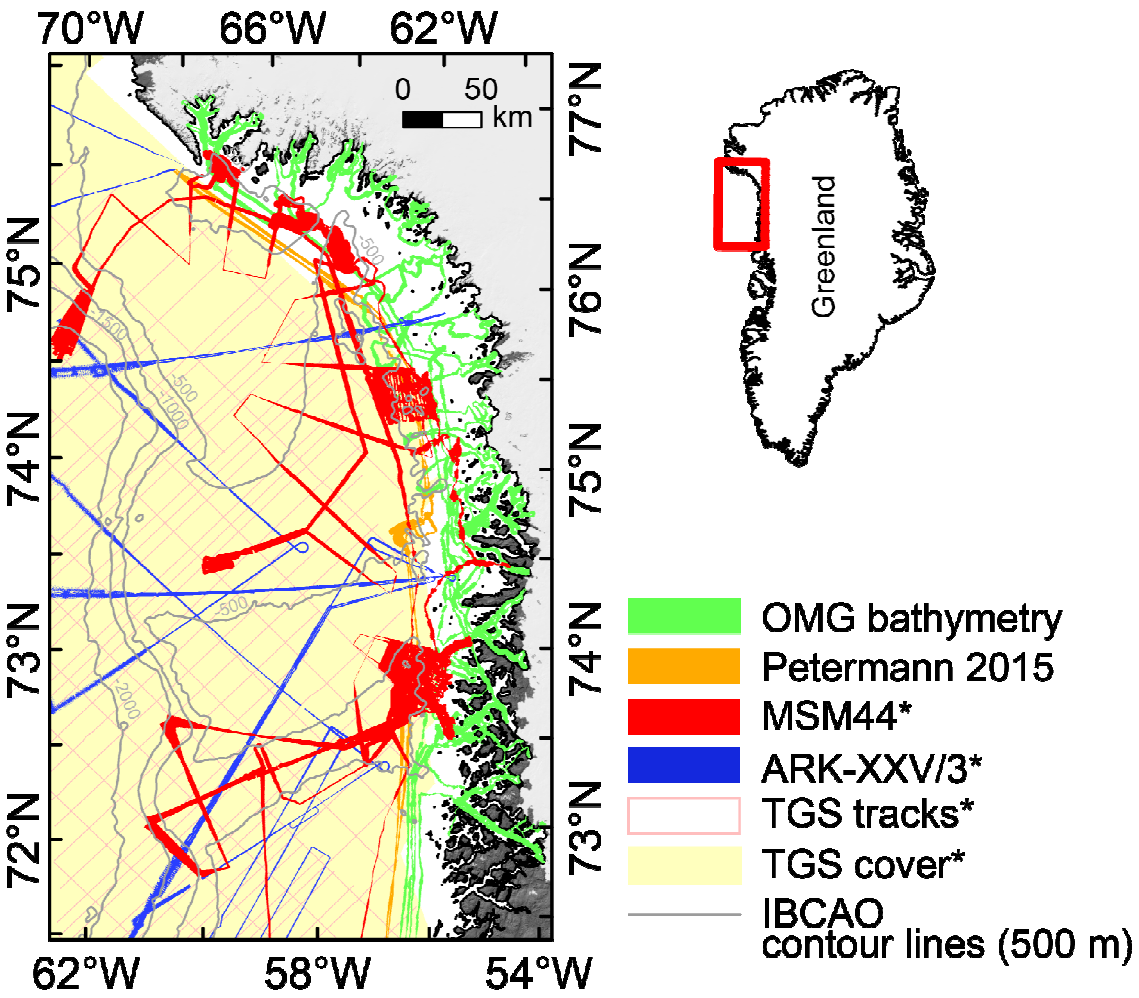

*Figure 2.1: Coverage of used multibeam echosounder datasets during this thesis. * indicates those datasets included in the first manuscript. The other datasets were added subsequently for preparation of the second and third manuscript. TGS tracks indicate a SBES dataset merged to a 500 m grid (TGS cover). Grey IBCAO contour lines (Jakobsson et al., 2012b) indicate the outline of the glacial cross-shelf troughs. Background topography is from GIMP (Howat et al., 2014).*

2.1. Principles of hydro-acoustic surveys

2.1.1. History of echosounders

First echosounders were invented after the RMS Titanic sank due to collision with an iceberg in 1912 (Lurton, 2004). They were primarily invented to detect icebergs under water. At the time, it became apparent that hydro-acoustic systems detected rather the seafloor than icebergs. The intense application and modification of hydro-acoustic systems in the military sector aided submarine discovery ever since. Already in the 1920s, the fishing industry used the modified echosounders to discover fish shoals in the water

column (Lurton, 2004). During the *RV Meteor* expedition in 1925-1927, a marine single beam echosounder was first used scientifically to map the depth of the south Atlantic along several east-west profiles, thus, discovering the Mid Atlantic Ridge (Heezen et al., 1959; Jakobsson et al., 2016). Since then, the echosounders have been further improved mostly by the military sector. In the 1970s, first multibeam echosounders were invented to map the seafloor with a swath of simultaneously recorded soundings (Lurton, 2004). Nowadays, they are widely used for mapping surveys for safety of navigation in harbours and other waterways and for scientific purposes.

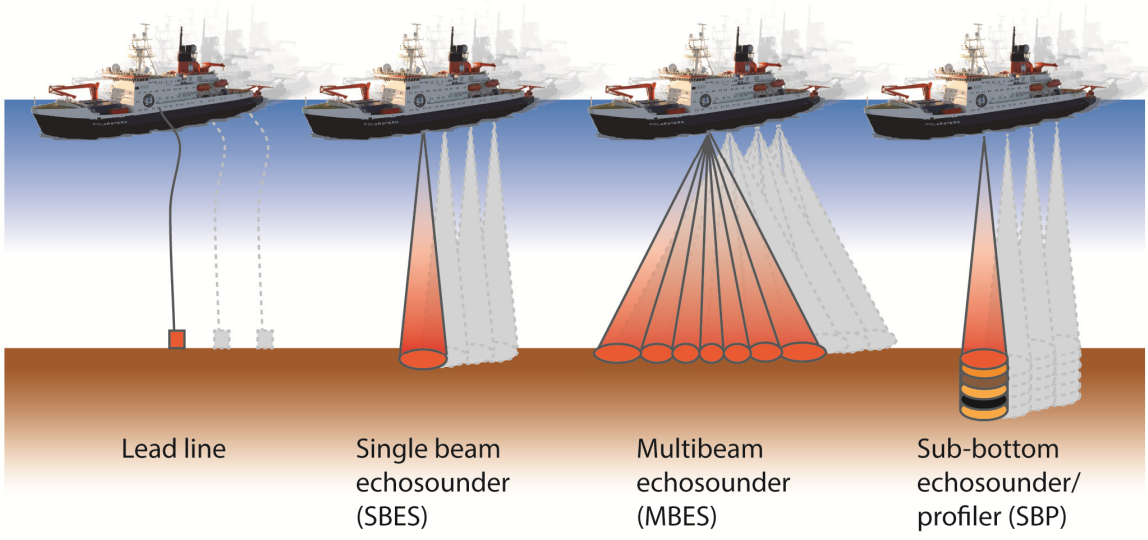

Figure 2.2: Schematic principles of bathymetric surveying

2.1.1.1. Single beam echosounder (SBES)

Once the benefit of hydro-acoustic systems for mapping the seafloor was demonstrated by the non-military sector to a wider public in the 1960s, single beam echosounders started to replace the former lead-line method (Fig. 2.2) to determine the water depth (Jakobsson et al., 2012b). Single beam echosounders (Fig. 2.2) transmit and receive an acoustic signal (ping; duration usually 0.1-1 ms in shallow water and 1-40 ms in deep water) (de Jong et al., 2002). This signal travels perpendicular to the ship as a narrow beam through the water column and reflects at the seafloor due to a different impedance between water and the sediment. The two-way travel time (t) between signal emission from the echosounder, reflection at the seafloor and reception of the signal at the

receiver can be measured. Divided by two, the one-way travel time multiplied with the sound velocity of water (v, ~1500 m/s) gives the water depth (s):

$$s = ½ v^* t \quad (1)$$

The opening angle of single beam echosounders is nowadays <5° resulting in small footprints on the seafloor, which means that a more precise point under the vessel is measured. Old models often had a wide beam width of up to 30° (de Jong et al., 2002) and broader footprints. The frequency of a single beam echosounder depends on water depth and application. For deep water, lower frequencies have to be used e.g. 12 kHz. The depth accuracy of these systems ranges at about 1% of water depth (Lurton, 2004).

2.1.1.2. Sub-bottom echosounder

A modification of the single beam echosounder is the sub-bottom echosounder or sediment profiler. These hydro-acoustic systems not only image the seafloor, but their signals also penetrate into the seafloor imaging the shallow sedimentary sequences (Fig. 2.2). For better seafloor penetration, sediment profilers rely on a signal with a lower frequency that reflects both at the seafloor, and at changes of impedance between sediment layers of different density. Sub-bottom echosounders can penetrate up to several hundreds of meters into the seafloor, imaging the shallow sediment architecture. Sediment penetration depends on the sedimentary structure. Highly consolidated sediments or rock may reflect rather than allow penetration into deeper layers. This is also typical for compressed glacial till as present in the study area.

Parametric sub-bottom echosounders of the type Atlas Parasound P70, which rely on the principle of the parametric effect, are installed on both *RV Polarstern* and *RV Maria S. Merian*. Therefore, two high, but slightly different frequencies (e.g. 18 and 22 kHz for Parasound P70) with high amplitudes are transmitted simultaneously (Lurton, 2004). Interferences of the two primary high frequencies produce a secondary low frequency of the difference of the primary frequencies (e.g. 4°) that can penetrate deep (up to 200 m) into the seafloor, depending on the sedimentary structure. Typically, sediment profilers have narrow beams with smaller footprints. For the P70, the opening angle of the beam is 4.5°.

For controlling the Parasound P70, the Atlas Hydromap Control software was used. Acquisition and recording of the signal was conducted using Atlas Parastore. The recorded ASD files were then converted to SGY format and visualized using IHS Kingdom software.

2.1.1.3. Multibeam echosounder (MBES)

Single beam echosounders record single depth soundings along a ships track (Fig. 2.2) that result in a 1D-profile (Jakobsson et al., 2016). Although this gives an impression of the seafloor depth, several parallel survey lines are required to provide spatial information on the seafloor morphology. Through advances in echosounding technology, multibeam echosounders were invented in the 1970s (Lurton, 2004). Rather than single soundings, they record a swath of soundings during each ping. Thus, they cover a wide stripe of the seafloor by recording simultaneously several depth points that are oriented perpendicular to the ship's track (Fig. 2.2). As a result, they provide a 2D-image of the seafloor that allows for geomorphological analysis (Jakobsson et al., 2016). Since the invention, multibeam systems have been continuously improved, constantly increasing the number of beams and the seafloor coverage. As first MBES systems had only 16 beams, later versions already provided 32 and nowadays up to 432 beams are regularly installed covering a wide swath width of up to >150°.

During the expedition in 2010, a hull-mounted Atlas Hydrographic Hydrosweep DS-2 was installed on *RV Polarstern*. Its transmitting frequency was 15.5 kHz and had 59 hardbeams (2x2.3° beam width) and 240 computed softbeams over a swath angle of 90-120°. Data acquisition was conducted using Hydromap Online software provided by Atlas Hydrographic. Caris Hips and Sips 6.1 was used for post processing. In 2015, on *RV Maria S. Merian*, the Kongsberg Simrad EM122 was installed. It transmits on 12 kHz (frequency range from 11.25 to 12.60 kHz in the different transmitting sectors), covering 111 beams with 2x2° beam width and a maximum swath angle of 150°. For this thesis, the data were reprocessed using Caris Hips and Sips 9.0. Then, the data were gridded and exported to ESRI ArcGIS and QPS Fledermaus for further analysis.

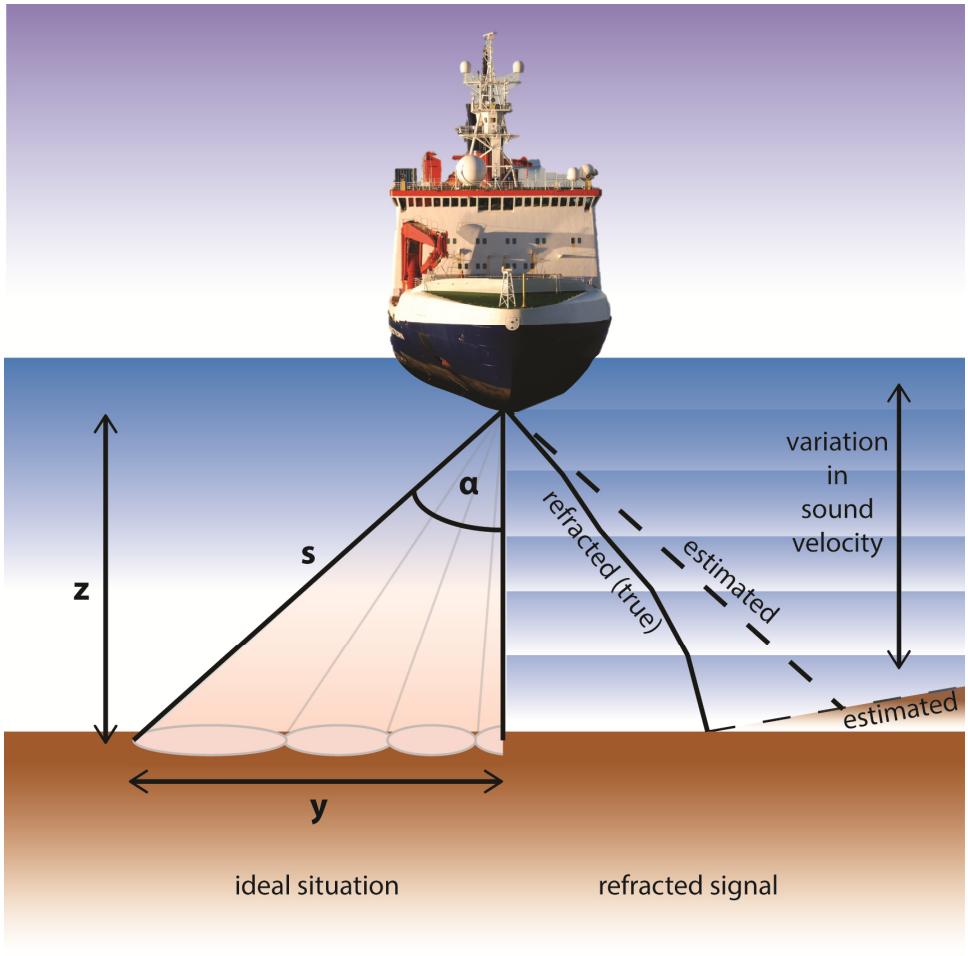

Figure 2.3: Slant range geometry (left) and geometric ray tracing due to changes in sound velocity in the water column (right).

MBES measuring principles

Simplified, for MBES, the slant range (s) of the beams is calculated similar to the depth measured by a SBES. However, the depth of the seafloor (z) and the distance to the centre beam (y) relies on a trigonometric computation and therefore the swath angle α needs to be considered (Fig. 2.3):

$$z = s * \sin(\alpha) = ½ v* t * \sin(\alpha) \quad (2)$$

$$y = s * \cos(\alpha) = ½ v* t * \cos(\alpha) \quad (3)$$

The more complex situation contains variations in sound velocity. The differently stratified layers of the water column refract the oblique ray paths of the sound wave and, thus, lead to different locations or depths of the data points at the seafloor (Fig. 2.3). The

signal refracts at the boundaries of water masses with different densities so-called pycnoclines. Therefore, true depth is different to the estimated depth and ray tracing is needed to account for the refraction in the water column (Fig. 2.3). Changes of the sound velocity in the water column can be measured directly using sound velocity probes (SVPs). SVPs consist of a small transducer that sends a signal over a short defined distance to its receiver. While lowering this sensor to the ground, the measured time of the signal between transducer and receiver changes and, thus, gives the water sound velocity. Density profiles for the water column can also be determined indirectly by measurement of the temperature and salinity of the water column with Conductivity-Temperature-Depth (CTD) sensors (Fig. 2.4). Densities and subsequently sound velocities can be computed from salinity, temperature and pressure using e.g. the formula published by Chen and Millero (1977).

Due to changing water masses, e.g. through currents and tides, it is necessary to regularly update the sound-velocity information of the water column and therefore deploy the SVPs as often as necessary. On board RV Polarstern, in 2010, the sound velocity was acquired using CTD sensors (Damm, 2010). On board RV Maria S. Merian, both, CTDs but also SVPs attached to other scientific instruments such as gravity and box cores were used (Dorschel et al., 2016).

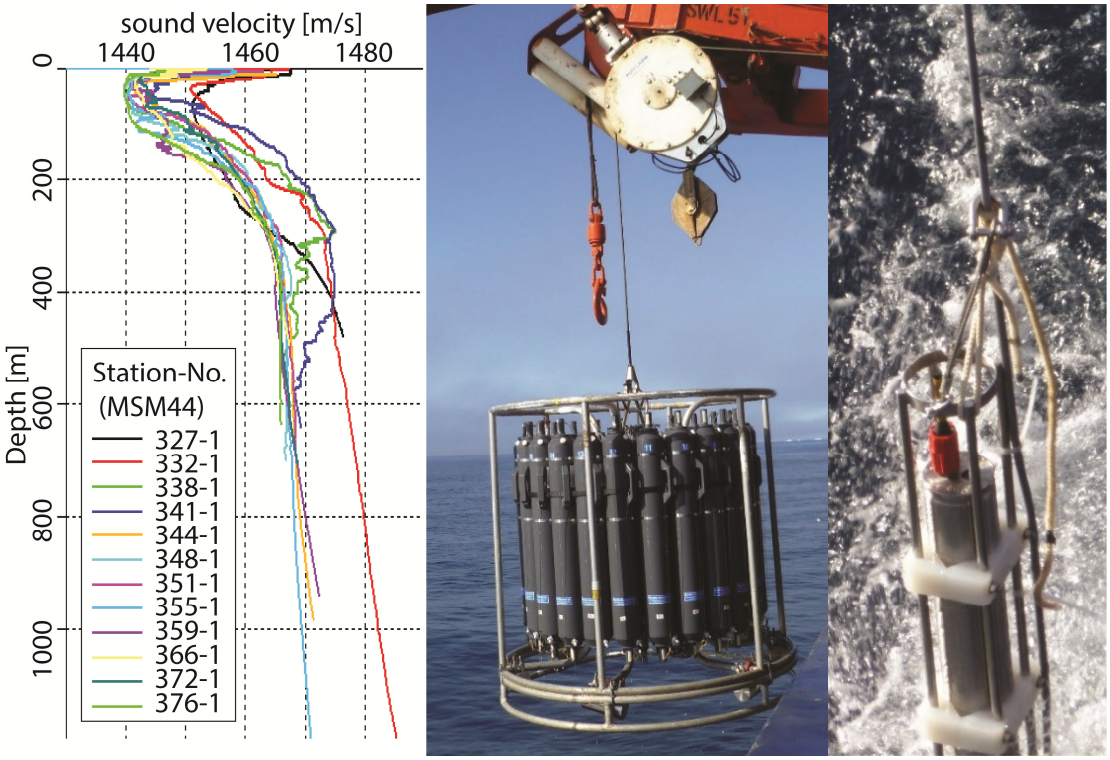

Figure 2.4: Example for SVP and CTD profiles acquired with individual instruments during MSM44 (left). Middle: CTD. Right: SVP.

Motion and position

Besides corrections for sound velocity, motion sensor data such as roll, pitch and heading of the survey vessel (Fig. 2.5), as well as time synchronisation and positioning (x, y, z) e.g. via GNSS (Global Navigation Satellite System) (Fig. 2.5) are required for correct locations of the measured data points at the seafloor. Therefore, the recorded depth soundings are continuously corrected for the ship's motion and position that are acquired and recorded simultaneously.

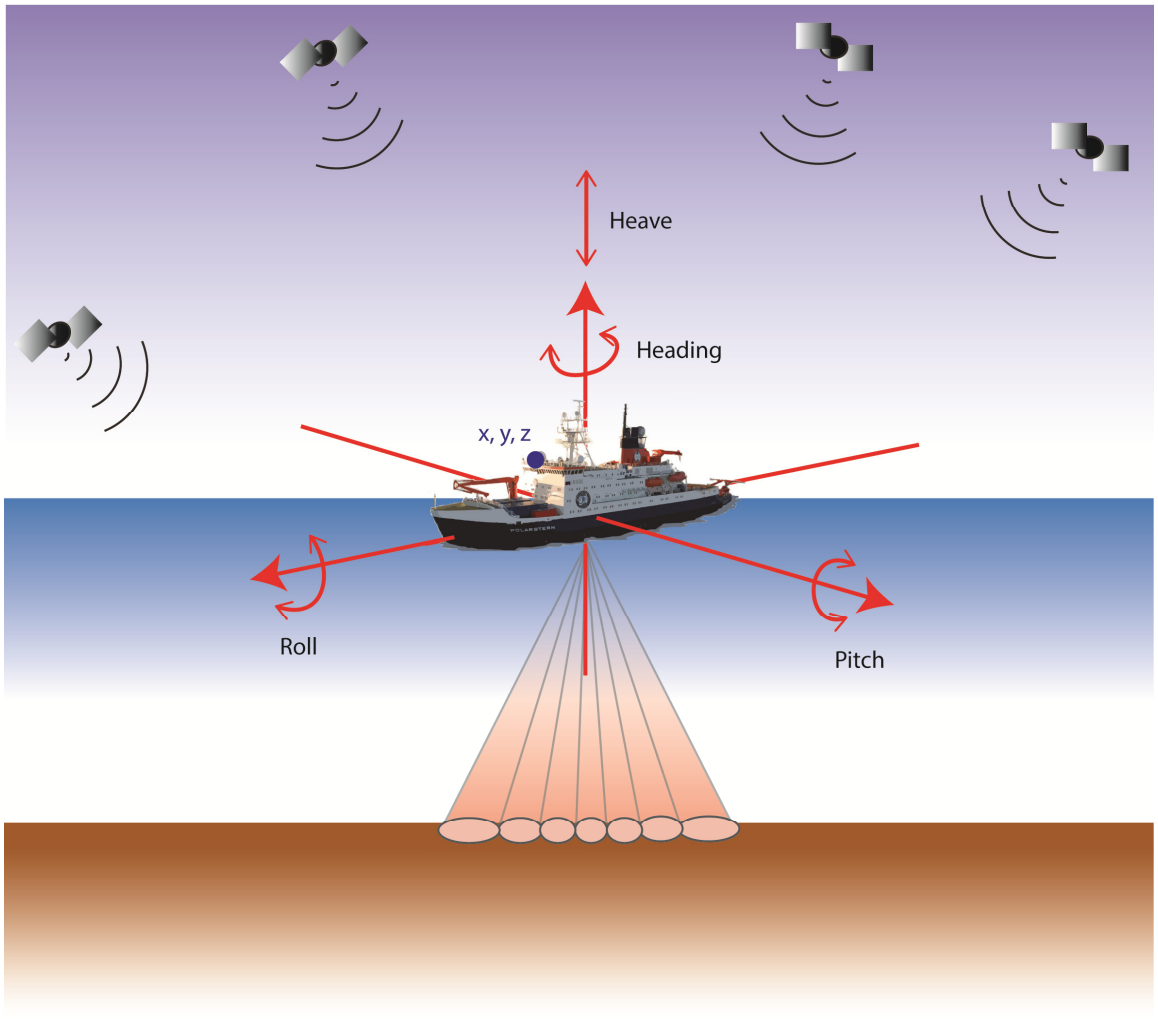

Figure 2.5: The ship's motion (roll, pitch, heave, and heading) is recorded by the marine inertial system. Simultaneously, GNSS measurements (e.g. GPS) give the geographic position (x, y, z) of the ship. Besides sound velocity corrections, both, motion and position are required for correction of the incoming depth measurements.

The inertial navigation system (INS) of the ship records the motion in space that consists of roll, pitch and heading (Fig. 2.5). The ships geographic position is required for absolute positioning of the soundings on the reference ellipsoid WGS84. Therefore, usually GNSS is used, giving the position, including the heave of the ship (Fig. 2.5). The GNSS comprises e.g. GPS (US Global Positioning System) and GLONASS (Russian GNSS Service).

At least four GNSS satellites are required to compute the position of the receiver antenna. DGPS (Differential GPS) is seldom used due to lack of local reference stations in the polar seas. For better precision, especially when GNSS satellites disappear behind the horizon in high latitudes, INS measurements complement the positioning. The INS is usually installed at the pivot point of the ship that inherits least motion. Whereas, the GPS antenna is generally installed on a high position on top of the ship for best exposition to satellite signals. Location of both systems within the ship's coordinate system needs to be known and applied for correct positioning of the ship and measured depths. On board RV Polarstern, a MINS (Marine Inertial Navigational System) is used, that incorporates both, motion sensor data but also positioning data received from two GPS antennas. Time synchronisation is essential to merge all incoming information to fit the position of the ship to its motion and adopt this information to the measured depth point and location.

2.2. Visual analysis and interpretation

When ice sheets extend and retreat, they deform sediments and bedrock beneath, resulting in significant glacial landforms that can be investigated. Glacial landforms may have both erosional and depositional character and vary in size and shape. Most glacial landforms have an up-ice and a down-ice side, thus, indicating former ice-stream orientation. Depending on their size, high-resolution (< 25 m) bathymetry is needed to identify glacial landforms that help reconstruct glacial retreat history.

A glossary of more significant glacial landforms that can be identified in the dataset from Melville Bay is provided below. They indicate former ice-sheet extensions, streaming directions and retreat dynamics. The specified dimensions give an overview of those landforms. Further explanations and visualizations of glacial landforms can be found in the scientific literature and summarizing textbooks like the *Atlas of Submarine Glacial landforms* (Dowdeswell et al., 2016) or *Glaciers and glaciation* (Benn and Evans, 2010).

Table 2.1: Overview of glacial landforms in Melville Bay

Landform	Description	Indication	Figure
Cross-shelf trough (CST)	Large u-shaped trough, often with reverse-gradient slope intersecting the sedimentary part of the continental shelf; 170-320 km long, 45-120 km wide, >800 m deep	Ice stream bed; indication of former ice-sheet extension across the continental shelf; paleo-ice-sheet drainage pathway	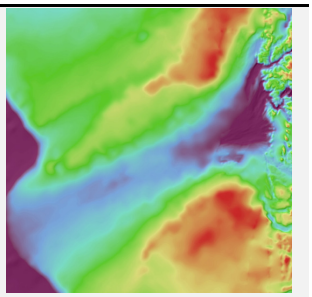
Trough	Elongated u-shaped trough, often with reverse-gradient slope on the bedrock of the inner continental shelf; 8-100 km long, 1.5-5 km wide, 150-700 m deep	Onset zone of the ice streams bedded in the CSTs; indicate ice and meltwater flow towards the outer shelf	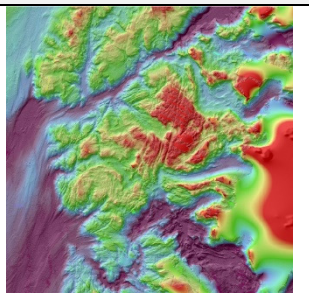
Crag-and-tail	Elongated, tear-shaped, streamlined hills, rocky crag-head, sedimentary tail, steep up-ice side; >400 m, 100-750 m wide, 30-150 m high, 7° up-ice slope, 1-2° down-ice slope	Ice streaming across the bedrock-crags with sediment deposition along the tails in ice-flow direction. Relative indicator of rapid ice-flow velocity and streaming direction	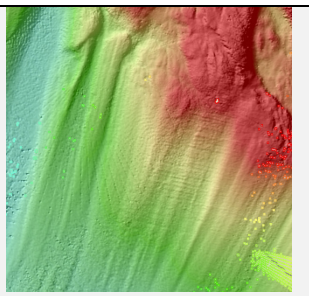

Roche moutonnée	Streamlined bedrock-hills with quarried down-ice side; 100-2000 m long, 100-1000 m wide, 15-40 m high	Ice streaming across crystalline bedrock; Quarried down-ice side is relative indicator of ice-flow direction	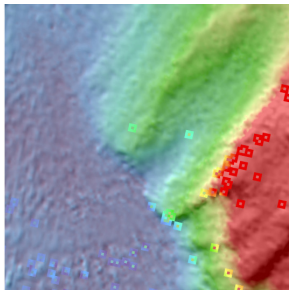
Glacial lineations (MSGL)	Elongated, parallel sedimentary ridges; related to crag-and-tails; 7-15 km long, 100-500 m wide, 4-15 m high	Ice streaming across soft sediment/till or sedimentary rock; relative indicator of rapid ice-flow velocity and direction	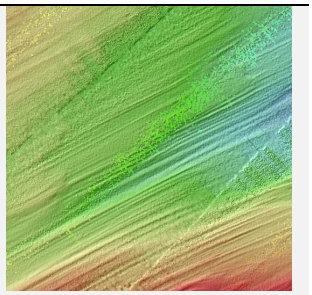
Lateral moraine	Elongated ridges at the lateral boundary of the trough; Sometimes asymmetric with steeper down-ice (2-3.5°), gentler up-ice slope (0.5-2°); several km long, 2-4 km wide, 15-60 m high	Deposition at the lateral boundary of streaming ice; relative indicator of ice-flow direction	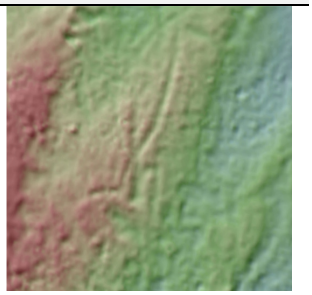
Marginal push-moraine	Elongated ridges, partially arcuate with steep up-ice (6-9°) and a gentle (2-6°) down-ice slope; 2-8 km long, 100-200 m wide, 5-10 m high	Indicate re-advances and stabilizations with subsequent retreat of the ice-stream margin	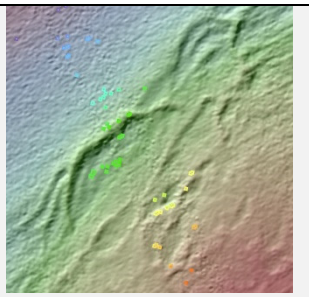
Arcuate push-moraine	Elongated, arcuate ridges, with gentle (1.5-2.2°) up-ice and steep (5-7°) down-ice slope; 200-800 m long, 100-200 m wide, 5-13 m high	Indicate re-advances and stabilizations with subsequent retreat of the ice-stream margin	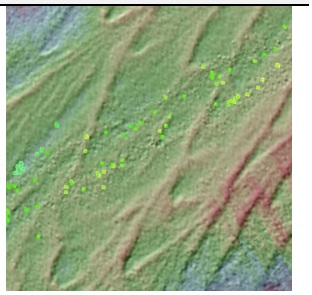

Grounding-zone wedge (GZW)	Wedges with steep down-ice sides (0.7-1.3°) and gentle rising up-ice sides (0.2-0.5); ~22 km long, >11 km wide, 20-70 m high	Subglacial sediment deposition at the ice-sheet margin during stabilization phases with subsequent retreat; Down-ice side and MSGL on top point in direction of former ice streaming	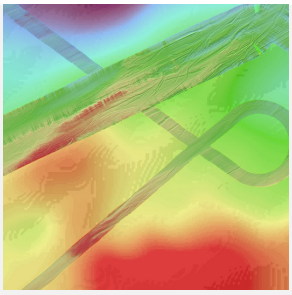
Subglacial till lobe	Small lobate wedges with steep down-ice slope (1.5-4°) and a gentle up-ice slope (0.3-0.5°); 1-6 km long, 1.5-2 km wide, 5-20 m high	Subglacial sediment deposition at the ice-sheet margin during stabilization phases; Down-ice side and MSGL on top point in direction of former ice streaming	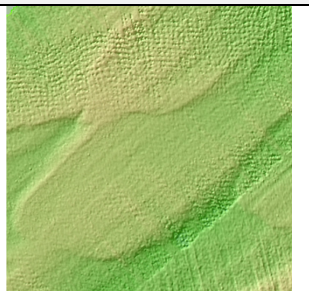
Iceberg scours/ ploughmarks	V-shaped to flat-bottomed elongated or chaotic incisions on shallow sedimentary seabed; 20-1500 m long, 30-300 m wide, 0.5-13 m deep	Irregular scouring of the seabed by grounded iceberg keels; Deposition of material adjacent as berms; indicate pathways of floating icebergs driven by wind and ocean currents	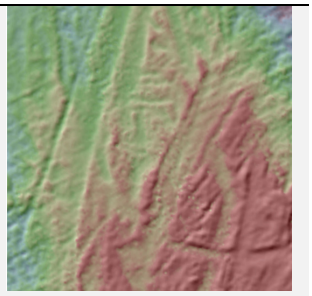
Lineaments	Mappable linear or slightly curvilinear surface expressions, e.g. bedrock fractures, parallel or sub-parallel to faults; 1-24 km long, 100-1000 m wide, 10-120 m deep	Pre-glacial structures exploited through erosion by rivers and ice-streams	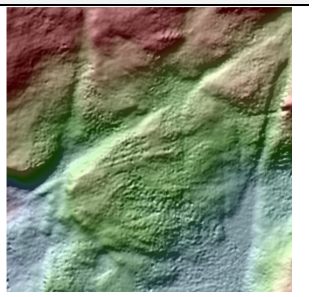

3. Contribution to scientific journals

My PhD thesis comprises three contributions to ISI-peer reviewed journals as first author, presented here in chronological order of their publication and submission:

Greenland ice sheet retreat history in the northeast Baffin Bay based on high-resolution bathymetry

Slabon, P., Dorschel, B., Jokat, W., Myklebust, R., Hebbeln, D. and Gebhardt, C. (2016)

Quaternary Science Reviews, 154, pp. 182-198. doi:10.1016/j.quascirev.2016.10.022

In this article, we analysed high-resolution bathymetric data from Melville Bay, northeast Baffin Bay. We identified and mapped glacial landforms indicative of grounded ice and its maximum extent. We interpreted their shapes, and resultant, we reconstructed a retreat pattern across the continental shelf.

I was part of the scientific crew on both AWI-expeditions to Baffin Bay (MSM44 and ARK-XXV/3), recording and processing the bathymetry data on board. I post-processed the data onshore and analysed the sub-bottom profiler data. I investigated the produced grid, digitized the glacial landforms and wrote the manuscript. Boris Dorschel and Wilfried Jokat supervised my work, provided scientific input and reviewed the manuscript. Reidun Myklebust provided data from TGS and revised the manuscript. Dierk Hebbeln provided the details concerning the gravity core data, the age dating information, and revised the manuscript. Catalina Gebhardt assisted with sub-bottom profiler data and revised the manuscript.

Bedrock morphology reveals drainage network in northeast Baffin Bay

Slabon, P., Dorschel, B., Jokat, W., Freire, F. (accepted, 2017), *Geomorphology*

In this article, we compiled the existing high-resolution bathymetric datasets from Melville Bay, northeast Baffin Bay with two new datasets from different institutions that complement and fill gaps within the data. In this compilation, we investigated the morphology of the inner continental shelf of northwest Greenland. We identified a paleo-subglacial drainage network that correlates with modern West Greenland fjords and inferred its formation by glaciofluvial erosion. Differences in channel morphology were investigated and related to changing bedrock morphology.

I compiled the data from in-house AWI-bathymetry and obtained data from newly available external resources (OMG-campaign from from NASA JPL and Petermann 2015). I investigated the created bathymetric grid for glacial landforms and other geological features and wrote the manuscript. Boris Dorschel and Wilfried Jokat provided scientific input, supervised my work, and revised the manuscript. Francis Freire provided bathymetric data from expedition “Petermann 2015” and revised the manuscript.

Influence of bedrock morphology on ice and meltwater orientation

Slabon, P., Dorschel, B., Jokat, W., Freire, F. (in review, 2017), *Geomorphology*

This article concentrates on the geomorphology and glacial activity of the northern part of Melville Bay, adjacent to the northern cross-shelf trough. We used the same high-resolution bathymetry dataset as was used for the article “Bedrock morphology reveals drainage network in the Northeast Baffin Bay” but focused on its northern part, which was not analysed in such detail before. We identified steep ridges that are expected to be part of the large volcanic Melville Bay and Thule dyke swarm systems. Glacial landforms indicate that the ridges likely fostered meltwater flow along subglacial channels and therefore probably influenced the ice-stream re-orientation.

I compiled the different datasets (see above) and analysed the northern part (>75°N) that was not discussed by the aforementioned article. I investigated the bathymetry for glacial landforms and geological features and wrote the initial manuscript. Boris Dorschel and Wilfried Jokat supervised my work, provided scientific input and revised the manuscript. Francis Freire revised the manuscript and provided bathymetric data from expedition “Petermann 2015”.

4. Greenland ice sheet retreat history in the northeast Baffin Bay based on high-resolution bathymetry

Patricia Slabon [a], Boris Dorschel [a], Wilfried Jokat [a,b], Reidun Myklebust [c], Dierk Hebbeln [d], Catalina Gebhardt [a]

[a] Alfred Wegener Institute Helmholtz Centre for Polar and Marine Research, Am Alten Hafen 26, 27568 Bremerhaven, Germany

[b] University of Bremen, Department of Geosciences, Klagenfurter Straße, 28359 Bremen, Germany

[c] TGS, Lensmannslia 4, P.O. Box 154, N-1371, Asker, Norway

[d] MARUM, Center for Marine Environmental Sciences, University of Bremen, Leobener Strasse, 28359 Bremen, Germany

Published in *Quaternary Science Reviews*, Vol. 154 (2016), p. 182-198, http://dx.doi.org/10.1016/j.quascirev.2016.10.022

Abstract

New swath-bathymetric data acquired in 2010 and 2015 indicate a variety of glacial landforms in cross-shelf troughs of the Melville Bay (northeast Baffin Bay). These landforms reveal that, at their maximum extent, ice streams in the troughs crossed the shelf all the way to the shelf edge. Moraines, grounding-zone wedges (GZWs) and subglacial till lobes on the continental shelf define a pattern of variable ice stream retreat in the individual troughs. On the outer shelf, in the northern cross-shelf trough, ice-stream retreat was slow compared to more episodic retreat in the central (at least one

stabilization on the outer shelf) and southern cross-shelf trough (re-advances at the shelf edge and fast retreat thereafter). Large GZWs on the mid-to inner shelf of the troughs indicate periods of grounding-zone stabilization. According to glacial landforms, the final retreat across the inner shelf (before 8.41 ka BP) was episodic to slow. Furthermore, evidence has been found for localized ice domes with minor ice-streams on inter-trough banks. The glacial landforms in Melville Bay, thus, indicate the varying and discontinuous ice sheet retreat history across the Northwest Greenland continental shelf.

Keywords

Ice-stream retreat; Grounding-zone wedge; Ice dome; Glacial landform, Greenland, Baffin Bay, Melville Bay

Highlights

- Ice streams reached the continental shelf edge through the cross-shelf troughs, presumably during the LGM.
- Discontinuous ice stream retreat of the Northwest Greenland ice sheet.
- Grounding-zone wedge complexes formed in mid-shelf position.
- Final ice stream retreat within the cross-shelf troughs occurred before 8.41 ka BP.
- Small ice streams occur on inter-trough banks.

4.1. Introduction

The Greenland Ice Sheet (GIS) is fast declining, contributing approximately 0.57 mm (Rignot and Kanagaratnam, 2006) to the annual global sea-level rise of ~3.3 mm (Cazenave and Remy, 2011). Accordingly, the ice-sheet dynamics of the GIS has received considerable attention in recent decades (IPCC, 2013). In this context, the extent of the GIS during the Last Glacial Maximum (LGM) is of interest to constrain predictions and models of sea-level rise. Melville Bay, in the northeast Baffin Bay area of the broad Northwest Greenland shelf (Fig. 4.1), hosts records of past ice sheets dynamics. Presently, about 13.5% by volume of annual GIS drainage is directed along glaciers that feed into Melville Bay (Rignot and Kanagaratnam, 2006). The catchment area feeding these glaciers covers approximately 11.5% of the GIS ice sheet. In this regard, the fast-flowing ice of the Northwest Greenland Ice Sheet (nwGIS) accounts for ~25.5 Gt, or ~7%, of the total annual mass loss of the GIS (Joughin et al., 2010; Khan et al., 2015; Kjær et al., 2012; Rignot and Kanagaratnam, 2006).

Thus, understanding the dynamics of the nwGIS is a prerequisite to assessment of the fate of the ice sheet in a time of accelerated global change. Evidence for ice sheet dynamics beyond the period of satellite observations (Box et al., 2012; Morlighem et al., 2014a; Nghiem et al., 2012) can be obtained from reconstructions of the nwGIS under past global warming events, namely during the last deglaciation, interpreted from glacial landforms.

In earlier studies, mass balance estimates and remote-sensing data supported the idea of acceleration of ice streams in Northwest Greenland (Joughin et al., 2004; Joughin et al., 2010; Khan et al., 2015; Kjær et al., 2012; Rignot et al., 2011). However, so far the role and extent of grounded ice, including fast-flowing ice streams, in Melville Bay draining the nwGIS during the last glacial Maximum (LGM) (~26.5 to ~19 ka BP) remains uncertain (Clark et al., 2009; Funder et al., 2011). The remote Melville Bay is only sparsely covered by high-resolution bathymetric surveys (ArcticNet, 2016; Jakobsson et al., 2012b; NOAA, 2016) and, as such, little is known about the distribution and shape of its glacial landforms. These landforms can, however, be used to interpret information on ice-stream advances and retreats across the shelf that is crucial to better understand past ice-sheet dynamics.

Recent studies from Uummannaq Trough, the Disko Trough area and Sisimiut (Fig. 4.1) (e.g. Dowdeswell et al., 2014; Hogan et al., 2016; Jennings et al., 2014; Ó Cofaigh et al., 2013b; Roberts et al., 2009; Sheldon et al., 2016) have improved glacial and deglacial reconstructions of West Greenland. Dowdeswell and Fugelli (2012) analyzed the characteristics of grounding-zone wedges (GZWs) identified on seismic profiles from Melville Bay (Fig. 4.1). Batchelor and Dowdeswell (2014, 2015) described Arctic glacial cross-shelf troughs, also from Baffin Bay, on the basis of IBCAO v.3.0 data (International

Bathymetric Chart of the Arctic Ocean) (Jakobsson et al., 2012b) and compared its GZWs to other Arctic and Antarctic GZWs to analyze their morphological characteristics. Freire et al. (2015), furthermore, interpreted high-resolution bathymetry of a small part (~220 km^2) of Melville Bay in terms of glaciogenic features and compared their morphology to onshore structures.

With regards to the timing of nwGIS dispersal since the LGM, studies along the entire West Greenland shelf (Fig. 4.1) indicate an asynchronous retreat of its ice streams (Bennike and Björck, 2002; Funder et al., 2011; Hogan et al., 2016; Ó Cofaigh et al., 2013b; Vasskog et al., 2015).

This pattern was not only influenced by climatic change accompanied by sea-level rise and the intrusion of warm water currents to grounding lines, but also by the topographic setting of individual ice streams. Topographic steering of the ice streams occurred as a result of the diverse underlying continental shelf topography. Internal ice-sheet dynamics have also been stated to have probably played a role in ice-stream retreat (Bennike and Björck, 2002; Long and Roberts, 2003; Ó Cofaigh et al., 2013b).

Due to its harsh sea-ice conditions, research cruises to Melville Bay have been limited. Consequently, LGM-time reconstructions of the nwGIS lack details about ice-stream retreat. We report the first systematic bathymetric survey (Fig. 4.2) along and across the cross-shelf troughs of Melville Bay, completed alongside geological sampling, which enables us to provide constraints on the ice sheet retreat in our research area. The data provide information along the axes of all major cross-shelf troughs in the bay, allowing us to reconstruct the history of ice-stream retreat between the LGM grounding zone and the present-day coast.

4.1.1. Regional setting

4.1.1.1. Seafloor topography and geomorphology

Melville Bay, as part of the Baffin Bay, covers ca. 120 000 km^2 of the up to 200-km wide continental shelf offshore Northwest Greenland (Figs. 4.1 and 4.2). It is characterized by three prominent cross-shelf troughs (Figs. 4.2 and 4.3), the northern, central and southern Melville Bay troughs (MVBTs) that count among the widest and deepest of Greenland's cross-shelf troughs (Funder et al., 2011). The troughs are 170-320 km long, 45-120 km wide and reach maximum depths between 740 and 1100 m. They are separated by shallow banks (up to 100-110 m below present sea level) termed inter-trough banks (ITBs) (Fig. 4.2), which are similar to those described from other glaciated shelf regions (Funder and Hansen, 1996; Ottesen et al., 2005; Rydningen et al., 2013; Weidick et al., 2004). The cross-shelf troughs along West Greenland were likely formed

by pre-glacial river systems draining the interior of Greenland during Neogene (Funder et al., 1989; Sommerhoff, 1979; Weidick and Bennike, 2007). Hofmann et al. (2016) state, that besides pre-glacial topography, structural boundaries related to fractures and faults zones also influenced ice stream routing. The river troughs were occupied and partly eroded by grounded ice during past glacials (Batchelor and Dowdeswell, 2014). As a result, Quaternary sedimentation in the MVBTs is dominated by glacial deposits and erosion (Knutz et al., 2015). The underlying Pliocene and Late Miocene successions are, in contrast, dominated by contourite deposits (Knutz et al., 2015). Close to the coast, Archaean and Proterozoic crystalline basement is exposed or covered by a thin veneer of sediment (Oakey and Chalmers, 2012).

*Figure 4.1: Overview of existing datasets from the north and eastern Baffin Bay concerning the last deglaciation. See legend for further details. Dashed red and violet lines (in Melville Bay) show conceptual maximum ice extent and mid-shelf stabilization based on thin multibeam surveys (this study). Thick red lines indicate the observed (partially minimum) LGM ice extent and thick violet lines show the retreat phases thereafter. Thin red and dark red lines indicate conceptual LGM ice extent proposed by Funder et al. (2011, 2004) and Ehlers and Gibbard (2007). White dots indicate dated sites (either radiocarbon dating or cosmogenic surface exposure ages). Thick colored numbers show important ages related to LGM and YD. The white asterisk (in Melville Bay) shows the location of Core GeoB 19920-1 (Dorschel et al., 2016) with its dated age (cal kyr BP). Inset shows the general location of the research area. Black box indicates location of Fig. 4.2. As background, regional bathymetry and topography is taken from IBCAO v.3.0 (Jakobsson et al., 2012b). [++] (Bennike and Björck, 2002; Kelley et al., 2013; Rinterknecht et al., 2014; Roberts et al., 2013); [x] and references therein; * (Dowdeswell et al., 2014; Funder et al., 2011, and references therein; Hogan et al., 2016; Ó Cofaigh et al., 2013a; Ó Cofaigh et al., 2013b; Sheldon et al., 2016); ** (Dowdeswell et al., 2014; Hogan et al., 2016; Ó Cofaigh et al., 2013b); GIS = Greenland Ice Sheet; LIS = Laurentide Ice Sheet, IIS = Innuitian Ice Sheet.*

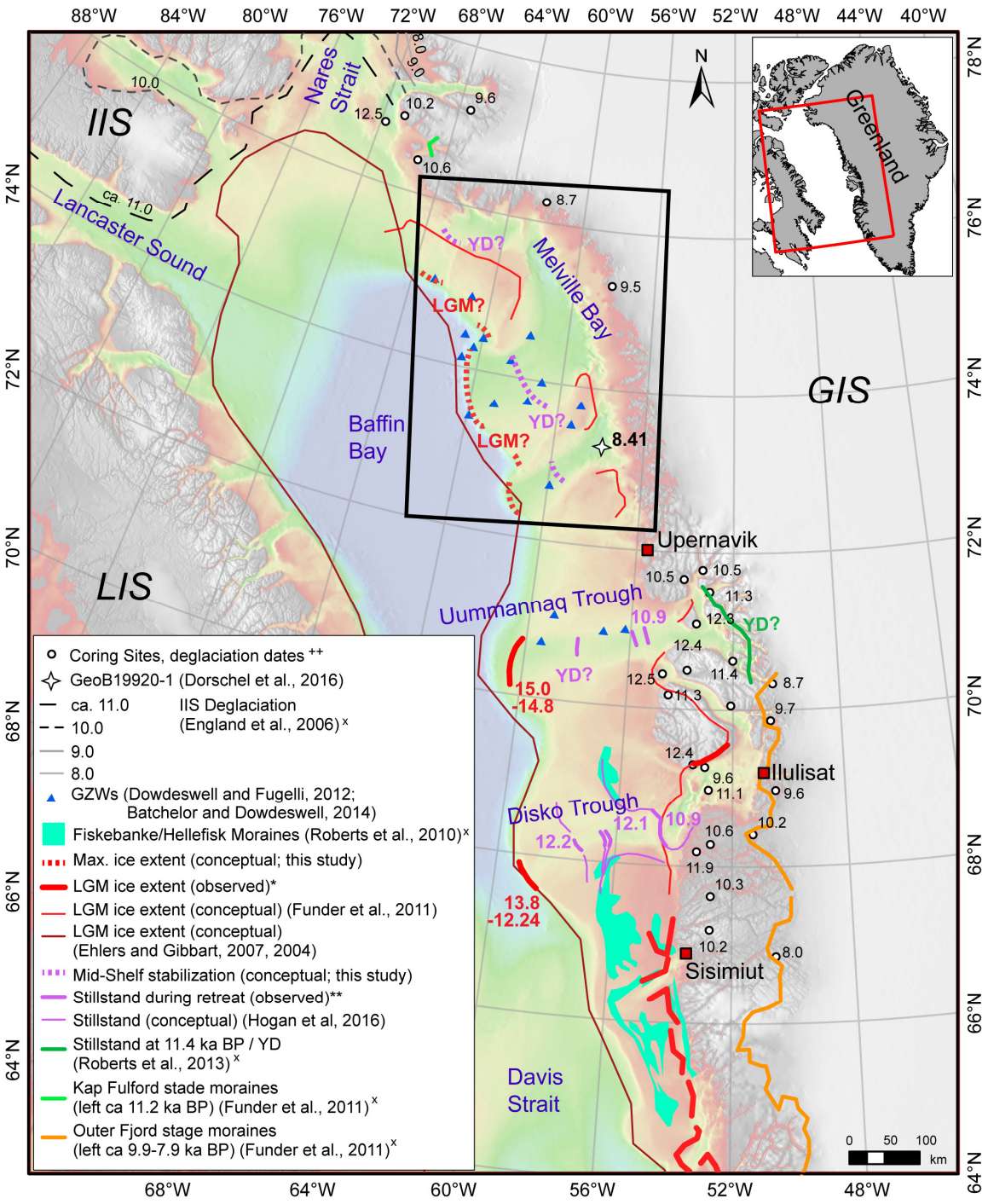
88°W
84°W
80°W
76°W
72°W
68°W
64°W
60°W
56°W
52°W
48°W
44°W
40°W
78°N
76°N
74°N
72°N
70°N
68°N
66°N
64°N
N
Greenland
IIS
LIS
GIS
Nares Strait
Lancaster Sound
ca. 11.0
Baffin Bay
Melville Bay
YD?
LGM?
8.41
Upernavik
Uummannaq Trough
15.0
-14.8
Disko Trough
12.2
13.8
-12.24
Illulisat
Sisimiut
Davis Strait
0 50 100
km
Coring Sites, deglaciation dates ++
GeoB19920-1 (Dorschel et al., 2016)
ca. 11.0
10.0
IIS Deglaciation (England et al., 2006)x
9.0
8.0
GZWs (Dowdeswell and Fugelli, 2012; Batchelor and Dowdeswell, 2014)
Fiskebanke/Hellefisk Moraines (Roberts et al., 2010)x
Max. ice extent (conceptual; this study)
LGM ice extent (observed)*
LGM ice extent (conceptual) (Funder et al., 2011)
LGM ice extent (conceptual) (Ehlers and Gibbart, 2007, 2004)
Mid-Shelf stabilization (conceptual; this study)
Stillstand during retreat (observed)**
Stillstand (conceptual) (Hogan et al, 2016)
Stillstand at 11.4 ka BP / YD (Roberts et al., 2013)x
Kap Fulford stade moraines (left ca 11.2 ka BP) (Funder et al., 2011)x
Outer Fjord stage moraines (left ca 9.9-7.9 ka BP) (Funder et al., 2011)x

4.1.1.2. Oceanographic setting and sea-level rise

During the LGM, global mean sea level was 120 -135 m below its present day sea level. Later, it rose almost continuously due to melting of most of the Northern Hemisphere ice sheets (Clark and Mix, 2002; Simpson et al., 2009, and references therein). At ~10 ka BP, sea level in Baffin Bay had reached ~100 m above LGM sea level (Funder and Hansen, 1996; Simpson et al., 2009), thus potentially destabilizing grounded ice on the continental shelf (Roberts et al., 2009).

The general present-day oceanographic conditions were established in central eastern Baffin Bay before ~14.0 ka BP (Sheldon et al., 2016) and by ~10.4-9 ka BP further to the North in northern Baffin Bay and Nares Strait (Knudsen et al., 2008; Levac et al., 2001). Since these times, the West Greenland Current (WGC) has functioned to transport warm Atlantic water along the West Greenland coast from the southern tip of Greenland to northern Baffin Bay (Seidenkrantz et al., 2013; Tang et al., 2004). The initial influx of this warm water was possibly responsible for the onset of ice stream retreat from the shelf edge (Knudsen et al., 2008; Levac et al., 2001; Seidenkrantz et al., 2013). Today, circulation in Baffin Bay is characterized by a thin low-salinity surface layer (in the upper ~100-300 m of the water column; derived from meltwater, runoff and precipitation) flowing above the warmer, high-salinity layers of the WGC (in ~150-1330 m depth) (Tang et al., 2004) that reach the base of marine terminating glaciers in West Greenland (Chauché et al., 2014).

4.2. Material and methods

Bathymetric data (Fig. 4.2) were acquired during *RV Maria S. Merian* expedition MSM44 in July 2015 (Dorschel et al., 2016) and *RV Polarstern* expedition ARK-XXV/3 in summer 2010 (Damm, 2010). On *RV Maria S. Merian*, the bathymetric data were acquired with a Kongsberg Simrad EM122 (12 kHz, 2° x 2° beam width, 130-150° swath angle, equidistant mode) deep-sea multibeam echosounder (MBES). The RV Polarstern data were acquired with an Atlas Hydrosweep DS-2 (15.5 kHz, 2° x 2.3° beam width, 90-120° swath angle, equidistant mode) MBES. The data were processed using Caris Hips and Sips v.9 and gridded to 50 x 50 m horizontal resolution for overview and 10 x 10 m resolution for detailed analysis. Additional bathymetric information was provided by TGS-NOPEC Geophysical Company ASA ('TGS') as 500 x 500 m grid (Fig. 4.2) based on TGS single-beam echosounder data. Regional bathymetry is taken from the International Bathymetric Chart of the Arctic Ocean version 3.0 (IBCAO v.3.0) (Jakobsson et al., 2012b) and terrestrial areas of Greenland are mapped according to the Greenland Ice Mapping Project digital elevation model (GIMP DEM, 90 m Grid) (Howat et al., 2014).

Gridded multibeam-bathymetric data and the TGS grid were imported to ESRI ArcView for subsequent analyses. In order to identify geomorphological landforms indicative of past ice-sheet development, the data were analyzed for slope angles and elevations and depressions using the standard ESRI raster computation tools for slope, hillshade, aspect, flow direction and focal statistics (Burrough and McDonell, 1998). Glacial landforms were then digitized manually.

The vertical resolution of the TGS grid is lower than that of the multibeam data. Slight elevation changes of 10-20 m cannot be identified within the TGS grid. Despite this drawback, it is still possible to trace some of the larger wedges of up to 70 m height, as observed in the high-resolution bathymetry, in the TGS grid. Sub-bottom profiler data were collected during expeditions MSM44 and ARK-XXV/3 with the Atlas Hydrographic Parasound P70 system. The acquisition settings of the Parasound system used during the expeditions are given in the respective cruise reports (Damm, 2010; Dorschel et al., 2016).

In order to obtain some age control on the deglaciation of Melville Bay inferred from glacial landforms, the base of sediment core GeoB 19920-1 was dated by Accelerator Mass Spectrometry (AMS) radiocarbon dating performed at the Laboratory of Ion Beam Physics at the ETH Zurich. Core GeoB 19920-1 was collected from the inner shelf of the southern MVBT (73°15.92'N, 57°50.95'W) at 998 m water depth (Figs. 4.1, 4.2 and 4.4). It has a total length of 1108 cm and consists largely of silty clays with only a few sandier layers (Fig. 4.7). The AMS ^{14}C date was analyzed on 3 mg calcium carbonate in mixed planktonic foraminifera picked from the >150 mm fraction at 1105 cm core depth. The obtained age was corrected for ^{13}C, and then converted to calendar years using the Calib.7.1.0 software (www.calib.qub.ac.uk) following the approach of Stuiver and Reimer (1993) and applying the INTCAL13 calibration curve (Reimer et al., 2013) (see Table 1 (Chapter 3.5) for details).

Figure 4.2: Overview of the bathymetric data acquired during Maria S. Merian expedition MSM44 and RV Polarstern expedition ARK-XXV/3 in Melville Bay in the Northeast Baffin Bay. Colors coincide with contour lines. White asterisk shows location of Core GeoB 19920-1. White dashed line indicates cross section shown in Fig. 4.2b. Inset shows the general location of the research area. Background is taken fromTGS (colored grid), IBCAO v.3.0 (blueish grid) (Jakobsson et al., 2012b) and GIMP (90mGrid, grey) (Bamber et al., 2013). MVBT: Melville Bay Trough. ITB: Inter-trough Bank. b: Cross section of Melville Bay.

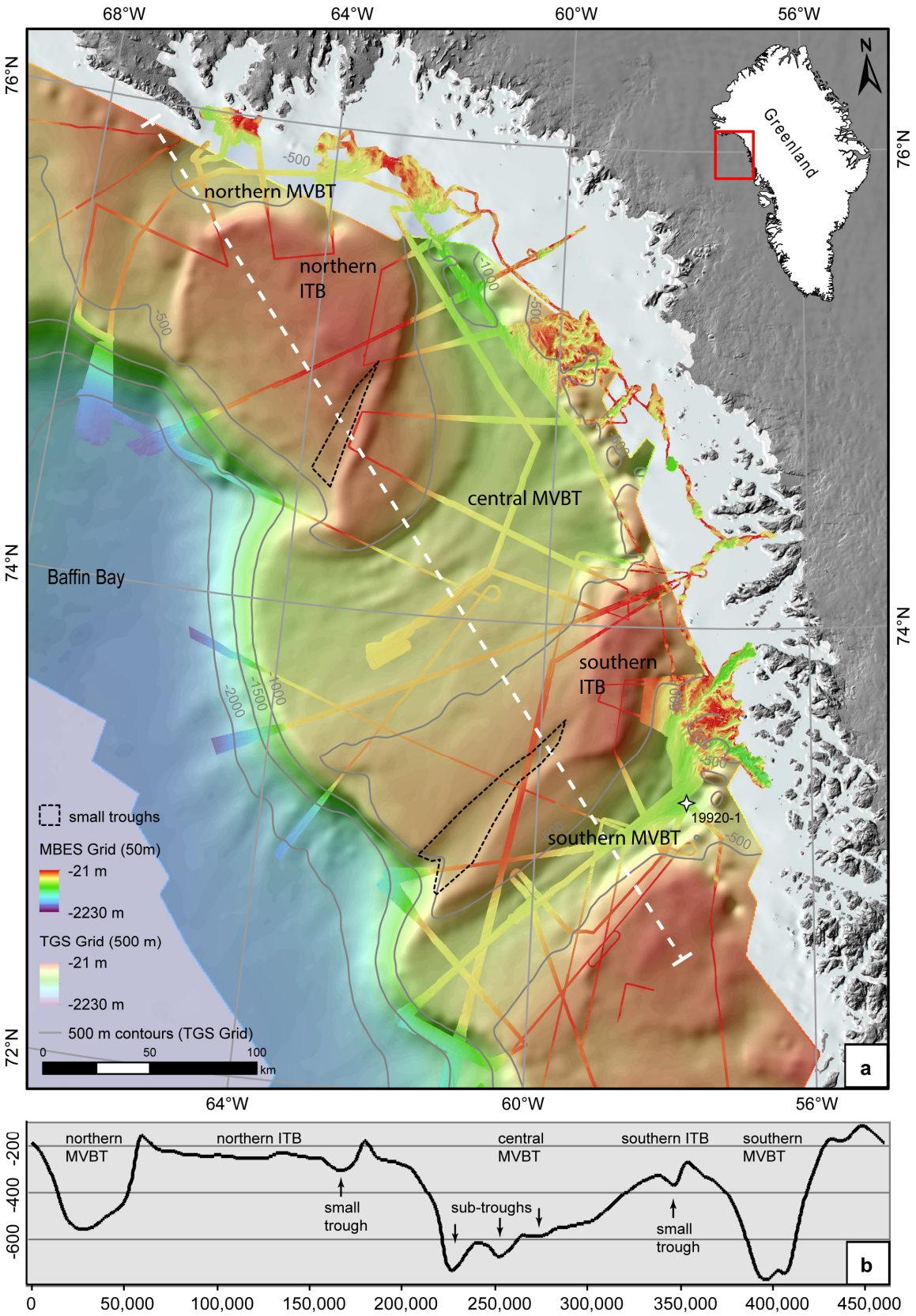
68°W
64°W
60°W
56°W
76°N
74°N
72°N
N
Greenland
northern MVBT
northern ITB
central MVBT
southern ITB
southern MVBT
Baffin Bay
19920-1
-500
-1000
-1500
-2000
small troughs
MBES Grid (50m)
-21 m
-2230 m
TGS Grid (500 m)
-21 m
-2230 m
500 m contours (TGS Grid)
0
50
100
km
a
northern MVBT
northern ITB
central MVBT
southern ITB
southern MVBT
small trough
sub-troughs
small trough
-200
-400
-600
0
50,000
100,000
150,000
200,000
250,000
300,000
350,000
400,000
450,000
b

4.3. Results and interpretation

4.3.1. Trough morphology

The three large MVBTs have reverse-gradient slopes, with water depths generally increasing landwards from the shelf edge (500-800m) to the overdeepened parts of the troughs on the inner continental shelf (750-950 m) (Fig. 4.3). Thalwegs of the MVBTs deepen from the shallow northern MVBT to the deep southern MVBT (Fig. 4.2b). The MVBTs are u-shaped to asymmetrical in cross section (Fig. 4.2b). The asymmetry is most pronounced in the middle to outer shelf of the central MVBT, which displays steep (~0.9°) northern and gentler (~0.1°) southern walls. The southern side of the central MVBT is furthermore incised by smaller sub-troughs (Fig. 4.2b), similar to those described from Belgica Trough, Antarctica (Graham et al., 2011). Small ridges on the middle shelf, in the troughs, rise to approximately 20-70 m above the adjacent trough floor (Fig. 4.3).

The northern and central MVBTs are curved and bend around the northern ITB (Fig. 4.2). Close to the coast, the onset of the northern and central MVBTs is divided by a prolongation of the ITB (200-500 m high, 20-30 km wide) (Fig. 4.5a). There, the ITB seems to extend further landwards between the central and the northern troughs. In contrast to the central and northern MVBT, the southern MVBT is straight in planform and separated from the central MVBT by the southern ITB (Fig. 4.2).

An elongated slight depression is observed in the middle of the southern ITB (Figs. 4.2 and 4.5b). The depression is flat-floored, u-shaped and incised into the southwestern flank of the ITB in water depths of 300-500 m. Its length is ~90 km, its width 20 km, and its depth 40-150 m (increasing towards the shelf edge). The depression trends straight southwestwards until a slight eastward curve at its lower end. This depression is delimited to the south by the high southern flank of the ITB. The landform thus resembles a small glacial trough that originates on the top of the ITB and extends to the shelf edge (Figs. 4.2, 4.4 and 4.5b). A similar but smaller flat-floored, u-shaped depression can be found on the northern ITB (Figs. 4.2 and 4.4). It is ~55 km long, up to 15 km wide, 15-80 m deep and located in water depths between 200 and 400 m. The trough is oriented south-southwest and is bordered to the south by a large elongated ridge (~10- 18 km wide, ~10-75 m high and ~80 km long). This ridge is straight except where it bends eastwards close to the shelf edge. These landforms are not oriented parallel to any underlying, older structural highs or lows described in the literature (Gregersen et al., 2013). We thus interpret them to be likely of glacial origin.

Furthermore, in front of the MVBTs, the continental slope is characterized by outward bulging contours indicating the presence of glacial trough-mouth fans (TMFs) (Fig. 4.2). This is supported by increased gradients of the upper continental slope (upper third of the slope) in the extension of the trough axes (2.9° in the northern, 2.8° in the central and 3.4° in the southern MVBT) that fit well with the findings of Batchelor and Dowdeswell (2014). The TMF of the northern MVBT, however, is smaller than those of the central and southern MVBT.

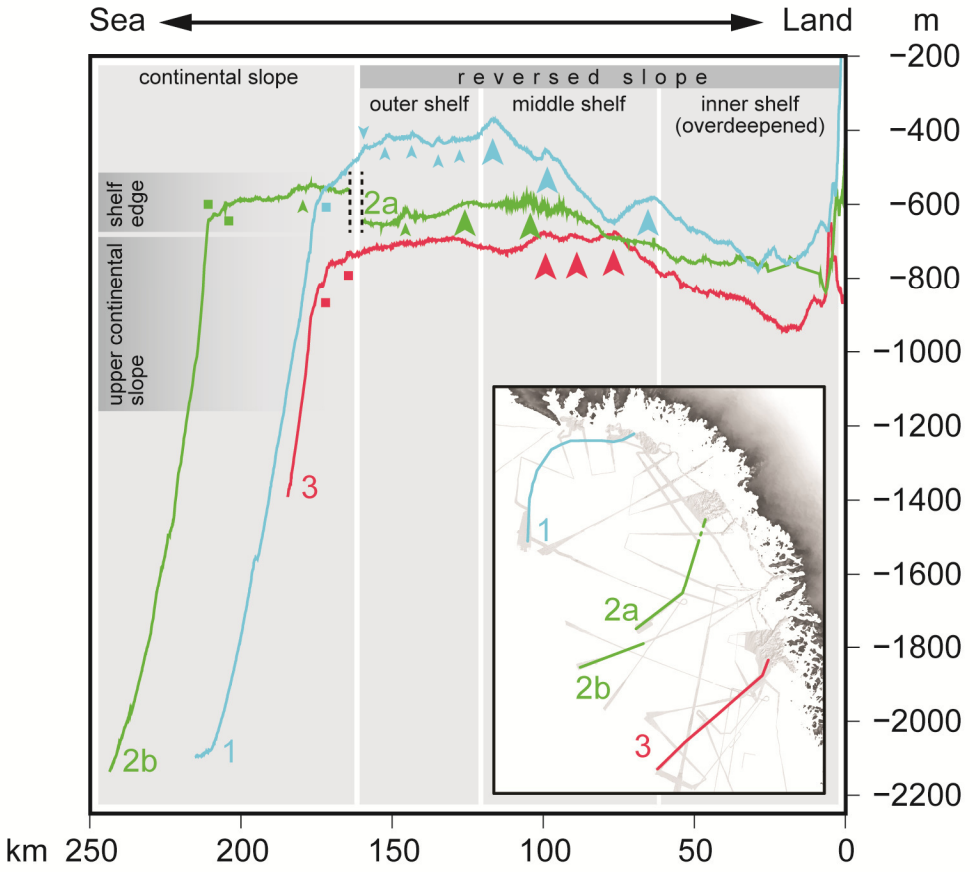

Figure 4.3: Bathymetric cross sections across the MVBTs. Note the reversed slope and the overdeepened inner shelf. Colors are similar in inset: Blue = northern trough (1); green = central trough (2a and b); red = southern trough (3). Large triangles indicate large GZWs, small triangles show small GZWs and colored squares indicate moraines, similar to Fig. 4.4. Each profile is displayed from the outer shelf to the inner shelf, based on the 50 m grid of MSM44 and ARK-XXV/3 bathymetric data. Grey boxes indicate approximate locations across the shelf described in the text.

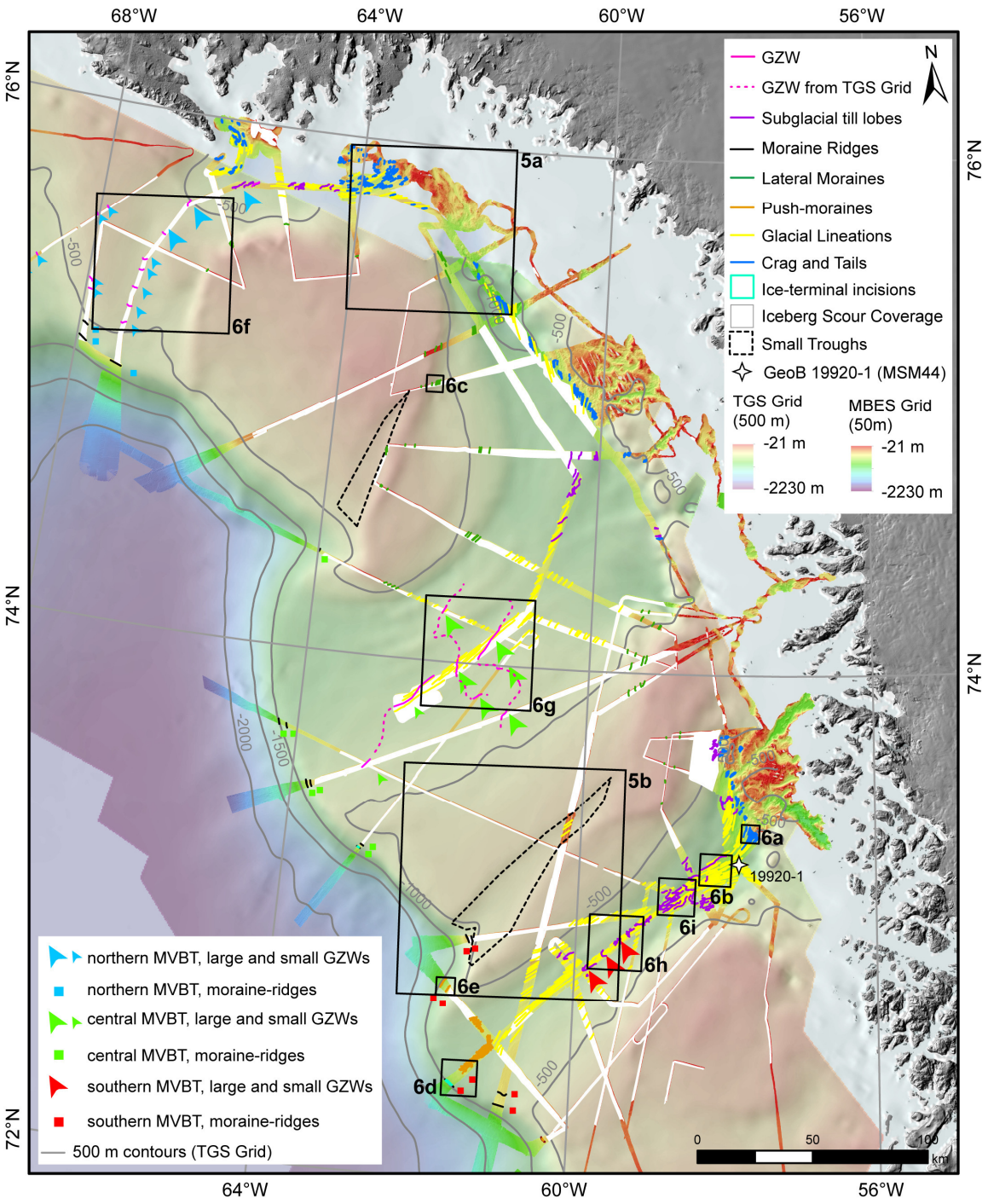

Figure 4.4: The different glacial landforms identified in the research area on the basis of the bathymetric grids (10 m resolution) and the TGS grid (500 m resolution). Iceberg scour coverage is colored areal white. The colored triangles and squares indicate the positions of GZWs and moraines identical to those in Fig. 4.3. Note that the GZWs in the southern MVBT are covered by subglacial till lobes. Subtle GZWs in TGS data are shown in dashed pink. As background data, a combination of IBCAO v.3.0 (Jakobsson et al., 2012b), GIMP (Bamber et al., 2013) and TGS data is displayed. Analyzed bathymetric data is colored according to depth. White asterisk shows location of Core GeoB 19920-1. Black boxes show location of Fig. 4.5a and 4.5b and 4.6a-i.

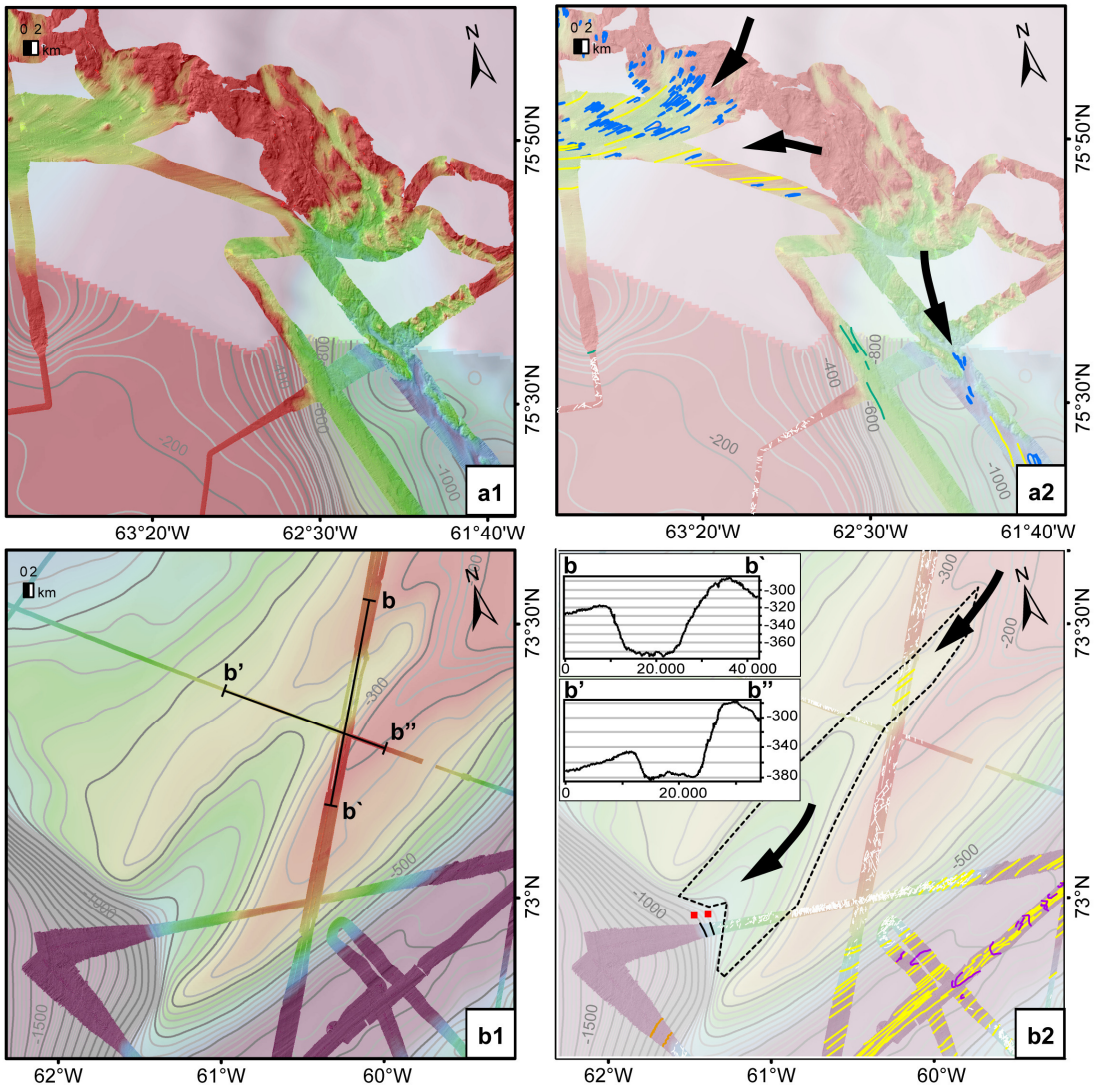

Figure 4.5: a) Crag-and-tails (blue) and glacial lineations (yellow) point in the individual troughs. They indicate a bifurcation of the ice-stream, thus, flowing into the northern and central MVBT around the northern ITB. Black arrows indicate suggested ice-flow. White lines on the ITB indicate iceberg scours. b) Zoom in on the small trough (dashed black line) on the southern ITB. Glacial lineations (yellow) on the upper part and moraines (black lines, red squares) on the lower end. White lines indicate iceberg scours. Black arrows indicate suggested ice-flow. Insets show cross sections (in meter) of the black profiles.

4.3.2. Along-trough glacial landforms

4.3.2.1. Crag-and-tail features

Elongated, streamlined hills occur in all three MVBTs on the inner shelf, at the transition from the crystalline bedrock near the coast to sedimentary sequences and at water depths between 300 and 1050 m (Figs. 4.4 and 4.6a). Slopes average around 7° on the up-ice sides of these hills and 1-2° downstream. Sub-bottom profiles show that the ice-facing sides are characterized by a higher amplitude reflector (Fig. 4.6a) likely indicating outcropping bedrock. The rocky ice-facing headlands vary in height between 30 and 150 m and in width between 100 and 750 m. The distal sides are covered by a smooth, partly stratified sedimentary tail (Fig. 4.6a). The lengths of the sedimentary tails vary from 400 m to several kilometers. These landforms are interpreted as crag-and-tails or rock drumlins (Benn and Evans, 2010). A special situation occurs at the connection between the northern and central MVBTs, where crag-and-tails oriented either west/southwest along the axis of the northern MVBT or south/southeast along the central MVBT (Fig. 4.5a) indicate divergence of the ice streams.

4.3.2.2. Glacial lineations

Smooth, elongated, and streamlined ridges (Figs. 4.4 and 4.6b) occur within all MVBTs at depths of 400-1050 m. They are 7-15 km long, 100-500 m wide and 4-15 m high. The ridges run parallel to the individual trough axes and, thus, trend on average towards the southwest. In the central and southern MVBTs, narrow and well defined ridges disappear close to the shelf edge. In the northern trough, these ridges are subtle and only occur in the deep inner shelf below 500 m water depth. The ridges often constitute the elongations of crag-and-tails (Figs. 4.4 and 4.6a) and are interpreted as glacial lineations (Benn and Evans, 2010; Clark, 1993; Ottesen et al., 2008). Subtle glacial lineations are also present in the upper part of the small trough on the southern ITB (Figs. 4.4 and 4.5b). They trend southwest and are, thus, parallel to those in the southern MVBT (Fig. 4.4).

In general, the glacial lineations are similar to those identified in the outer Uummannaq Trough, south of Melville Bay, where they are interpreted as indicators of fast-flowing ice and former ice-flow directions (Benn and Evans, 2010; Clark, 1993; Dowdeswell et al., 2014; Ó Cofaigh et al., 2013a, 2013b; Spagnolo et al., 2014).

4.3.2.3. Lateral moraines

Smooth, elongated ridges occur at the lateral boundaries of the MVBTs (Figs. 4.4 and 4.6c). They are 15-60 m high and have a width of 2-4 km across. In the northern MVBT, those ridges are located in water depths of 215-380 m while, in the central MVBT, they seem to occur over a greater depth range (215-800 m depth). In the southern MVBT, lateral ridges can only be observed in the multibeam data on the southern flank of the southern ITB in depths of 100-190 m (Figs. 4.4 and 4.6c). Some of the ridges are asymmetrical with a steeper down-ice slope (2-3.5°) oriented towards the adjacent ITB and a gentler up-ice slope (0.5-2°).We interpret these ridges as lateral moraines as they only occur at the boundaries of the troughs (Benn and Evans, 2010).

Figure 4.6: Selected examples for identified and digitized seafloor features: a) blue = crag-and-tails, yellow = glacial lineations; b) yellow = glacial lineations; c) green = lateral moraines, black arrows indicate exemplary three of the several iceberg scours and their direction; d) turquoise = ice-terminal shelf-edge incisions, orange = push moraines, black dashed = moraine; e) dark red = push moraines at the shelf edge; f) pink = GZW, black = iceberg scours, blue arrows = small and large GZWs (see Figs. 4.3 and 4.4); g) pink = GZW, dashed pink = subtle GZWs in TGS data, black = iceberg scours, yellow = glacial lineations; h) purple = subglacial till lobes covering GZWs, red arrows = large GZWs (see Figs. 4.3 and 4.4), yellow = glacial lineations; i) purple = subglacial till lobes, yellow = glacial lineations; Insets show cross sections and sub-bottom profiles of the black profiles. Cross sections are in meter. Offset (sub-bottom profile) shows distance in meters to start of Line. TWT = two-way travel time in seconds. Annotations on the sub-bottom profile in Fig. 4.6g are in meter. Cross section in Fig. 4.6h shows high-resolution bathymetry (black) and TGS grid (dashed black).

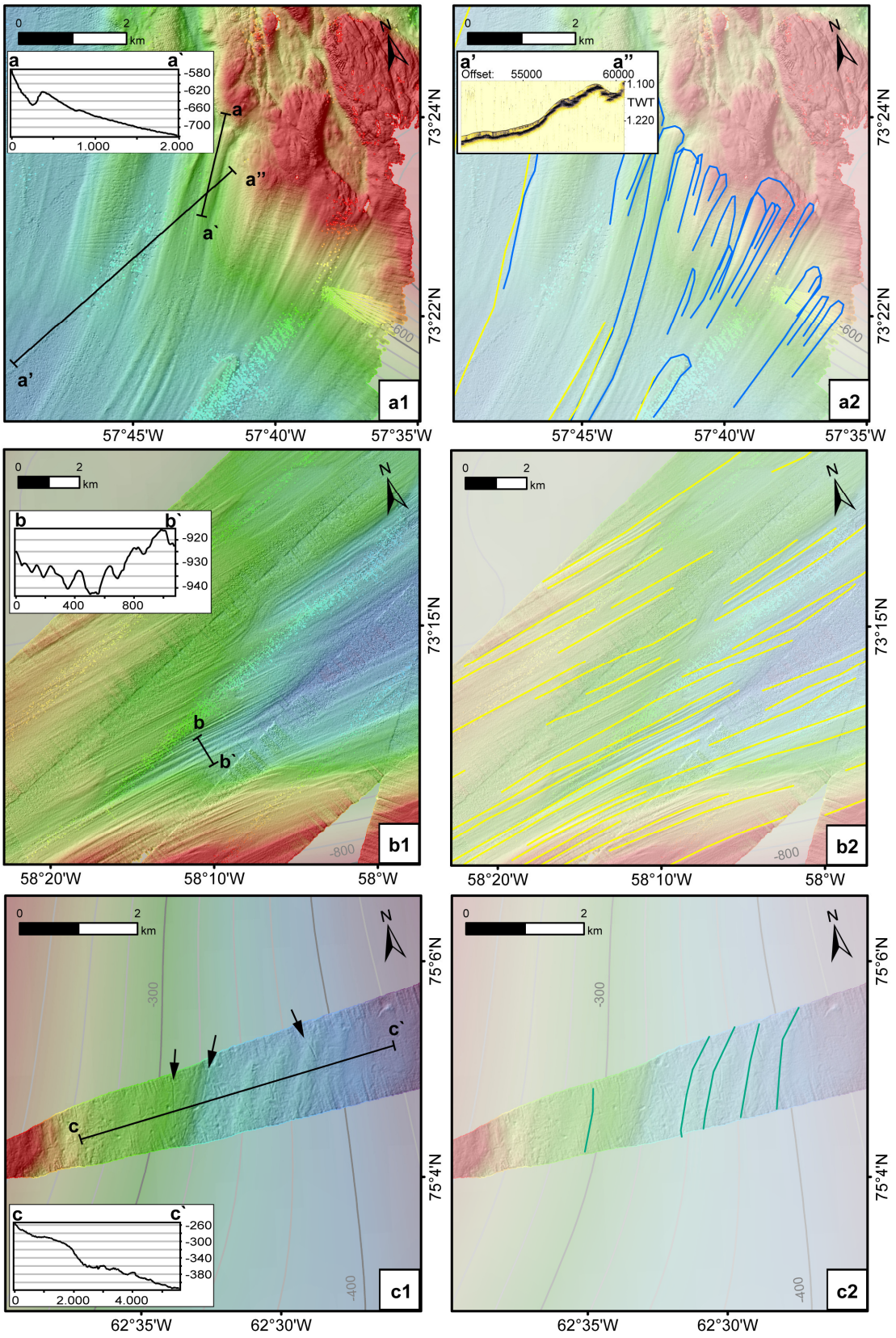
a1
a2
b1
b2
c1
c2
0 2 km
N
a
a`
a'
a''
-580
-620
-660
-700
0 1.000 2.000
Offset: 55000 60000
-1.100
TWT
-1.220
b
b`
-920
-930
-940
0 400 800
c
c`
-260
-300
-340
-380
0 2.000 4.000
-600
-800
-300
-400
73°24'N
73°22'N
73°15'N
75°6'N
75°4'N
57°45'W
57°40'W
57°35'W
58°20'W
58°10'W
58°W
62°35'W
62°30'W

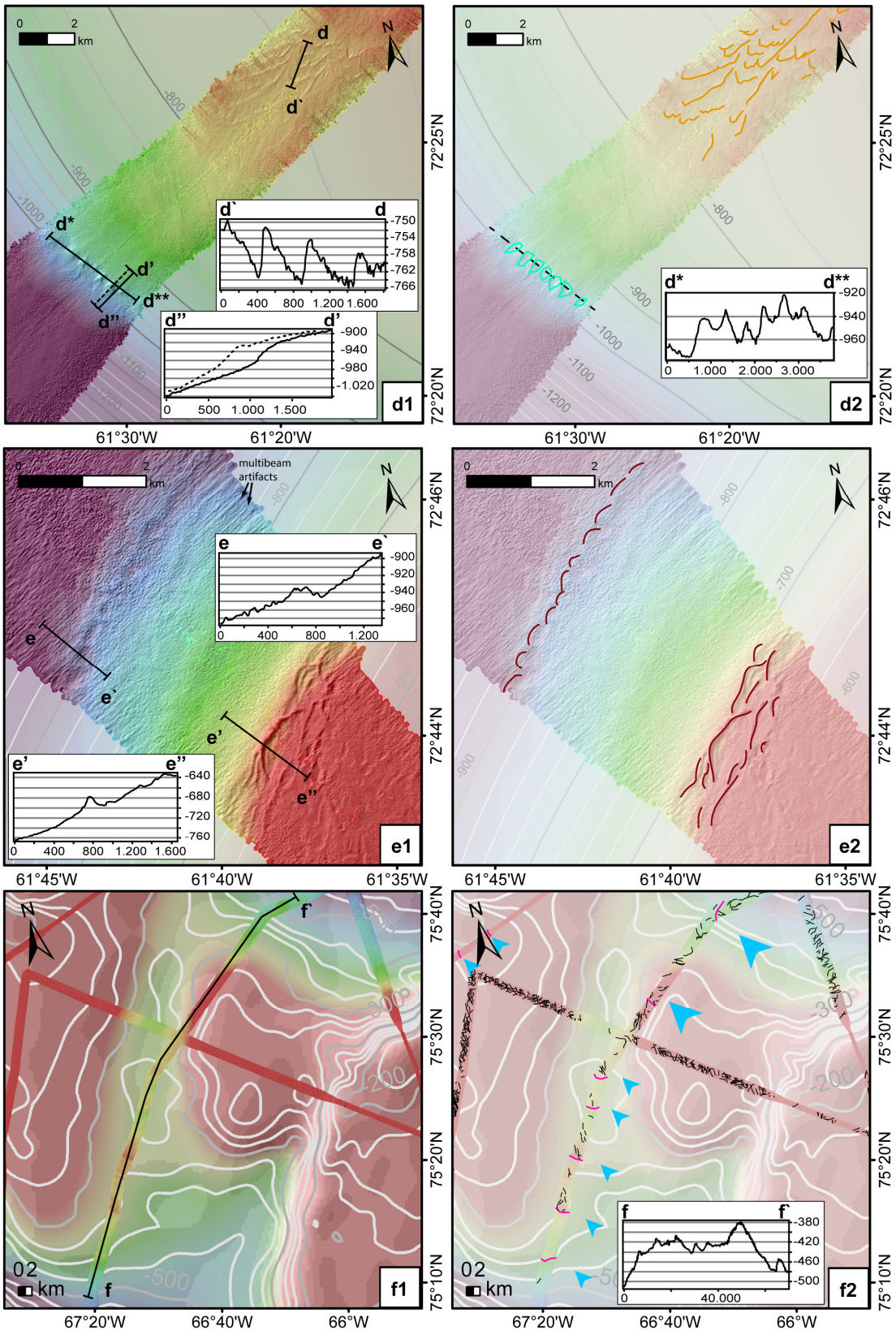
d1
d2
e1
e2
f1
f2
multibeam artifacts
0 2 km
N
72°25'N
72°20'N
72°46'N
72°44'N
75°40'N
75°30'N
75°20'N
75°10'N
61°30'W
61°20'W
61°45'W
61°40'W
61°35'W
67°20'W
66°40'W
66°W
02 km

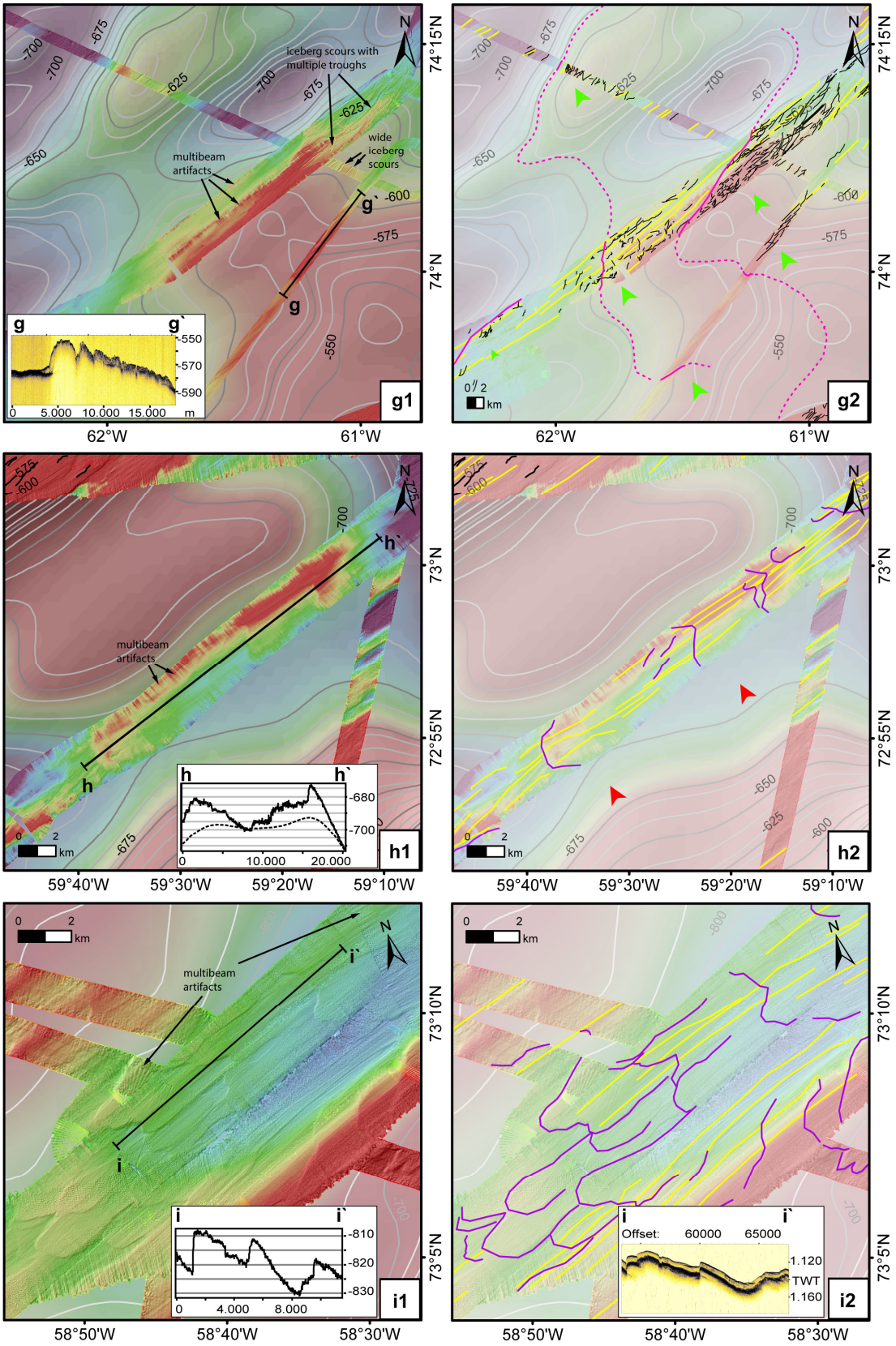
iceberg scours with multiple troughs
wide iceberg scours
multibeam artifacts
g
g`
h
h`
i
i`
g1
g2
h1
h2
i1
i2
Offset:
TWT
km
N
62°W
61°W
74°15'N
74°N
59°40'W
59°30'W
59°20'W
59°10'W
73°N
72°55'N
58°50'W
58°40'W
58°30'W
73°10'N
73°5'N

4.3.3. Across-trough glacial landforms

4.3.3.1. Moraine ridges

Elongated ridges of varying shapes are observed running oblique to the axes of all three cross-shelf troughs and at the seaward edges of the small troughs on the ITBs of the Melville Bay outer shelf (Figs. 4.4, 4.5b and 4.6d, 4.6e). The elongated ridges in the northern and central MVBTs measure up to 45 m in height, 500-1000 m in width and 2-6 km in length. They are relatively smooth and most of them have an asymmetric profile with a steep up-ice- slope (6-9°) and a gentler down-ice slope (2-5°).

Compared to the northern and central MVBTs, the ridges on the outer shelf of the southern MVBT are more arcuate (Figs. 4.4 and 4.6d). These ridges are 5-13 m high, 100-200 m wide, 200-8000 m long and are typically asymmetric with a steep (~5-7°) down-ice slope and a gentle (1.5-2.2°) up-ice slope. In plan form, most of them are convex to the shelf edge, but some are almost sub-parallel to the trough axis. The ridges appear to continue across the southern trough and probably also onto the ITBs, forming an embayment in the deepest, central part of the trough (Figs. 4.4 and 4.6d). Similar arcuate ridge segments occur at the shelf edge and on the upper continental slope of the southern MVBT (Figs. 4.4 and 4.6e). In plan form these ridge segments are convex to the shelf edge and are 2-8 km long, 5-10 m high and 100-200 m wide with a steep up-ice slope (~6-9°). The down-ice slope is equal to slightly shallower (2-6°).

We interpret these landforms as ice-terminal moraines that developed at the shelf edge, similar to those described from Svalbard and Norway (Ottesen et al., 2007, 2005). The arcuate ridges near the shelf edge of the southern MVBT (Fig. 4.6d and 4.e) are interpreted as recessional push moraines, based on their similarity in shape, size, and asymmetry to ridges on Iceland (Bennett, 2001; Bennett and Glasser, 2009).

4.3.3.2. Grounding-zone wedges (GZWs)

Wedge-shaped landforms of varying size have been identified within the multibeam data. Large wedges (large triangles in Figs. 4.3, 4.4 and 4.6f, 4.6g, 4.6h) occur on the reverse-gradient slopes of the mid-to inner shelves of all three MVBTs. They are ~20-70 m high, ~22 km long, in places >11 km wide and occur in water depths of 350-700 m. Their down-ice slopes are steeper (0.7-1.3°) than their up-ice slopes (0.2-0.5°). The transverse spacing of the back-stepping wedges that build a stack in the individual troughs is 9-22 km. Small wedges (small triangles in Figs. 4.3, 4.4 and 4.6f, 4.6g) are ~10-20 m high, ~1-6 km long and occur in water depths of 440-650 m on the outer shelf of the northern and central MVBT. Their width could not be entirely mapped but exceeds 1.7 km. Their down-ice slopes are also steeper (0.7-1.3°) than their up-ice slopes (0.2-0.3°) and the transverse spacing of back-stepping wedges in the stack is 7.5-10 km. Large wedges can be traced

across the central MVBT in the TGS grid, albeit only as subtle images (Figs. 4.4 and 4.6g). Glacial lineations can be traced in the multibeam data over the tops of most of the large wedges (Figs. 4.4, 4.6f and 4.6g).

We interpret these landforms as recessional wedges in GZW-complexes. The locations of the observed GZWs roughly coincides with those identified in seismic data (Batchelor and Dowdeswell, 2015; Dowdeswell and Fugelli, 2012). GZWs at the reverse-gradient slope are rather unusual but have been also identified with similar sizes in the Uummannaq (Dowdeswell et al., 2014) and Disko troughs (Hogan et al., 2016) south of Melville Bay.

4.3.3.3. Subglacial till lobes

Small, wedge-shaped landforms that are streamlined and lobate to sinuous in planform occur on the inner shelf and partially also on the mid-shelf in all three MVBTs (Figs. 4.4, 4.6h and 4.6i). They are 1-6 km long, 1.5-2 km wide and 5-20 m high. The landforms have a steep down-ice slope (1.5-4°) and a shallow up-ice slope (0.3-0.5). They occur in 650-880 m water depths and are stacked with a transverse spacing of 1.5-2 km. The axes of the lobate wedges are oriented approximately parallel to the trough-axes.

They are overprinted by narrow (100-200 m wide) glacial lineations. Sub-bottom profiles (Fig. 4.6i) indicate that those wedges are generally deposited on a basal till layer with a relatively clear defined boundary. We interpret these lobes as recessional subglacial till lobes. On the inner northern MVBT and on the entire southern MVBT, the subglacial till lobes overprint the large GZWs and are likely part of it (Figs. 4.5 and 4.6h). Similar grounding zones consisting of streamlined lobes have been described from Larsen Inlet, Antarctica (Evans et al., 2005).

4.3.4. Ice-terminal shelf-edge incisions

U- to v-shaped incisions to depths of 25 m are present in front of the southern MVBT, along a shelf-edge moraine at 920 m depth (Figs. 4.4 and 4.6d). These incisions are 350-500 m wide and ~1000 m long. Although the origin of these landforms is unclear, their location suggests that they are probably associated with ice-terminal processes during maximum ice-sheet extent.

4.3.5. Iceberg scours

V-shaped to flat-bottomed incisions of various sizes (~0.5-13 m deep, 20-1500 m long and 30-300 m wide) cover almost all surveyed areas shallower than 650 m (except in areas with exposed bedrock at the seafloor) (Fig. 4.4). They are especially dense on the shallow ITBs where they occur with multiple cross-cutting orientations (Figs. 4.4, 4.5a and 4.5b). Some of the incisions have berms at their sides of up to 6 m. They are typical iceberg scours (Benn and Evans, 2010).

In the MVBTs, the main orientation of the iceberg scours is west to southwest, roughly parallel to the trough axes. On the shallow ITBs, the orientations are more chaotic with a stronger northwest component on the northern ITB and a stronger southwest component at the southern ITB. On the outer shelf, the scours trend more southeastwards (Fig. 4.6f). On the middle to outer shelf, some of the iceberg scours show multiple troughs (Fig. 4.6g). These can be interpreted as the products of multi-keeled icebergs. Relatively wide iceberg scours (Fig. 4.6g) are ploughed by small tabular icebergs. Most of the iceberg scours near the cross-shelf trough axis are straight to slightly curved (Fig. 4.6f).

4.3.6. Radiocarbon dating

Radiocarbon dating from 1105 cm core depth of sediment core GeoB 19920-1 (Fig. 4.7) revealed an uncalibrated age of 7925 radiocarbon years. This has been calibrated to 8410 cal yr BP (8.41 ka BP) (Table 1). Thus, the dated sediments are post-glacial in age and provide a minimum estimate for the deglaciation at the location of core GeoB 19920-1. Till deposits were not recovered in this core.

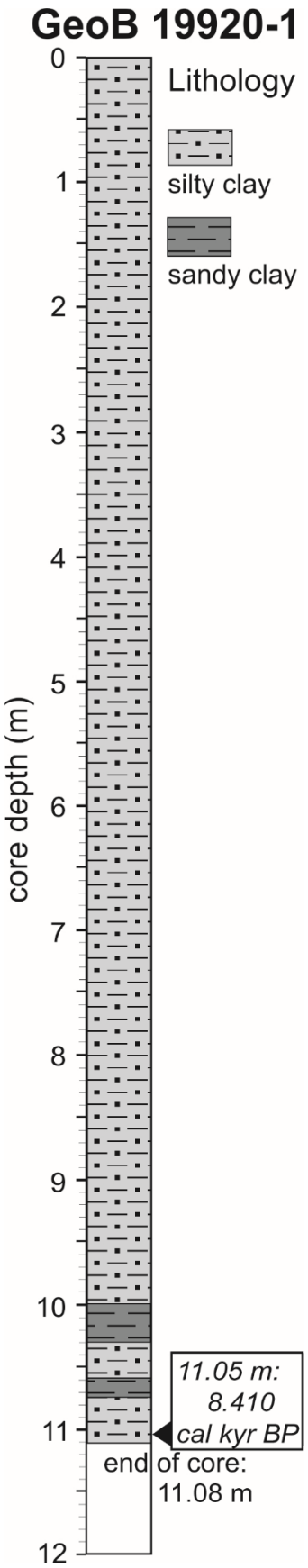

Figure 4.7: Lithological log of sediment core GeoB 19920-1 from the southern Melville Bay Trough.

Table 4.2: Raw data and calibration of the radiocarbon dating on core GeoB 19920-1

Core	lab code	sample depth (cm)	materia	^{14}C age	cal yr BP range [a] 1 sigma [b] 2 sigma	calibrated age
GeoB 19920-1	ETH-66277	1105	mixed planktic forams	7925 +/- 75	8334 - 8498 [a] 8231 - 8583 [b]	8410

Calibration was done using the Marine13.14c dataset and Calib Rev 7.1.0. A ΔR of -22 (+/- 31) was applied based on the average of 3 data points from West Greenland (Upernavik, Thule (Mörner and Funder, 1990) and Uummannaq (McNeely et al., 2006)) as listed in the http://calib.qub.ac.uk/marine/ data base.

4.4. Discussion

4.4.1. Maximum ice-sheet extent

In all three MVBTs, the occurrence of moraines at the shelf edge (Fig. 4.4) indicates that grounded ice of the nwGIS covered the entire troughs at some time in the past. The shelf-edge moraines in the MVBTs are terminal moraines, which record the furthest ice-stream advance across the continental shelf. In addition, the presence of glacial landforms in the small troughs on the ITBs suggests that these areas were also occupied by grounded ice and possibly drained by small ice streams from the banks to the shelf edge. Furthermore, the TMFs in front of the MVBTs indicate that the ice streams may have extended to the shelf edge repeatedly during past glacial periods (Batchelor and Dowdeswell, 2014).

No direct dates are available for the timing of ice-stream advances and retreats in the Melville Bay area due to lack of dateable material from the outer shelf. However, by comparing the ice-terminal landforms from Melville Bay to those of the Uummannaq and Disko troughs (Fig. 4.1), which have been dated to the LGM LGM (Dowdeswell et al., 2014; Ó Cofaigh et al., 2013b), we can suggest that the ice-terminal landforms in Melville Bay are also LGM features (Fig. 4.8a). The few terrestrial exposure dates and radiocarbon ages from coastal moraines and related landforms in and around Melville Bay do not contradict this interpretation (Funder et al., 2011 and references therein).

With our new observations on maximum former ice-sheet extents at the Melville Bay shelf edge it is now evident that ice streams reached the shelf edge via the cross-shelf

troughs along the entire West Greenland Coast during past glacials (Fig. 4.1). Furthermore, GZWs at the shelf edge and on the outer shelf of the northern and central MVBTs as described by Dowdeswell and Fugelli (2012) and Batchelor and Dowdeswell (2015), coincide with the locations of GZWs and moraines identified in our bathymetric data set. These features are likely of Late Weichselian age, which does not contradict the LGM interpretation. Nevertheless, our data suggest that most of the landforms identified at the shelf edge are moraines, rather than GZWs. We suggest therefore that the GZWs described by Dowdeswell and Fugelli (2012) and Batchelor and Dowdeswell (2015) might be overprinted or superimposed by those smaller moraines. Furthermore, the margins of wide ice streams might have created GZWs and moraines simultaneously at different lobes and a complex composite of both landforms (Bennett and Glasser, 2009) is also possible.

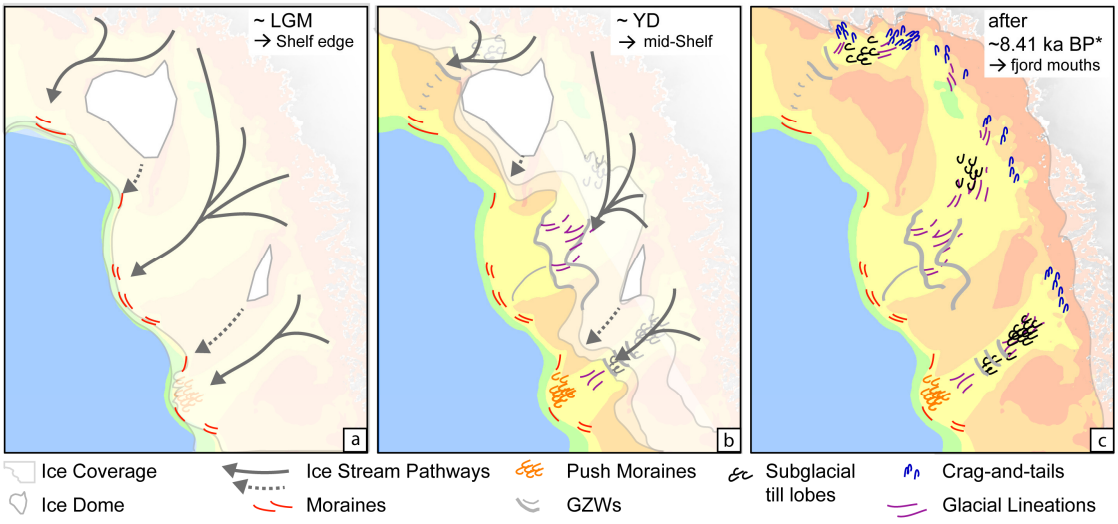

*Figure 4.8: Simplified sketch representing the assumed glacial retreat in Melville Bay. a) During LGM, ice domes and topography divide the ice streams that drain the nwGIS. Dashed grey arrows indicate possible small ice streams fed by the ice domes. Moraines at the shelf edge indicate the maximum extent. b) Varying retreat from the shelf edge is indicated by the distribution of the signatures of GZWs, moraines and glacial lineations. The retreat stopped on the mid-shelf, probably during the Younger Dryas (YD). c) Retreat from the midshelf occurred thereafter, uncovering more glacial landforms on the inner shelf, e.g. subglacial till lobes and crag-and-tails. The overdeepened inner shelf was free of grounded ice before 8.41 ka BP. * GeoB 19920-1.*

4.4.2. First nwGIS retreat

The investigation of the three MVBTs allows a comprehensive reconstruction of the retreat of major ice streams of the nwGIS. Nevertheless, due to a lack of dated samples for the moraines at the shelf edge of Melville Bay (Figs. 4.3 and 4.4), information on the chronology of ice-stream retreat has to be extrapolated from adjacent cross-shelf troughs. Dates from Nares Strait (Fig. 4.1) indicate a late (by ~12.5 ka BP) start of deglaciation north of the survey area (Knudsen et al., 2008). According to Ó Cofaigh et al. (2013b), ice-stream retreat in the Uummannaq Trough further south commenced earlier at ~14.8 ka BPSheldon et al. (2016), however, suggest slightly earlier retreat in Uummannaq Trough, starting prior to 15.0 ka BP. In front of Disko Trough the onset of ice-stream retreat has been dated later, at between 13.8 and 12.24 ka BP (Ó Cofaigh et al., 2013b) (Fig. 4.1). This information implies the onset of ice stream retreat in Melville Bay at some time between 15 and 12.24 ka BP.

4.4.3. Retreat from the outer shelf

The variability of glacial landforms on the outer continental shelves of the MVBTs also suggests slight variability in the conditions of ice-stream retreat between the individual MVBTs. All of the MVBTs display shelf-edge moraines (Figs. 4.3 and 4.4). The small GZWs on the outer shelf in the northern MVBT (Figs. 4.3, 4.4 and 4.6f) form a retreating stack. This stack indicates short phases of stabilization and, thus, an episodic to relatively slow retreat (Dowdeswell et al., 2008; Ó Cofaigh et al., 2008). Accordingly, retreat of the grounding zone in the northern MVBT to the middle shelf may have been a stepwise affair, similar to that suggested for episodic to slowly retreating ice streams in the Belgica Trough and Ross sea, Antarctica (Dowdeswell et al., 2008; Ó Cofaigh et al., 2008; Shipp et al., 2002). In the central MVBT, just one small GZW occurs on the outer shelf (Figs. 4.3, 4.4 and 4.6g), indicating at least one stabilization of the ice stream margin during its retreat across the outer shelf. GZWs are absent from the outer shelf in the southern MVBT. Here, instead, recessional push-moraines (Bennett, 2001; Ottesen et al., 2007, 2005) occur close to the shelf edge (Figs. 4.4, 4.6d and 4.6e). These moraines indicate an episodic to relatively slow initial retreat with small re-advances. Furthermore, the configuration of the push-moraines resembles a calving bay (Benn and Evans, 2010; Hogan et al., 2016; Leventer et al., 2006) in the deepest, central part of the trough (Fig. 4.6d). Here, it seems the grounding line was stable on the shallower banks but lay farther inland in the deeper trough. Glacial lineations to the east of the push moraines (Fig. 4.4) indicate fast retreat of the ice stream grounding-zone on the outer shelf in this part of the trough.

To summarize, the evidence from the outer shelf shows that ice streams in the MVBTs retreated with contrasting styles. Retreat in the northern MVBT was continuous and stepwise. Retreat in the central MVBT was interrupted by at least one stillstand phase.

Retreat from the southern MVBT occurred rapidly after an initial advance and retreat phase. This pattern of varying stabilization (Ó Cofaigh et al., 2008; Shipp et al., 2002) can be expected to be related to some combination of the effects of underlying topography (Bennike and Björck, 2002; Long and Roberts, 2003; Ó Cofaigh et al., 2013b), sea-level rise (Clark and Mix, 2002; Funder and Hansen, 1996; Simpson et al., 2009), advancing warm WGC (Chauché et al., 2014; Dyke et al., 1996; Knudsen et al., 2008; Levac et al., 2001; Sheldon et al., 2016) and internal factors of the ice sheet (Benn and Evans, 2010).

4.4.4. Large GZWs on the mid-shelf

A complex of large recessional GZW landforms is observed on the middle shelf in all three MVBTs (Figs. 4.3, 4.4 and 4.6f, 4.6g, 4.6h), roughly coincident with the mid-shelf GZWs interpreted from seismic reflection data (Fig. 4.1) (Batchelor and Dowdeswell, 2015; Dowdeswell and Fugelli, 2012). The GZWs represent periods of significant ice stream stabilization (Anandakrishnan et al., 2007; Dowdeswell and Fugelli, 2012; Engelhardt and Kamb, 1997).

The mid-shelf stabilization in the MVBTs might have been climatically induced, and can tentatively be related to the Younger Dryas (YD) cooling event (Fig. 4.8b). This interpretation relies on comparisons of the large GZWs of Melville Bay to those of Uummannaq (~13.9 ka BP to ~11.5 ka BP) (Dowdeswell et al., 2014; Sheldon et al., 2016) and Disko troughs (12.24-12.08 ka BP) (Hogan et al., 2016; Ó Cofaigh et al., 2013b) (Fig. 4.1) and requires that the NE Baffin Bay region responded to the YD cooling event with a regional mid-shelf grounding-zone stillstand. The ice stream in Uummannaq Trough seems not to have been naturally conditioned to facilitate stabilization during retreat, leading to interpretations of its Bølling-Allerød- to YD-aged stillstand as climatically induced (Hogan et al., 2016; Sheldon et al., 2016). By analogy, the icestreams within Melville Bay's MVBTs may have been similarly forced.

4.4.5. Subglacial till lobes on the inner shelf

Deposition of recessional subglacial till lobes on the inner shelf (and in parts on the mid-shelf) in all three MVBTs (Figs. 4.4, 4.6h, 4.6i) indicates re-advancing ice-stream lobes at the grounding zone during ice-stream retreats. The processes forming theses subglacial till lobes might be similar to those forming the larger subglacial GZWs. The position of the lobes within the MVBTs (Fig. 4.4), thus, likely infers episodic to slow retreat (Dowdeswell et al., 2008; Ó Cofaigh et al., 2008) over the inner shelf with several grounding-zone stabilizations of a sinuous to lobate ice-stream margin. Similar landforms on the inner shelf of Uummannaq Trough have been interpreted as GZWs indicating an episodic retreat (Dowdeswell et al., 2014).

Subglacial till lobes and glacial lineations occur everywhere seawards of the exposed basement on the inner shelf. Most of the glacial lineations develop as elongated tails from rock drumlins and crag-and-tails (Figs. 4.4, 4.6a, 4.6b, 4.6h) that record streaming ice-flow. Again, similar crag-and-tails are recorded from the inner Disko (Hogan et al., 2016) and Uummannaq troughs (Dowdeswell et al., 2014; Ó Cofaigh et al., 2013b). These features are generally formed during periods of major glacial erosion at the transition between bedrock and sedimentary rocks (Harrison et al., 2008; Margold et al., 2015). Analogous crag-and-tails from Antarctica (cf. Ó Cofaigh et al., 2002; Wellner et al., 2001) have been used to show how bedrock controlled down-flow transitions in terms of ice-stream bed geomorphology.

The radiocarbon date from the inner shelf (GeoB 19920-1) provides a minimum age of 8.41 ka BP for ice-free conditions at the inner shelf of the southern MVBT (Fig. 4.8c). Two additional deglacial ages from the present day coastline (Fig. 4.1) indicate that Melville Bay was ice-free by 9.5-8.7 ka BP (Bennike and Björck, 2002; Funder et al., 2011; and references therein). To the south in the Uummannaq and Disko Bay region the ice retreated beyond the present day coastline between 12.5 and 10.5 ka BP (Bennike and Björck, 2002, and references therein). This indicates that ice streams in Melville Bay retreated probably later to their present position compared to those in the southern areas.

4.4.6. The role of ITBs

Well-preserved crag-and-tails and glacial lineations in the northern and central MVBT, at the landward prolongation of the northern ITB (Figs. 4.4, 4.5a), indicate a bifurcation of the ice stream in this area. This bifurcation was likely established by streaming ice adopting pre-glacial river valleys around the northern ITB (Fig. 4.4, 4.5a). This situation might have facilitated the development of stable domes of ice on top of the ITB (Fig. 4.8a) (Domack et al., 2006; Lavoie et al., 2015), analogous to the Siple Ice Dome on the inner Ross Ice Shelf (Fretwell et al., 2013; Horgan and Anandakrishnan, 2006; Lavoie et al., 2015). The topographic setting of the inner Ross Ice Shelf resembles the configuration of Melville Bay. The small troughs with their terminal shelf-edge moraines on the ITBs (Fig. 4.4, 4.5b) indicate the action of small ice streams, which can be seen as further evidence for past ice domes. Similarly, few glacial lineations occur on the southern ITB (Fig. 4.4, 4.5b), implying streaming ice. Lavoie et al. (2015) discussed how similar small troughs host ice streams draining the suggested Marr, Brabant and Livingston ice domes on the western Antarctic Peninsula. To summarize, we conclude that ice domes might have existed on the ITBs (Fig. 4.8a).

4.5. Conclusion

The submarine glacial landforms (GZWs, moraines etc.) identified in the Melville Bay provide a fresh view on the former extent and retreat history of the nwGIS.

- The glacigenic features identified in the study area indicate that grounded ice streams of the nwGIS reached the continental shelf edge through the MVBTs, where they deposited moraines likely of LGM age.
- Across the MVBTs, the number, dimensions and locations of the recessional wedges within GZW-complexes indicates that the detailed style of ice-stream retreat from the shelf edge varied between the MVBTs.
- Retreat on the outer shelf was slow, continuous and stepwise in the northern MVBT, but more episodic in the other MVBTs (with at least one stabilization on the outer shelf in the central MVBT and re-advances at the shelf edge followed by fast retreat in the southern MVBT).
- Mid-shelf stabilizations, revealed by the presence of large GZW-complexes, occurred in all three MVBTs in post LGM times, presumably during the YD. This interpretation is based on analogy to the findings from most West Greenland troughs.
- Recessional subglacial till lobes on the mid-to inner shelf indicate re-advancing ice-stream lobes during episodic to slow final ice-stream retreat towards the coast.
- The final ice-stream retreat in the inner southern MVBT took place before 8.41 ka BP.
- Ice domes probably developed on the ITBs during glacials, channeling the faster ice streams around them. Inferred small glacial troughs on the seaward flanks of the ITBs indicate that minor ice-streams were flowing along the axes of the ITBs.

Acknowledgments

We thank the crew and scientists of R/V Maria S. Merian expedition MSM44 and especially the bathymetry group for their assistance during the cruise. Furthermore, we thank Volkmar Damm and the crew and scientists of R/V Polarstern expedition ARK-XXV/3 for the good collaboration during the cruise. We acknowledge TGS for providing us with a bathymetric data grid and we thank Graeme Eagles for providing language help. Kelly A. Hogan and an anonymous reviewer are thanked for their thorough and very constructive comments and suggestions, which helped to improve the manuscript. Finally, we wish to thank the German Science Foundation (DFG) for providing ship time on R/V MARIA S. MERIAN.

5. Bedrock morphology reveals drainage network in northeast Baffin Bay

Patricia Slabon [a], Boris Dorschel [a], Wilfried Jokat [a,b], Francis Freire [c]

[a] Alfred Wegener Institute Helmholtz Centre for Polar and Marine Research, Am Alten Hafen 26, 27568 Bremerhaven, Germany

[b] University of Bremen, Department of Geosciences, Klagenfurter Straße, 28359 Bremen, Germany

[c] Geological Survey of Sweden (SGU), Villavägen 18, 751 28 Uppsala, Sweden

Submitted to *Geomorphology*, accepted 2017

Abstract

A subglacial drainage network underneath the paleo-ice sheet off West Greenland is revealed by a new compilation of high-resolution bathymetry data from Melville Bay, northeast Baffin Bay. This drainage network is an indicator for ice streaming and subglacial meltwater flow toward the outer shelf. Repeated ice sheet advances and retreats across the crystalline basement together with subglacial meltwater drainage had their impact in eroding overdeepened troughs along ice stream pathways. These overdeepenings indicate the location of a former ice sheet margin. The troughs inherit characteristics of glacial and subglacial meltwater erosion. Most of the troughs follow tectonic weakness zones such as faults and fractures in the crystalline bedrock. Many of these tectonic features correspond with the orientations of major fault axes in the Baffin Bay region. The troughs extend from the present (sub) glacial fjord systems at the Greenland coast and parallel modern outlet-glacier pathways. The fast flowing paleo-ice streams were likely accelerated from the meltwater flow as indicated by glacial landforms within and along the troughs. The ice streams flowed along narrow tributary troughs and merged to form large paleo-ice streams bedded in the major cross-shelf troughs of Melville Bay. Apart from the troughs, a rough seabed topography characterises the

bedrock, and we see a sharp geomorphic transition where ice flowed onto sedimentary rock and deposits.

Keywords

meltwater; glacial landform; drainage network; paleo-ice sheet

Highlights

- Overdeepened dendritic trough network in bathymetric data
- Troughs link to cross-shelf troughs and extend subglacially under the modern GIS
- Overdeepenings indicate former ice-sheet margin
- Deep troughs likely channel warm Atlantic water to the modern ice sheet.

5.1 Introduction

Today, the polar regions are more and more of public interest because of the increased mass loss and partial retreat of the glaciers (IPCC, 2013). With an area of ~1,710,000 km², the Greenland Ice Sheet (GIS) covers ~80% of the Greenland mainland that, if entirely melted, would contribute 7 m to global mean sea-level rise (IPCC, 2013). Since 2001, the average GIS ice-loss has accelerated significantly from 34 to 215 Gt/a (e.g. Enderlin et al., 2014; IPCC, 2013; Rignot et al., 2011), which equals the increase from 0.0952 to 0.602 mm/a of global sea-level rise. The negative ice sheet mass balance of the GIS is mainly controlled by dynamic thinning and calving caused by submarine melting from warm water inflow of the West Greenland Current (Rignot et al., 2010; Rignot et al., 2011; Thomas et al., 2009), together with an increased surface melt (Nghiem et al., 2012; Tedesco et al., 2013). Nevertheless, it remains unclear, how exactly the GIS will continue to respond to changing climatic conditions. Information about the responses of the GIS to past climate changes, e.g. since the Last Glacial Maximum (LGM), are therefore crucial to better model and understand the GIS behaviour in the future.

During past glacial cycles, the GIS experienced repeated advances and retreats across the continental shelf (Funder et al., 2011, and references therein) creating glacial landforms. The intensity and detailed development of the ice-sheet advances remains, however, uncertain. Most significant future response will likely be focused along the outlet glaciers that drain the GIS (Bennett, 2003). The marine-based glaciers on Greenland are channelled along deep troughs that are partly overdeepened below sea level under the modern ice sheet (Morlighem et al., 2014a) (Figs. 5.1, 5.2). This topography makes the GIS more vulnerable to submarine melting by warm Atlantic water inflow (Rignot et al., 2010; Rignot et al., 2011; Thomas et al., 2009) and thus susceptible to rapid ice sheet collapse (Schoof, 2010).

Future changes of GIS evolution may be predicted based on similarities to past ice-sheet behaviour that is recorded by glacial landforms (Stokes and Clark, 2001). Applying this premise in northern Greenland where it is mostly covered with ice would imply that the study of glacial landforms is best done on the ice-free submarine landscape where high-resolution bathymetric surveys can provide information of past glacial processes. However, the availability of high-resolution bathymetry is limited in the Melville Bay, northeast Baffin Bay, owing to its remote location. Few multibeam echosounder data exist at present that can be used to map the glacial imprint from past glacials on the West Greenland continental shelf (Dowdeswell et al., 2014; Freire et al., 2015; Funder et al., 2011; Gyllencreutz et al., 2016; Hogan et al., 2016; Jennings et al., 2014; Newton et al., 2017; Ó Cofaigh et al., 2013b; Roberts et al., 2009; Sheldon et al., 2016; Slabon et al., 2016).

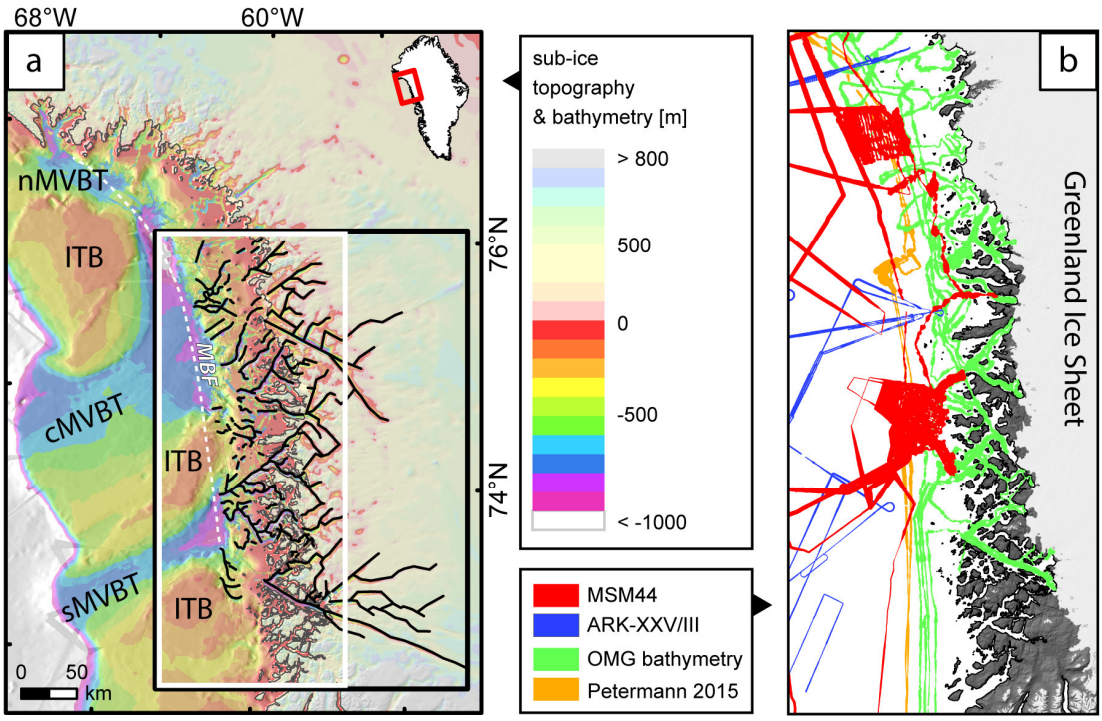

Figure 5.1: Overview of Melville Bay (northeast Baffin Bay) and adjacent Greenland sub-ice topography from Morlighem et al. (2014a). Note the large cross-shelf troughs (CSTs) and the related trough network (black) in continental shelf and sub-ice topography. Present day coastline is shown as a dark grey line. Dashed white line indicates location of the Melville Bay Fault (MBF) (Gregersen et al., 2013). nMVBT = northern Melville Bay CST, cMVBT = central Melville Bay CST, sMVBT = southern Melville Bay CST, ITB = inter-trough bank. White outline indicates location of Fig. 5.1b, black outline indicates location of Fig. 5.2. Fig. 5.1b: Coverages of used datasets. Bedrock topography in grey with Greenland Ice Sheet (GIS) coverage in white from GIMP (Howat et al., 2014). See section 5.2 for details. Note the wide gaps between datasets in the right figure.

Most previous studies concentrated on the analysis of glacial landforms within the glacial cross-shelf troughs. These studies indicate that the ice streams were active during the LGM when they likely reached the continental shelf edge (Dowdeswell et al., 2014; Hogan et al., 2016; Sheldon et al., 2016; Slabon et al., 2016).

This study provides a comprehensive compilation of the most recent high-resolution bathymetry from a previously almost unmapped part of Melville Bay, northeast Baffin Bay. As former studies did focus merely on a relatively small part of crystalline bedrock in Melville Bay (Freire et al., 2015; Gyllencreutz et al., 2016), we could show here, based on additional data, that the inferred trough system extends far across the inner shelf toward the modern Greenland Ice Sheet. Three areas with dense high-resolution bathymetric data coverage located adjacent to the cross-shelf troughs are selected for further analysis

(Figs. 5.1b, 5.2). They show different characteristics of the trough system that we interpret are related to morphology and the impact of glaciofluvial erosional forces. The data presented here show a more detailed picture of the crystalline bedrock on the inner continental shelf that allows a more detailed analysis of its morphology in terms of glacial and fluvial landforms.

5.1.1 Regional setting, geomorphology and geology

5.1.1.1 Melville Bay Bathymetry

Melville Bay is located on the northeast part of the Baffin Bay, an ~650,000 km² basin between Canada and Greenland. Recent high-resolution multibeam echosounder surveys (Freire et al., 2015; Gyllencreutz et al., 2016; Slabon et al., 2016), partly combined with seismic data (Newton et al., 2017), reveal detailed seafloor topography. High-resolution bathymetric data collected during the NASA Oceans Melting Greenland (OMG) mission in 2015 (OMG-Mission, 2016) supplement the datasets close to the coast and in most of the accessible fjords of West Greenland (Fenty et al., 2016; Morlighem et al., 2016). The glaciers bordering these coastal areas are likely influenced by the inflow of warm Atlantic water to their base, similar to the glaciers in the fjords of central West Greenland (Rignot et al., 2012; Rignot et al., 2015; Rignot et al., 2016; Rignot et al., 2010; Rignot et al., 2011). There, the topography channels warm water into the fjords. The topography of the newly mapped region in Melville Bay may have similarly influenced ice behaviour and enhanced glacial retreat along the troughs during past interglacial periods and since the LGM. The characteristic troughs that may have acted as passages for ice and meltwater, but also warm Atlantic water, need further investigation for glacial and fluvial landforms. Glacial and fluvial landforms indicate the presence of former ice streams with subglacial meltwater at their base. The processes forming glacial landforms are still unresolved. However, an accepted theory is that they develop by subglacial erosion, such as abrasion and quarrying, when ice and subglacial meltwater loaded with sediments slide over bedrock (e.g. Glasser and Bennett, 2004). More common are depositional and deformable landforms, where ice and meltwater are thought to form e.g. sedimentary tails behind bedrock bumps such as crag-and-tails, or mega-scale glacial lineations along the ice-stream path (e.g. Clark, 1993; King et al., 2009; Spagnolo et al., 2014; Stokes et al., 2011; Stokes et al., 2013). These landforms may show the (re-)orientation of ice streams across and along major obstacles or passages (e.g. Jakobsson et al., 2012a; Klages et al., 2015; Margold et al., 2015; Ó Cofaigh et al., 2010). However, they may not directly indicate warm water inflow, as could analysis of specific foraminifera picked from sediment

samples (e.g. Jennings et al., 2017a; Jennings et al., 2017b; Jennings et al., 2011) that we do not focus on here.

5.1.1.2 Coastal Geology

The coast of Melville Bay is characterised by a cratonic basement (Knutz et al., 2015) consisting of crystalline, gneiss-based Archaean and reworked (Paleo-) Proterozoic rock (Freire et al., 2015; Gyllencreutz et al., 2016; Harrison et al., 2011; Whittaker et al., 1997). On land, the basement is partly overlain by Paleoproterozoic metaturbidite sediments of the Karrat Group (Steenfelt et al., 1998). The crystalline basement east of the Melville Bay Fault (Fig. 5.1a) is characterised by a scoured and fractured, partly hilly relief associated with a typical 'knock-and-lochan' morphology of knolls and basins as indicated similarly for a relatively small region (~220 km²) in Melville Bay (Fig. 5.2) (Freire et al., 2015; Gyllencreutz et al., 2016). This landscape is likely caused in part by stripping of weak saprolite from weathering during pre-Quaternary uplift above sea level (e.g. Bonow, 2005; Bonow et al., 2006a; Bonow et al., 2006b; Bonow et al., 2007; Japsen et al., 2006). The morphology is furthermore associated with subsequent reshaping from deep glacial and fluvial erosion (Krabbendam and Bradwell, 2014; Krabbendam and Glasser, 2011). This eroded basement continues from the coast up to 100 km seaward to the steeply dipping (up to 40°) Melville Bay Fault (Fig. 5.1a).

The overall geology below the seafloor of Melville Bay and the entire northern Baffin Bay shows several faults related to horst and graben structures and a sub-parallel inverted halfgraben (Harrison et al., 2011). They result from rifting, tilting, uplift, and subsidence of tectonic blocks during the opening of Baffin Bay in the late Mesozoic to early Cenozoic (Chalmers and Pulvertaft, 2001; Gregersen et al., 2013; Whittaker et al., 1997). Some of the tectonic blocks of West Greenland may have been sub-aerially exposed during those rifting phases (Bonow et al., 2007). Among the tectonic grabens is the Melville Bay Graben that is located west of the Melville Bay Fault (Fig. 5.1a). It aligns parallel to the coast and marks the transition from the crystalline bedrock to the Mesozoic and Cenozoic sedimentary sequences (Gregersen et al., 2013; Knutz et al., 2015). At the Melville Bay Fault, the crystalline basement is downthrown to the west and buried beneath sedimentary successions of Miocene to Pleistocene age that are up to 9-11 km thick in the Melville Bay Graben (Altenbernd et al., 2014, 2015; Knutz et al., 2015). For the continental shelf of southwest Melville Bay, models indicate ~5 km of sedimentary successions on top of the crystalline crust (Suckro et al., 2012). Most of these successions are of glacial and glaciofluvial origin with sedimentation intensified since GIS expansion between 3.3 and 2.7 Ma ago (Jansen et al., 2000; Knutz et al., 2015). Erosion by currents as well as glacial activity reworked the sedimentary deposits in Melville Bay (Knutz et al., 2015).

Three large paleo ice-stream cross-shelf troughs (Fig. 5.1a) characterise the topography in Melville Bay (Batchelor and Dowdeswell, 2014; Slabon et al., 2016). They stretch across the continental shelf from the Melville Bay Fault to the shelf edge and are separated by shallow inter-trough banks (Fig. 5.1a). The troughs are 45-120 km wide, 170-320 km long, and up to 1100 m deep. Each has a reversed topographic profile (Slabon et al., 2016) and is deepest close to the Melville Bay Fault. Glacial landforms in the cross-shelf troughs indicate that they have been completely occupied by grounded ice-streams during several glaciations (Slabon et al., 2016). This resulted in an intense isostatic adjustment of the continental crust in West Greenland that is still deforming and reacting to the glacial load (e.g. Groh et al., 2014). During the slow to episodic retreat from the shelf edge, the ice streams deposited glacial landforms such as moraines and grounding-zone wedges (Slabon et al., 2016).

The Nussuaq Basin around Disko Bay is a volcanically-influenced region. Its centre is located ~400 km south of Melville Bay. During opening of Baffin Bay (~65 Ma ago), flood basalts spread across the seafloor in a huge area stretching from south of Disko Island up to the southern Melville Bay (Fig. 5.5a) (Gregersen et al., 2013). This area of flood basalts is ~500 km long and 40-160 km wide (Harrison et al., 2008; Harrison et al., 2011; Whittaker et al., 1997). The associated volcanoes were active during the early Palaeocene and the preserved associated flood basalt sequences in the Disko Bay region, south of Melville Bay, are between 1 and 5 km thick (Storey et al., 1998). These volcanic sequences belong to the West Greenland Tertiary Volcanic Province (Buchan and Ernst, 2004).

Figure 5.2: Overview of the trough network in Melville Bay bathymetry (this study) and Greenland sub-ice topography from Morlighem et al. (2014). Note the network of deep troughs at the seafloor that extends under the Greenland Ice Sheet within the sub-ice topography. For location, see black box in Fig. 5.1a. Boxes indicate location of associated Figs. 5.3-5.5. Box with hachures indicates location of study area from Freire et al. (2015) and Gyllencreutz et al. (2016). Faint coloured background bathymetry is from IBCAO v. 3.0 (Jakobsson et al., 2012).

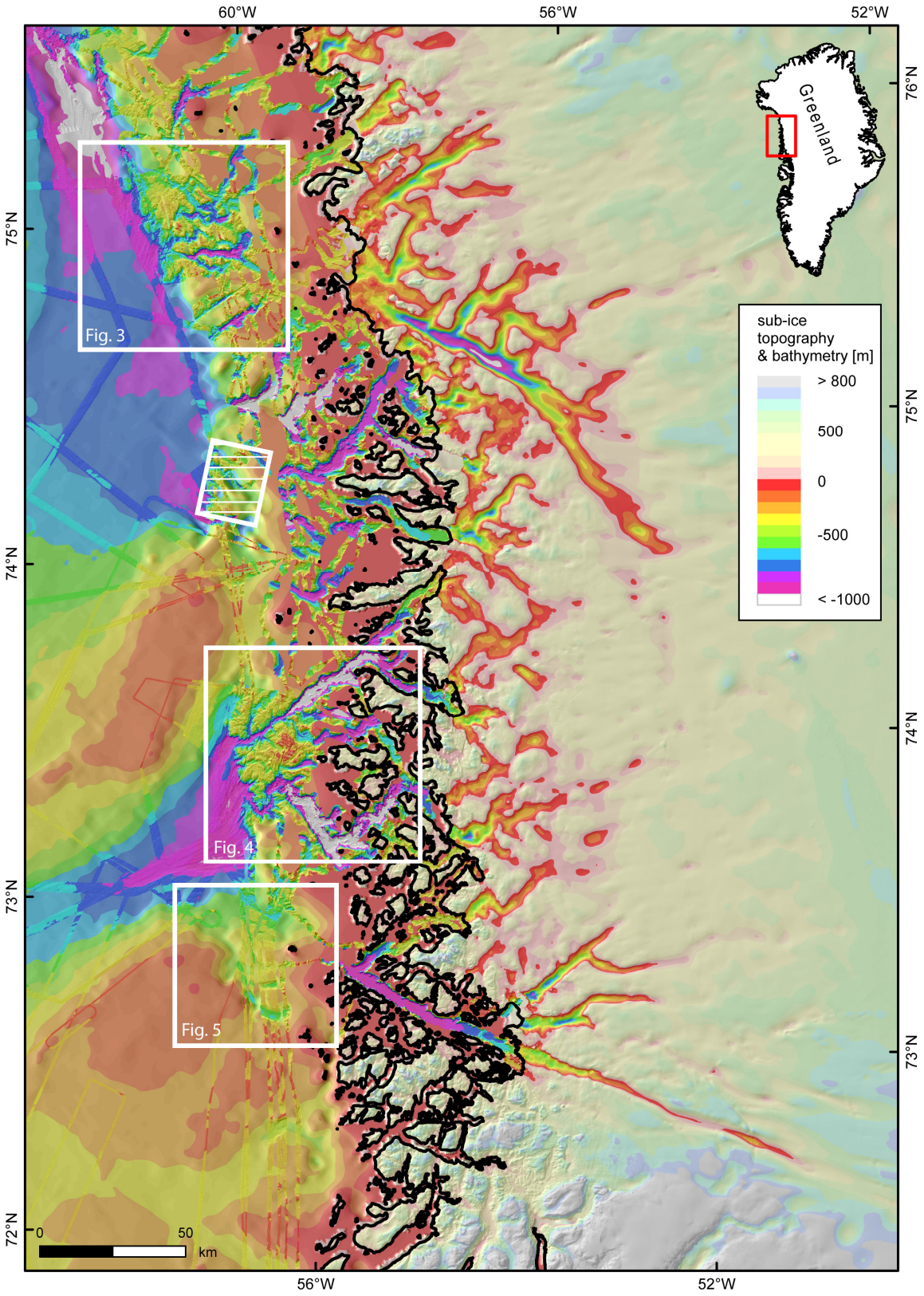
60°W
56°W
52°W
76°N
75°N
74°N
73°N
72°N
Greenland
Fig. 3
Fig. 4
Fig. 5
sub-ice
topography
& bathymetry [m]
> 800
500
0
-500
< -1000
0
50
km

5.2 Material and methods

The high-resolution bathymetric data sets compiled in this study (Fig. 5.1b) were acquired during four research cruises in the past 7 years. Bathymetric surveys were conducted during *RV Maria S. Merian* expedition MSM44 in July 2015 using a Kongsberg multibeam echosounder EM122 (12 kHz, 2°x2° beam width, 130-150° swath angle, equidistant mode) (Dorschel et al., 2015) and *RV Polarstern* expedition ARK-XXV/3 in summer 2010 using an Atlas Hydrographic Hydrosweep DS-2 (15.5 kHz, 2°x2.3° beam width, 90-120° swath angle, equidistant mode) (Damm, 2010). Further data were acquired during *RV Oden* 'Petermann expedition' in summer 2015 using a Kongsberg multibeam echosounder EM122 (12 kHz, 2°x2° beam width, 130-150° swath angle, equidistant mode) (Department of Geological Sciences, Stockholm University) and NASA OMG mission using the portable Teledyne Reson SeaBat 7160 multibeam echosounder system (44 kHz, 1.5°x2° beam width, 150° swath angle, equidistant mode) on board *RV Cape Race* in summer 2015 (OMG-Mission, 2016). The data were individually processed and compiled as separate xyz grid files with 10 to 25 m resolution. They were then gridded to a merged grid of 10 m (partly artificial) resolution. The shaded relief illumination of bathymetry and topography in all figures is from northwest (azimuth 315°, altitude 45°). As background data, the IBCAO v.3.0 grid is used (Jakobsson et al., 2012b). Sub-ice topography is taken from Morlighem et al. (2014a) and provided at 150 m resolution. The ice surface is from the Greenland Ice Mapping Project digital elevation model (GIMP DEM), in 90 m resolution (Howat et al., 2014). Sediment echosounder data were collected simultaneously with multibeam echosounder data during expeditions MSM44 and ARK-XXV/3 using the Parasound P70 system (Damm, 2010; Dorschel et al., 2015).

Based on available multibeam echosounder data coverage, three study areas were selected (Figs. 5.1b, 5.2). The new, high-resolution bathymetric data cover large parts of the inner continental shelf of Melville Bay from the coast to the Melville Bay Fault (Fig. 5.1a). They complement the IBCAO v.3.0 grid that lacks data in this part of the bay. The grids were analysed using ESRI ArcMap to identify glacial landforms and geological features. The landforms in the three predefined study areas were manually digitised and analysed using the standard ESRI raster computation tools for slope angles, elevations, and depressions. The NRCAN (2159A) map from Harrison et al. (2011) was used to compare landforms to larger geological structures. The projection EPSG 3413, NSIDC Polar Stereographic North was used for the project.

5.3 Results

5.3.1 Troughs and channels

An extensive drainage network of dendritic and partly meandering troughs that cut into the crystalline bedrock characterises the coast of Melville Bay. Most troughs' cross-profiles close to the coast are U-shaped or flat floored with steep, partly asymmetric walls (20-65°) (Figs. 5.3c, 5.4c, 5.5b), similar to glacial troughs. The troughs become narrower and more V-shaped toward the outer shelf (e.g. Fig. 5.4c, line h-h' and f-f'). Where troughs strike oblique to the former ice-streaming direction, one wall is often steep and quarried while the other is rather smooth (Figs. 5.3a, 5.3c, 5.3e, 5.4a, 5.4c, 5.4e).

At the transition to the sedimentary strata, few linear channels of similar size to the troughs occur that are entirely V-shaped (Figs. 5.3a, 5.3b, lines B-B', C-C'). For differentiation, we call them channels instead of troughs. The channels are similarly overdeepened and seem to initiate and terminate abruptly or have only small and narrow meandering tributaries (Fig. 5.3a).

In the northern and central study areas (Figs. 5.3, 5.4), the drainage network shows sinuous troughs and few linear channels fed by shallow tributaries, similar to glacial hanging valleys. The undulating, stepped thalwegs of the troughs and channels are partly reversed, with a major overdeepening (300-500 m deep) ~50 km from the coast. From this point farther seaward, thalwegs of the troughs and channels rise again while the cross-profiles of the troughs narrow to a V-shape (Figs. 5.3, 5.4). At the transition from crystalline basement to sedimentary rocks and deposits at the Melville Bay Fault, they terminate. There, the troughs and channels add to the wide main trunk of the cross-shelf trough. In the southern area (Fig. 5.5), the drainage network varies compared to the other areas. There, the troughs have a similar but shallower thalweg with overdeepened basins (~150 m deep). The troughs show several elongated terraces cut into relatively smooth and low-relief bedrock (150-400 m). Those terraces are 20-60 m apart in elevation, 200-500 m wide and stretch along the walls (Figs. 5.5d-f).

In plan view, the troughs and channels in all three study areas generally trend SW or NW with minor variations, revealing a slightly rectangular pattern (Figs. 5.1-5.5). Across the bedrock, they connect with the outlet glaciers along the modern Greenland coastline and with the large Melville Bay cross-shelf troughs (Figs. 5.1, 5.2). Furthermore, the drainage network shows more significant sediment infill near the modern coast that results in the flat seafloor along most of the troughs and U-shaped cross profiles (Fig. 5.4f).

Table 5.1: Troughs and channels of the drainage network

Study area	Width (m)/ Length (m)/ Depth (m)/ Water depth (m)	profile	main orientation (plan view)	Description
north	2,000-4,000/ 20,000/ 350-700/ 150-950	overdeepened profile, shallow near the fault	NW, W, SW	flat floored, U-shaped, steep walls, some also V-shaped, linear and sinuous
central	1,500-5,000/ 8,000-100,000/ 200-500/ 150-1,300	overdeepened profile, shallow near the fault	NW, SW, S	flat floored, U-shaped, linear and sinuous, in parts V-shaped
south	3,000-5,000/ >30,000/ 150-350/ 150-650	overdeepened profile, shallow near the fault	N, NW, W	U-shaped, overdeepened on the inner shelf, V- shaped on the low-relief bedrock; small terraces alongside the trough-axes, sinuous

Figure 5.3: Northern study area. Geomorphological interpretation of the crystalline bedrock adjacent to the central Melville Bay cross-shelf trough. Dashed black lines show location of cross sections presented in Figs. 5.3b and 5.3c. Fig. 5.3b: Lines A-C show the long profiles with overdeepenings of the major troughs and channels. Fig. 5.3c: Lines a-g show the U- and V-shaped cross profiles of the troughs and channels. Scales are in metres. Note the different scales. Fig. 5.3d: Identified fractures, crag-and-tails and mega-scale glacial lineations (MSGLs) and location of flow marks. Black square indicates location of figure 5.3e. Fig. 5.3e: Example of abraded and quarried landforms. Background is IBCAO v. 3.0 (Jakobsson et al., 2012) in fainted colours, similar to high-resolution bathymetry.

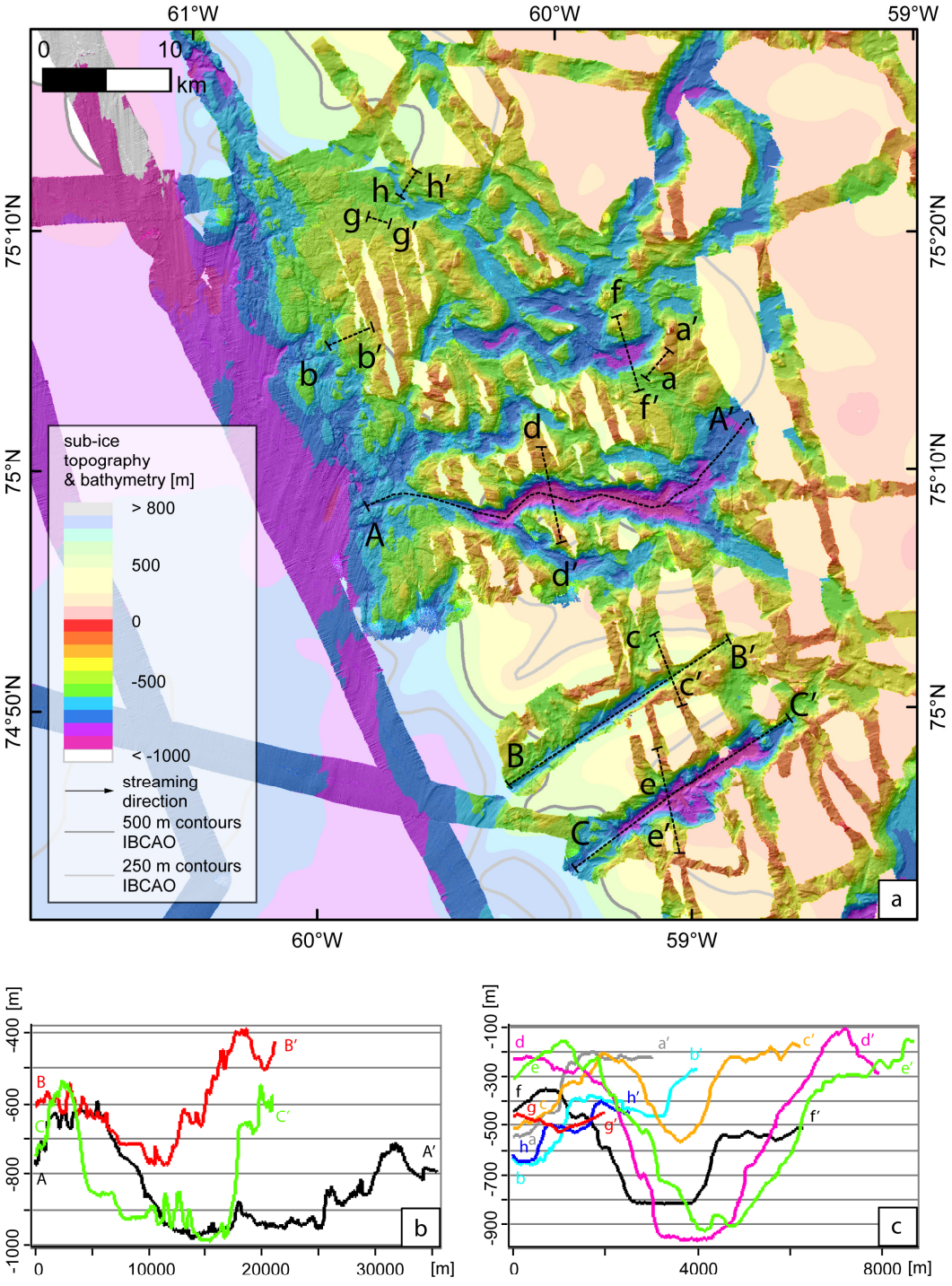
61°W
60°W
59°W
75°10'N
75°N
74°50'N
75°20'N
75°10'N
75°N
0
10
km
sub-ice
topography
& bathymetry [m]
> 800
500
0
-500
< -1000
streaming
direction
500 m contours
IBCAO
250 m contours
IBCAO
A
A′
B
B′
C
C′
a
a′
b
b′
c
c′
d
d′
e
e′
f
f′
g
g′
h
h′
a
b
c
d
e
f
g
h
-400 [m]
-600
-800
-1000
0
10000
20000
30000
[m]
-100 [m]
-300
-500
-700
-900
4000
8000 [m]

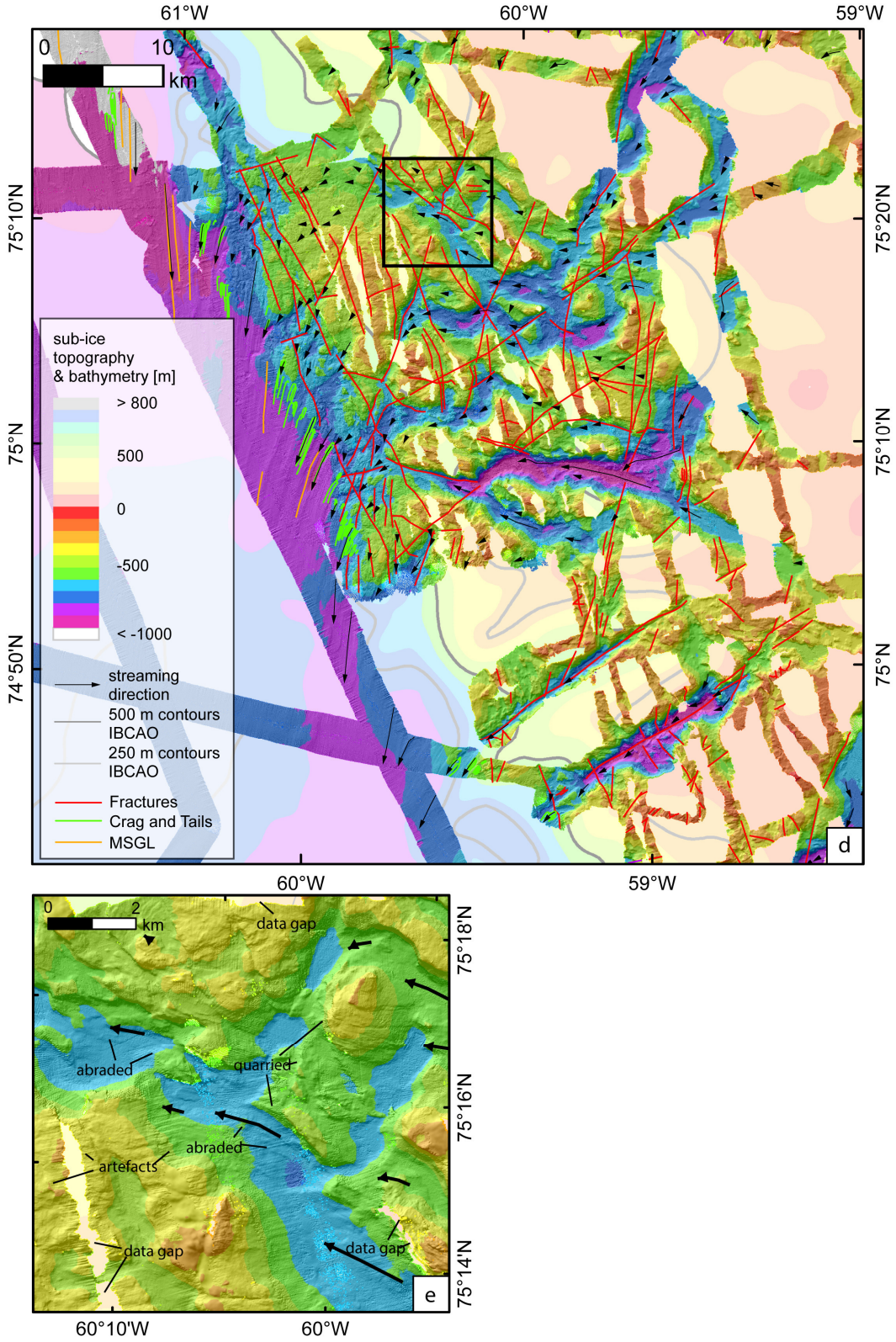
61°W
60°W
59°W
75°10'N
75°N
74°50'N
75°20'N
75°10'N
75°N
0
10
km
sub-ice
topography
& bathymetry [m]
> 800
500
0
-500
< -1000
streaming
direction
500 m contours
IBCAO
250 m contours
IBCAO
Fractures
Crag and Tails
MSGL
d
60°W
59°W
0
2
km
data gap
75°18'N
75°16'N
75°14'N
abraded
quarried
abraded
artefacts
data gap
data gap
e
60°10'W
60°W

5.3.2 Lineaments

Lineaments are any mappable linear or slightly curvilinear surface expressions that differ distinctly from adjacent features (O'Leary et al., 1976). In this study, lineaments are expressed as fractures and faults in the bedrock (Figs. 5.3c, 5.3d, 5.4d, 5.5e), similar to the definition for the bedrock expressions in the study area of Freire et al. (2015) in central Melville Bay (Fig. 5.2). Therefore, they differ from the expression of the troughs and channels described above. The coastal part of Melville Bay mainly consists of crystalline basement with low relief that is clearly identifiable as rough and rugged, rocky seafloor as seen from the bathymetric data (Fig. 5.2). The crystalline basement shows a highly fractured surface (Figs. 5.3b, 5.4b, 5.5b). The fractures are 10-120 m deep incisions (e.g. Fig. 5.3c, line g-g'), 1-24 km long, 100-1000 m wide and occur in a wide depth range from 100-1150 m. The fractures are generally straight linear to slightly sinuous. They are oriented in four main directions N, NW, W, and NE that are inclined parallel and sub-parallel to major Baffin Bay faults (Harrison et al., 2011). Some troughs and channels are partially bedded along the axes of pre-existing fractures of the basement. There, erosion further deepens and widens the bed. Apart from the troughs and channels that bend toward the CST, the fractures continue straight within the shallow, low-relief part of the bedrock, (Figs. 5.3d, 5.4d).

Figure 5.4: Central study area. Geomorphological interpretation of the crystalline bedrock adjacent to the southern Melville Bay cross-shelf trough. Dashed black lines indicate the location of cross sections. Fig. 5.4b: Lines I and II indicate the long profiles of the major troughs. Note the overdeepenings. Fig. 5.4c: Lines a-i show the U- to V-shaped cross profiles of the major troughs. Note the different scales between the diagrams. Fig. 5.4d: Identified fractures, crag-and-tails, MSGLs and location of flow marks. Fig. 5.4e: Cross section z-z' shows the sub-bottom profile of the large trough in the north.

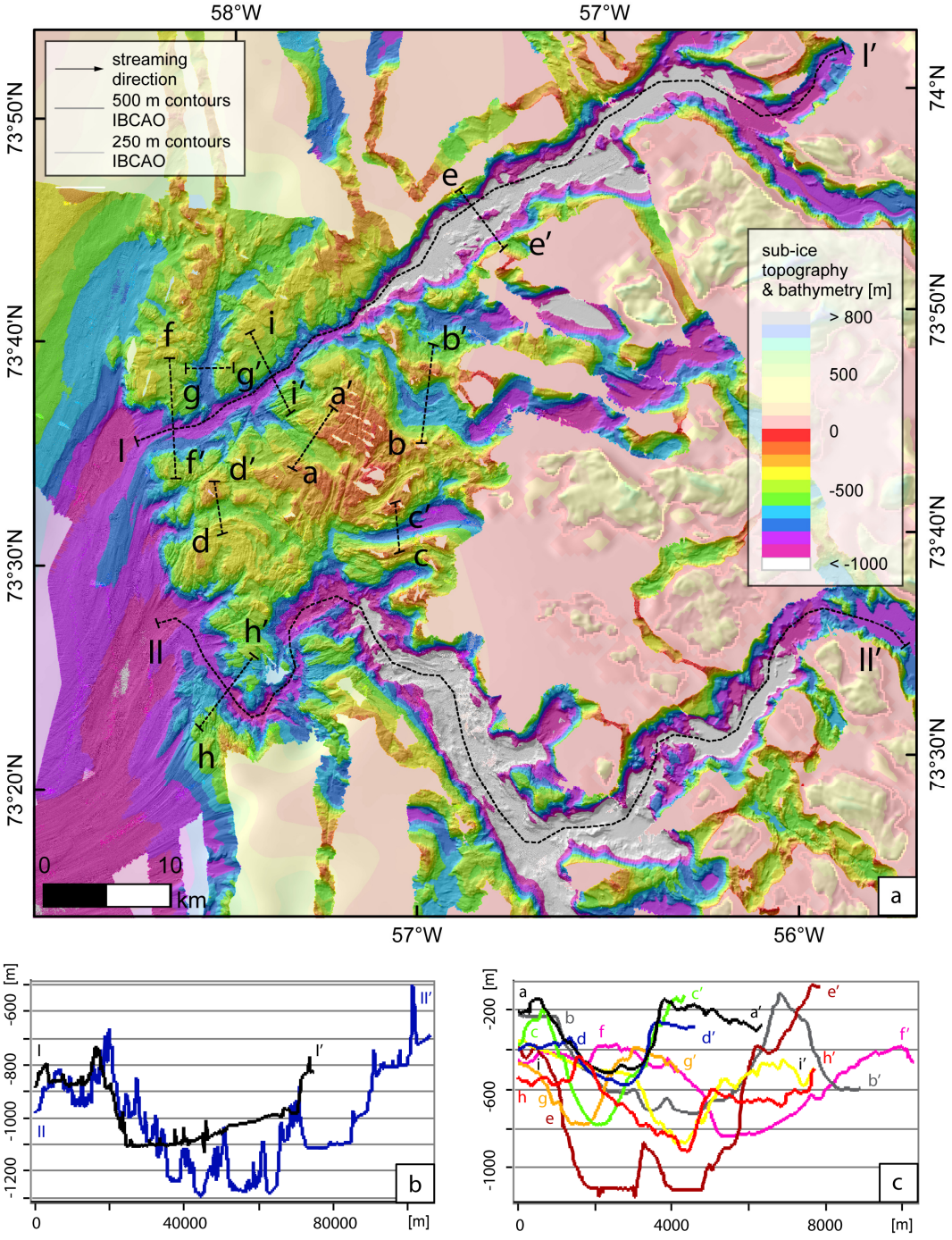
58°W
57°W
56°W
73°50'N
73°40'N
73°30'N
73°20'N
74°N
streaming direction
500 m contours IBCAO
250 m contours IBCAO
sub-ice topography & bathymetry [m]
> 800
500
0
-500
< -1000
0
10
km
a
b
-600
-800
-1000
-1200
[m]
40000
80000
c
-200
-600
-1000
4000
8000

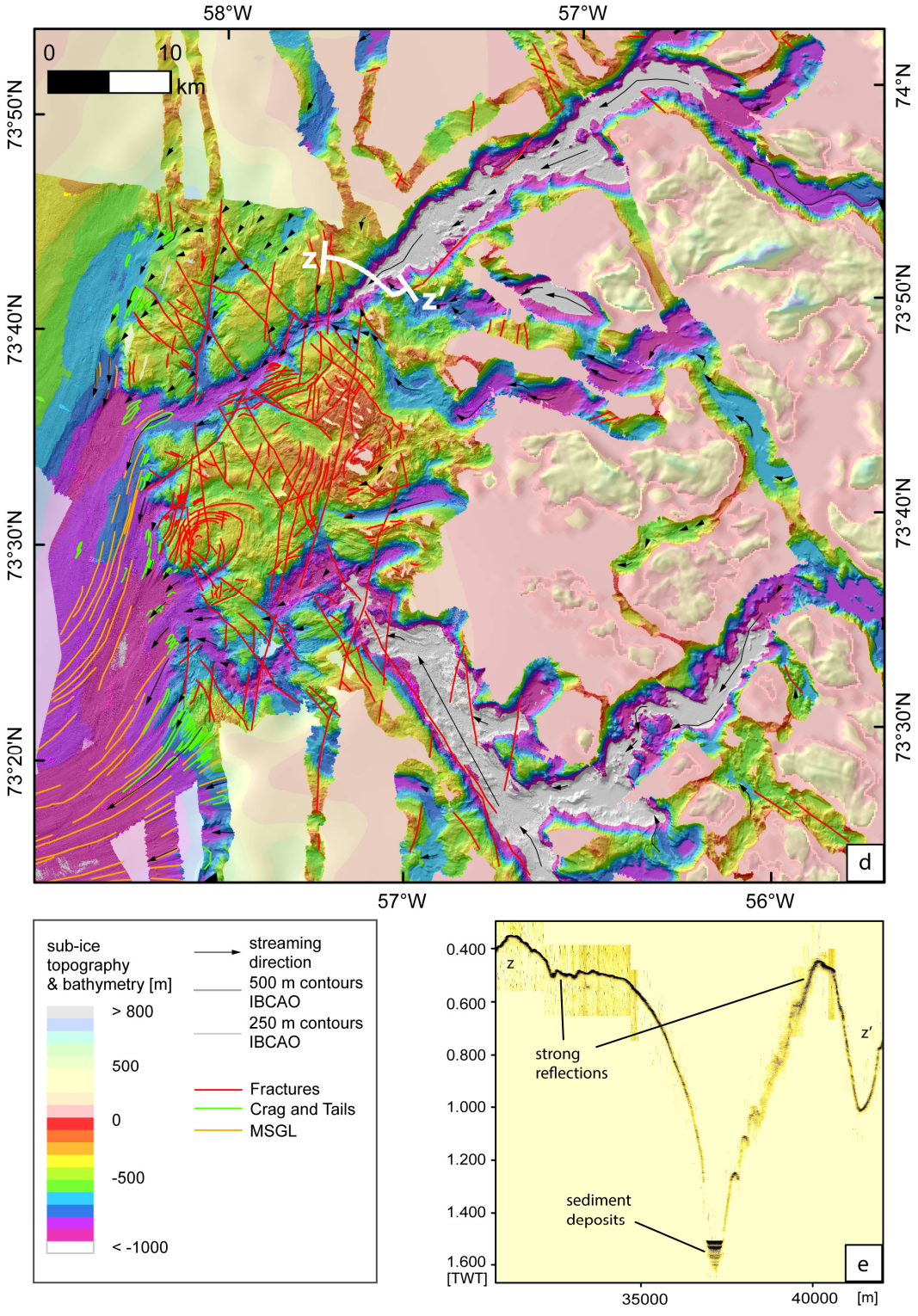
58°W
57°W
0
10
km
73°50'N
73°40'N
73°30'N
73°20'N
74°N
73°50'N
73°40'N
73°30'N
z
z'
d
57°W
56°W
sub-ice topography & bathymetry [m]
> 800
500
0
-500
< -1000
streaming direction
500 m contours IBCAO
250 m contours IBCAO
Fractures
Crag and Tails
MSGL
0.400
0.600
0.800
1.000
1.200
1.400
1.600
[TWT]
z
z'
strong reflections
sediment deposits
e
35000
40000
[m]

5.3.3 Landforms as flow marks

The bedrock of Melville Bay is highly eroded by glacial activity. Glacial landforms that indicate fast ice flow (e.g. as part of crag-and-tails and mega-scale glacial lineations) are found on the mid to outer continental shelf or are confined to the troughs and channels close to active glaciers along the modern coastline (Figs. 5.1a, 5.2). These landforms however are not commonly seen on bedrock. The landforms observed in our data are the small abraded or quarried landforms like streamlined hills (crag-and-tails, whalebacks) or stoss-and-lee forms (roche moutonnées) and overdeepened rock basins that are part of the troughs and channels within the drainage network. Abraded, streamlined hills (Fig. 5.3e) are described as smooth, rounded, and slightly elongated ridges, carved out of the bedrock. Roche moutonnées-type landforms show a smooth, partly rounded stoss side and a quarried lee side (Fig. 5.3e). Most features could be clearly identified within the drainage networks, while a few are also preserved on the shallow jointed bedrock, in shallow but wide bedrock depressions (Figs. 5.3c, 5.4c). Some regions inherit no significant features. Most streamlined landforms are oriented parallel to the troughs and channels in which they are located (Figs. 5.3d, 5.4d) and taper seaward. Inshore of the Melville Bay Fault, some crag-and-tails are oblique to the drainage network, or occur independent to it, also tapering seaward (Figs. 5.3d, 5.4d). These glacial landforms indicate that paleo-ice and meltwater flow was toward the bay. In the southern study area (Fig. 5.5e), similar flow marks are widely absent. There, the meandering form with intervening, pointing bars of the troughs is indicative of flow direction (Fig. 5.5e).

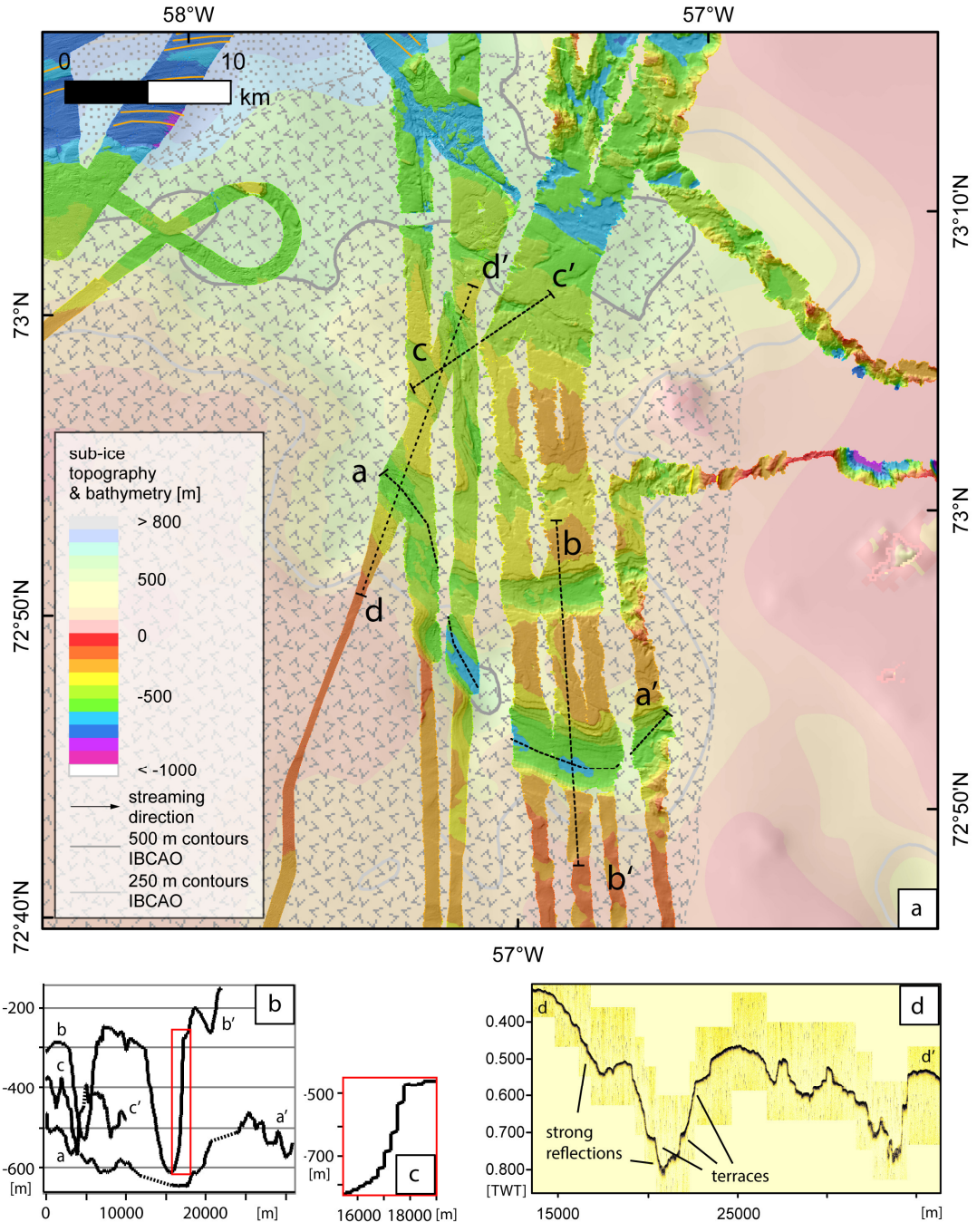
58°W
57°W
0
10
km
73°10'N
73°N
72°50'N
72°40'N
sub-ice
topography
& bathymetry [m]
> 800
500
0
-500
< -1000
streaming
direction
500 m contours
IBCAO
250 m contours
IBCAO
a
b
c
d
a′
b′
c′
d′
a
b
-200
-400
-600
[m]
0
10000
20000
[m]
-500
-700
[m]
16000
18000
[m]
c
d
0.400
0.500
0.600
0.700
0.800
[TWT]
strong
reflections
terraces
15000
25000
[m]

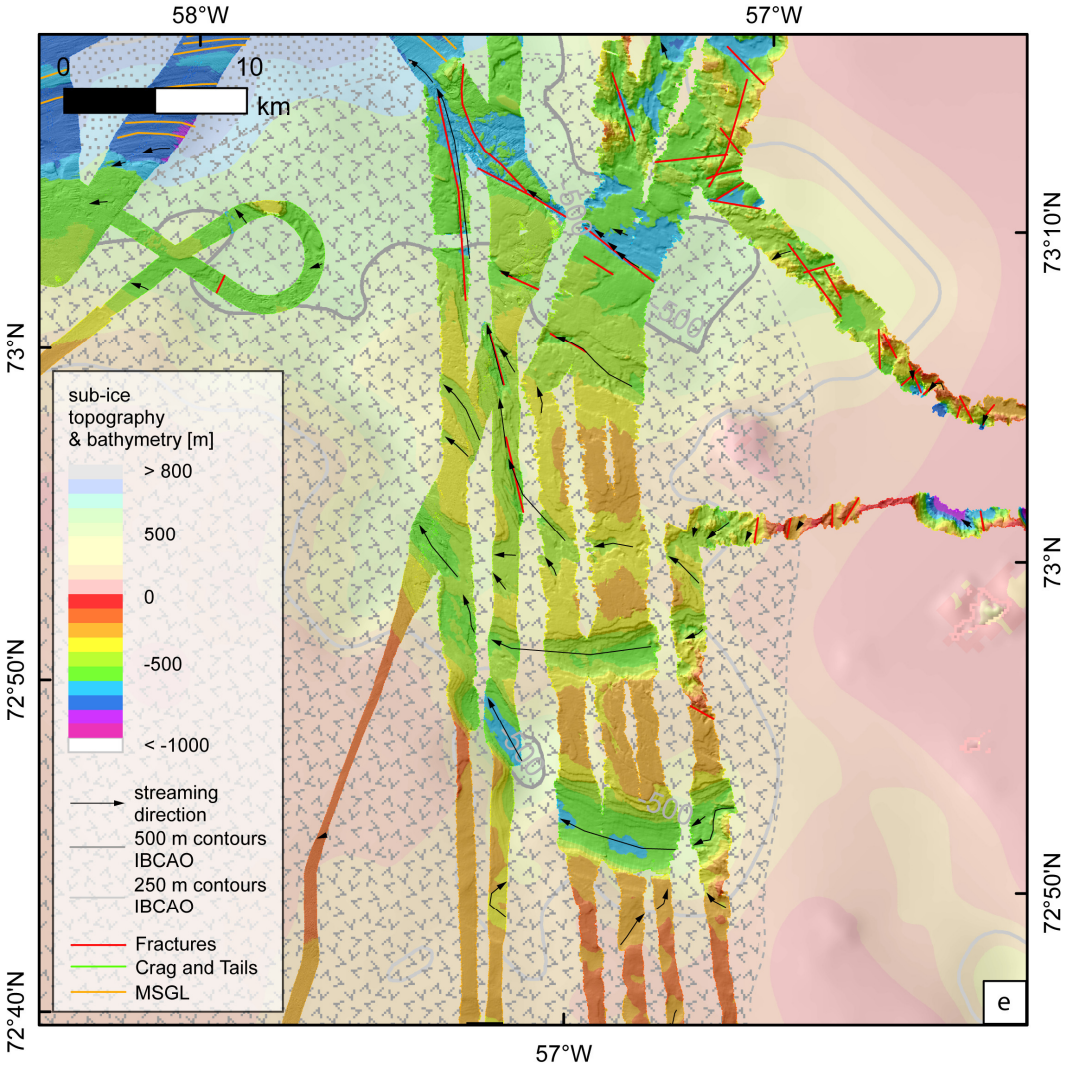

Figure 5.5: Southern study area. Geomorphological interpretation of the crystalline bedrock adjacent to the southern Melville Bay cross-shelf trough. Smooth troughs with terraces in the seafloor. Grey dotted area in the upper part is sedimentary strata that are Cretaceous and younger (145.5-0.0 Ma). Grey ornaments in the area below indicate outcrop of mafic extrusive rocks of Paleocene and Eocene (63.5-33.9 Ma) age, characteristic for Paleogene flood basalts from the Nussuaq Basin in central West Greenland. The area with no marks indicates Archaean and Paleoproterozoic (4000-1600 Ma) metamorphic, undivided crystalline rocks. This background information is from Harrison et al. (2011). Dashed black lines indicate along and across profiles of the troughs presented in Figs. 5.5b-d. Fig. 5.5b: long profiles and cross sections of the troughs. Fig. 5.5c: Note the escarpments in the red box indicating terraces. Fig. 5.5d: The sub-bottom profile d-d' shows the lack of sediments and strong reflections from the sea bed. The seafloor in this area is interpreted as flood basalts. Fig. 5.5e: Identified fractures and MSGLs, and location of flow marks across the seafloor.

5.4 Discussion

5.4.1 Eroded Bedrock topography

The shallow, low-relief bedrock topography between the troughs and channels with its partly abraded and quarried knolls (low hills) and lochs (basins) in the form of, e.g., roche moutonnées (Fig. 5.3e) and bedrock gouges fits to the description of a region of areal scour (Glasser and Bennett, 2004) also called 'knock-and-lochan' morphology (Krabbendam and Bradwell, 2014, and references therein). When this part underwent pre-Quaternary uplift above sea level, as suggested for the adjacent central West Greenland coast, chemical and physical weathering likely had a strong contribution in moulding this landscape (Bonow, 2005; Bonow et al., 2006a; Bonow et al., 2006b; Bonow et al., 2007; Japsen et al., 2006). Thus, as the crystalline basement of Melville Bay mainly consists of granite and gneiss, the rough knock-and-lochan morphology with its initial overdeepenings along fracture zones, is likely eroded by stripping of weak pre-glacial saprolite from the Paleocene. After subsequent subsidence of the basement block, glaciofluvial erosion and reshaping to highly overdeepened troughs and channels occurred along the faults and fracture zones as similarly suggested for parts of central West Greenland (Bonow, 2005; Bonow et al., 2006a; Bonow et al., 2006b; Bonow et al., 2007; Japsen et al., 2006) but also other regions, e.g., Scotland (Krabbendam and Bradwell, 2014; Shaw, 1997). Freire et al. (2015) and Gyllencreutz et al. (2016) came to a similar conclusion for their survey area on the bedrock in central Melville Bay (Fig. 5.2).

5.4.2 Re-occupied drainage network

The bedrock area is crossed by a network of dendritic troughs. Near the coast, they inherit more characteristics of glacial troughs, whereas, near the sharp geomorphic transition onto sedimentary rock, they fit to the definition of large subglacial meltwater channels from Glasser and Bennett (2004). As the bedrock suffered pre-glacial erosion (Bonow, 2005; Bonow et al., 2006a; Bonow et al., 2006b; Bonow et al., 2007; Japsen et al., 2006), the channels and troughs are likely the result of glaciofluvial widening and deepening along exploited fracture zones that previously may have hosted a pre-glacial river system, as similarly suggested by Freire et al. (2015) for their study area in Melville Bay. A pre-glacial river system has been previously suggested for Melville Bay by Funder et al. (1989), Sommerhoff (1979) and Weidick and Bennike (2007). This paleo-river could be one explanation for the initial V-shape of some parts of the troughs and channels, as well as their partly meandering path across the bedrock. Similar suggestions have been drawn e.g. for parts of southern Norway (Bonow et al., 2006b).

However, the overdeepenings of the troughs and channels, follow the general assumptions from Alley et al. (2003) for the bed of highly erosive ice streams. The well

preserved narrow, V-shaped, and steeply rising down-ice profile of the troughs at the transition to the sedimentary rock indicates flow of supercooled meltwater that is below its freezing point and that developed under high pressure of the overlying ice. This supercooling of the meltwater at the steep seaward slope likely restricted further seaward erosion, as it tends to refreeze under reduced pressure. However, simultaneous up-ice erosion by ice and sediment-laden meltwater produced further overdeepening and, thus, an increase of the gradient of the reverse slope (Alley et al., 2003).

We therefore suggest that also the abruptly initiating V-shaped channels (Fig. 5.3a) have been similarly occupied by ice streams with subglacial meltwater flow at its base. We furthermore suggest that they are supplied by meltwater flow through glacier crevasses and moulins near the paleo ice-sheet margin that were in part responsible for the abrupt initiation. Similar conclusions have been drawn for ice-marginal subglacial channels in Sweden described by Kleman (1994) and Glasser and Bennett (2004). There, like most linear trending channels in Melville Bay, the V-shaped channels are oriented along bedrock fractures. This is consistent with results of studies from several glaciated regions, e.g., Ellesmere Island, on the opposite side of Baffin Bay. The authors of those studies came to the similar conclusion that the orientations of fjords and valleys are closely related to structural lineaments and intrusions (England, 1987; Glasser and Ghiglione, 2009; Nesje and Whillans, 1994).

Furthermore, caused by high ice discharges, overdeepenings also often form at the junctions of tributary troughs or narrowings of their cross profile (Løken and Hodgson, 1971), which in Melville Bay generally is also the case (Figs. 5.3a, 5.4a, 5.5a). Tributaries often occur as shallow hanging valleys, when they are less eroded than their adjacent main trunks. Once a glacier has started to erode a main trough, erosion occurs more quickly along that trough as a result of faster ice flow and greater pressure and hence more basal melting at its bed.

The supercooling of meltwater with subsequent overdeepening of the troughs and channels often occurs near the ice-stream margin. This lets us infer that the ice streams stabilized in this position over long timescales or repeated glacial cycles to produce such overdeepenings in resistant bedrock. As all those major overdeepenings occur in a range of 50 km from the modern coast, we suggest an overall ice-sheet margin stabilization on the crystalline bedrock. Nevertheless, the extensive trough network incised into bedrock is expected to be the product of several glaciations with abundant flow of subglacial meltwater and persistent ice-sheet coverage. We therefore suggest that glacial erosion from repeated ice-sheet advances and retreats across the continental shelf, possibly since the Pliocene as proposed for southwest Greenland (Nielsen and Kuijpers, 2013), were likely responsible for the overdeepened incisions along the troughs and channels.

The high concentration of meltwater channels in this region is likely the result of low permeability of the crystalline bedrock that leads to deep erosion, but perhaps also as a result of the high preservation potential of landforms eroded into crystalline bedrock. Variations in channel morphology might be the result of variable impermeability and resistance of the bed as seen in Amundsen Sea, Antarctica (Graham et al., 2009). In Melville Bay, this is likely a consequence of the presence of different types of crystalline basement blocks with variable properties.

5.4.3 Troughs interconnect with fjord system

The troughs and channels connect the huge cross-shelf troughs of Melville Bay with modern outlet glaciers along the Greenland coast (Figs. 5.1a, 5.2). Beyond the coast, the trough network continues underneath the modern West GIS farther inland (Figs. 5.1a, 5.2) as indicated by the sub-ice topography (Morlighem et al., 2014a). According to their similar size and shape, we suggest that the troughs within the bathymetry are equivalent to the bed of modern outlet glaciers. The troughs are, thus, a continuation of the fjord system. There, similar overdeepenings occur close to the modern ice-sheet margin (Fig. 5.2). Thus, as suggested above, the overdeepenings of the troughs at the seabed likely mirror the location of a former glacial margin. The overdeepenings in the sub-ice topography of the modern GIS, therefore, may indicate supercooled meltwater and additional overdeepening in places with highly reversed down-ice slopes near the modern coastline.

Seemingly, the submarine trough network acted as tributary for the large paleo-ice streams that filled the CSTs. Erosional glacial flow marks (Figs. 5.3d, 5.4d) within and along the troughs indicate that fast streaming ice was bedded within the troughs. This may furthermore indicate meltwater occurrence, as it acts as lubricant for streaming ice. Furthermore, the rough morphology of the crystalline basement adjacent to the channels might be responsible for higher friction, resulting in stagnant to slow flowing ice and limited glacial quarrying between the branches of the channel network. Thus, on the basis of the glacial landforms in the study areas, slow-flowing ice on low-relief bedrock was intersected by fast ice-streams bedded in glacial troughs, as seen at the modern GIS margin, e.g., in data from Joughin et al. (2010). Some erosional marks striking oblique across the troughs (Figs. 5.3d, 5.4d) likely record broader streaming of the ice, similar to suggestions from Glasser and Bennett (2004) for abrasion and quarrying. Furthermore, the troughs and channels show in part an asymmetric cross profile that also conforms to the abrasion and quarrying of roche moutonnées and streamlined landforms (Figs. 5.3e). This broad streaming that is in parts independent of the underlying topography occurs similar in some locations of the modern GIS, as seen in velocity data from Joughin et al. (2010) compared to sub-ice topography from Morlighem et al. (2014b). There, high ice-

sheet velocities do not necessarily coincide with the orientation of troughs in the sub-ice topography. This broad streaming across the bedrock may be the result of nearby ice-sheet reorganization or could have occurred, when the ice-sheet margin was located seaward of the study area, e.g., near the continental shelf edge. Analogues to this ice streaming across crystalline bedrock have been similarly identified in south and west Greenland, northwest Scotland, Antarctica, and North America (Glasser and Warren, 1990; Graham et al., 2009; Hogan et al., 2016; Krabbendam and Bradwell, 2014; Larter et al., 2009; Ó Cofaigh et al., 2010).

5.4.4 Flood basalts

The characteristic terraces along the troughs in the southern study area are interpreted as the result of flood basalts that were incised by channels of glaciofluvial origin. Paleogene flood basalts (Fig. 5.5a) from the Nussuaq basin in central West Greenland are known to extend towards the southern Melville Bay (Chalmers et al., 1999; Gregersen et al., 2013; Harrison et al., 2011). After glaciofluvial erosion, those terraces likely represent several outcropping sheet flows that thin out north of 73°10'N (Fig. 5.5a). A frequent occupation by ice streams with subglacial meltwater flow likely gave them their overall U-shape and their overdeepened long profile (Fig. 5.5b). To some extent, the observed landforms resemble the flood-basalt escarpments described from Disko Trough and onshore Disko Island (Hogan et al., 2016) but are less inclined and reveal no significant dip direction, which could be caused by the large distance from the volcanic centre. In the Disko region, the escarpments indicate individual sheet flows; whereas the steps in height between the terraces in Melville Bay likely represent stacked piles of lava flows, as they exceed the average 5 m thickness (Storey et al., 1998) of sheet flows per eruption event. Ice and meltwater likely followed pre-glacial lines of weakness, but were not constrained to them to form this trough morphology.

5.4.5 Morphology and oceanography

The channel network in Melville Bay reaching to the modern outlet glaciers of the GIS (Figs. 5.1a, 2) is deeper than 250 m. This allows Atlantic water of the West Greenland Current, reported at depths >250 m below sea level (Morlighem et al., 2016; Rignot et al., 2016), to flow into the fjords and towards the glaciers. The mixing of this dense warm water with meltwater continuously outflowing at several marine-terminating glaciers at the modern West GIS margin (Fenty et al., 2016; Rignot et al., 2016; Xu et al., 2013), produces a turbulent plume, melting the ice front from underneath (Holland et al., 2008; Morlighem et al., 2014a; Rignot et al., 2015; Rignot et al., 2016). This accelerates the glacier melt and, thus, likely its retreat. This oceanographic condition was established in Baffin Bay during deglaciation after LGM (Funder and Weidick, 1991; Knudsen et al., 2008; Levac et al., 2001; Seidenkrantz et al., 2013; Sheldon et al., 2016). Thus, a similar

mechanism of Atlantic water inflow through the channels probably resulted in a rapid landward retreat of the paleo-ice sheet across the crystalline bedrock after the LGM.

5.5 Conclusion

The new high-resolution bathymetric compilation from Melville Bay, northeast Baffin Bay, provides a more detailed representation of the crystalline basement on the inner shelf than previously available from isolated single beam and multibeam soundings. Three study areas in which we have good multibeam data coverage are analysed in detail for geomorphology and flow patterns. The main points are stated below:

- A network of undulating, dendritic, and overdeepened troughs that likely hosted supercooled paleo-subglacial meltwater at its bed crosses the crystalline bedrock of Melville Bay, northeast Baffin Bay. It indicates a former ice-sheet margin on the inner continental shelf.
- The trough network sub-glacially extends under the modern Greenland Ice Sheet.
- The network is likely a re-occupied drainage network that developed along fractures during pre-glacial uplift, and was widened and deepened by subsequent glaciofluvial processes after subsidence.
- Erosional landforms along and across the channels indicate the pathways of ice streams and subglacial meltwater across the formerly glaciated bedrock.
- A different erosional morphology is observed in the southern study area that we suggest is caused by channels incised into outcropping flood basalts.
- The overall deep profile of the channels likely facilitated warm Atlantic water inflow toward the ice-sheet margin, which might have accelerated the ice-sheet retreat after the LGM.

Acknowledgements

Parts of the data used in this study were collected during *RV Maria S. Merian* cruise MSM44, *RV Polarstern* cruise ARK-XXV/3 and *RV Oden* expedition Petermann 2015. We thank the German Science Foundation (DFG) for providing ship time on *R/V MARIA S. MERIAN*. Thanks to NASA JPL for providing the OMG-bathymetry data collected on board *RV Cape Race*. Furthermore, we thank the crew and scientists on board for help with data acquisition during the expeditions. We thank Rob Larter and two anonymous reviewers, as well as the editor Richard A. Marston for the valuable comments on the manuscript.

6. Influence of bedrock morphology on ice and meltwater orientation in northern Baffin Bay

Patricia Slabon [a], Boris Dorschel [a], Wilfried Jokat [a,b], Francis Freire [c]

[a] Alfred Wegener Institute Helmholtz Centre for Polar and Marine Research, Am Alten Hafen 26, 27568 Bremerhaven, Germany

[b] University of Bremen, Department of Geosciences, Klagenfurter Straße, 28359 Bremen, Germany

[c] Geological Survey of Sweden (SGU), Villavägen 18, 751 28 Uppsala, Sweden

Submitted to *Geomorphology*, in review 2017

Abstract

High-resolution multibeam echosounder data reveal steep ridges characterizing the seafloor close to the West Greenland coast in northern Melville Bay, northeast Baffin Bay. Although they slightly resemble ribbed moraines formed by glacial overprinting, they are likely of different origin. The ridges are remarkably parallel to volcanic dykes swarms (Neoproterozoic Thule dyke swarms and Paleoproterozoic Melville Bugt dyke swarms) in this region and possibly related to the faults of the Thule halfgrabens that intersect the Proterozoic Thule Supergroup. They are higher and steeper than most glacial landforms in this region and, thus, may have partly restricted subglacial meltwater flow. This likely had an influence on ice streaming in northern Melville Bay. At the shallow bedrock between the northern and central cross-shelf trough of Melville Bay, we observe glacial landforms partly oblique to steep ridges and channels that indicate the reorganization of ice streams during retreat and subsequent re-advance. The landforms eroded into bedrock are likely older and caused by several ice-sheet advances, compared to the fresh

glacial deposits in the sedimentary part. Therefore, for this part of the study area, ice is expected to first have streamed southwards into the central cross-shelf trough, while after reorganization, it streamed westwards into the northern cross-shelf trough of Melville Bay.

Keywords

glacial landform; dyke; meltwater channel; ice-stream reorganization

Highlights

- Steep ridges in Melville Bay related to large dyke swarm systems
- Ice stream reorganization between northern and central cross-shelf trough
- Ridges partly influenced meltwater and ice-stream orientation

6.1. Introduction

Increased mass loss and partial retreat of the glaciers attract public attention to Greenland's melting ice sheet (IPCC, 2013). To model future melt and retreat scenarios for this ice sheet, it is necessary to understand past ice-sheet development. This can be studied in formerly ice-covered regions. As nowadays 80% of Greenland itself is covered by snow and ice and, thus, shielded from direct observations, it helps studying the adjacent seafloor. There, glacial landforms are imprinted that indicate the impact of former glaciations and meltwater flows.

Here, we study the seafloor of the northwest Greenland continental shelf. Due to its remoteness and tough sea-ice conditions, high-resolution bathymetric surveys have been limited in northern Baffin Bay. Most of them focussed on the large cross-shelf troughs (CST) in Melville Bay that have been occupied by paleo-ice streams during past glaciations (Batchelor and Dowdeswell, 2014; Dowdeswell and Fugelli, 2012; Slabon et al., 2016). Latest datasets, also including seismic data (Freire et al., 2015; Gyllencreutz et al., 2016; Newton et al., 2017; OMG-Mission, 2016; Slabon et al., 2016), show the detailed seafloor topography and reveal glacial landforms as imprints from former ice-sheet dynamics on both sedimentary rock and partly crystalline bedrock. Recent bathymetry datasets have been compiled to a 150 m grid (Morlighem et al., 2017) that already gives a good impression on the seafloor morphology and, for this area, improve previous, lower resolution map products such as the International Bathymetric Chart of the Arctic Ocean (IBCAO v.3.0) (Jakobsson et al., 2012b). Those datasets covering the crystalline basement on the inner continental shelf of northwest Greenland (Figs. 6.2a, 6.2b) (OMG-Mission, 2016; Slabon et al., 2016) have been compiled for this study with additional data from Petermann expedition 2015 to give an overview on the high-resolution bathymetry in this part of northern Melville Bay. There, the bedrock morphology with its glacial landforms overprinted on major geological structures indicates paleo ice-sheet dynamics with corresponding meltwater influence.

The study area is located in the Baffin Bay, a ~650 000 km² large basin between Canada and Greenland. We focus on the Melville Bay, the northeast part of Baffin Bay. Melville Bay is characterized by three large overdeepened CSTs that are 45-120 km wide, 170-320 km long and up to 1100 m deep (Fig. 6.1). The study area covers the northernmost part of Melville Bay near Kap York (Figs. 6.1, 6.2a), adjacent to the northern CST. In this area, the bathymetric data extend into the De Dødes Fjord and the Sidebriksfjord (Fig. 6.3a). The water depth in this part is 48 m close to the coast and up to 988 m in the central parts of the fjords. There, the study area covers large parts of smooth, sedimentary rock and deposits. The eastern part of the study area (Fig. 6.4a) covers the shallow bedrock region separating the northern and central Melville Bay CST, already described in parts by Slabon

et al. (2016). Here, water depths range between 111 m and 1057 m. This part of the study area shows outcropping low relief crystalline basement, characterized by a rough and rugged seafloor within the bathymetry (Fig. 6.4a). Strong reflections from the surface and limited to no sediment coverage characterize the basement within sediment echosounder data. Only in few basins, successions of smooth sediment can be found (Fig. 6.4f).

6.1.1 Regional setting and geology

Northern Melville Bay consists in parts of cratonic basement and sedimentary rock. The cratonic basement comprises crystalline Archaean and reworked (Paleo-) Proterozoic rock (Harrison et al., 2011; Knutz et al., 2015; Whittaker et al., 1997) stretching onshore and offshore along the coast. Furthermore, sedimentary rocks from the Proterozoic Thule Supergroup crop out onshore. It is likely that sedimentary sequences continue offshore in northern Melville Bay (Dawes, 1997, 2006; Harrison et al., 2011). The Thule Supergroup is partly of continental and shallow marine sediments deposited during the Proterozoic (Dawes, 2006). Its older units contain basaltic volcanic rock e.g. from dykes or sills, but also younger volcanism is observed intruding in the younger sedimentary layers (Dawes, 1997). The dykes and sills developed simultaneously along the faults of the Proterozoic Thule half-graben system in northern Baffin Bay and the adjacent Nares Strait (Chalmers et al., 1999; Dawes, 2006; Neben et al., 2006) (Fig. 6.1). As the dykes exploited those local faults and fractures, most dykes trend WNW and NW, and are, thus, parallel to the halfgraben. However, some dykes trend also sinuous (Dawes, 2006). Reactivation of faults in Baffin Bay likely occurred during Cretaceous to Paleocene rifting prior to seafloor spreading in the Baffin Bay, but also later, during Eocene, when Baffin Bay partly underwent compression (Chalmers and Pulvertaft, 2001; Gregersen et al., 2013; Harrison et al., 2006; Harrison et al., 2011; Oakey and Chalmers, 2012; Whittaker et al., 1997). The extension and subsequent compression of Baffin Bay resulted in several partly linked horst and graben structures as well as tilted fault blocks that characterize the geology of Melville Bay below the seafloor (Fig. 6.1). In central Melville Bay, the grabens are covered by 9-11 km thick sedimentary successions of Miocene to Pleistocene age (Altenbernd et al., 2014, 2015; Knutz et al., 2015), whereas in the southwest Melville Bay, sediment thickness yields only ~5 km (Suckro et al., 2012). The most prominent tectonic structure in the study area is the Melville Bay Graben aligning parallel to the west coast of Greenland (Fig. 6.1). The eastern flank of the graben is the Melville Bay Fault that trends NW to WNW. This fault builds the sharp transition from the crystalline basement to the partly reworked and eroded sedimentary successions of Miocene to Pleistocene age that fill the graben (Gregersen et al., 2013; Knutz et al., 2015).

Diabase sills and dykes developed along the previously described faults. They cross the Thule Supergroup and are related to the (Neohelikian) and Franklin (Hadrynian) magmatic episodes (Dawes, 1997). They are part of large volcanic dyke swarms of the same age that stretch across the basement of Melville Bay (Buchan and Ernst, 2004, and references therein). The Thule dyke swarms (Fig. 6.1), which are an expression of the Franklin magmatism, are of Neoproterozoic age (1.00-0.545 Ga) and trend WNW-ESE (Buchan and Ernst, 2004; Dawes, 2006; Dawes and Christie, 1991; Dawes and Rex, 1986). The Melville Bugt dyke swarms (Fig. 6.1) are of Paleoproterozoic age (2.50-1.60 Ga), trending from WNW-ESE in the north to NW-SE in the southeast (Buchan and Ernst, 2004; Dawes, 2006; Kalsbeek, 1986; Nielsen, 1990). Poorly constrained Nigârfivik dyke swarms (Fig. 6.1) trend NNE-SSW (Buchan and Ernst, 2004; Dawes, 2006; Dawes and Christie, 1991; Dawes and Rex, 1986) and, thus, are oblique to the former ones. Most dykes within the Thule strata form sharp ridges as they occur generally vertical or with steep dip (up to 75°) (Dawes, 2006). Some exceed even 200 m thickness. However, within bedrock outcrops, they also often form as depressions (Dawes, 2006).

Figure 6.1: Overview of high-resolution bathymetry data in northern Melville Bay, northeast Baffin Bay. Background bathymetry is in part from Morlighem et al. (2017). Greenland topography with ice coverage is from GIMP (Howat et al., 2014). Note the Thule dyke swarms coloured in pink and Melville Bay dyke swarms in green that trend parallel and sub-parallel to the faults and (half-) graben in Baffin Bay (modified from Harrison et al., 2011). Thule halfgraben in northern Melville Bay and across Nares Strait, north of it, are from Dawes (2006). nCST: northern cross-shelf trough (CST), cCST: central CST, sCST: southern CST, ITB: inter-trough bank, MBF: Melville Bay Fault, MBG: Melville Bay Graben. Thick black outline indicates location of Figs. 6.2a and 6.2b. Note in dashed orange the location of the modern ice divide.

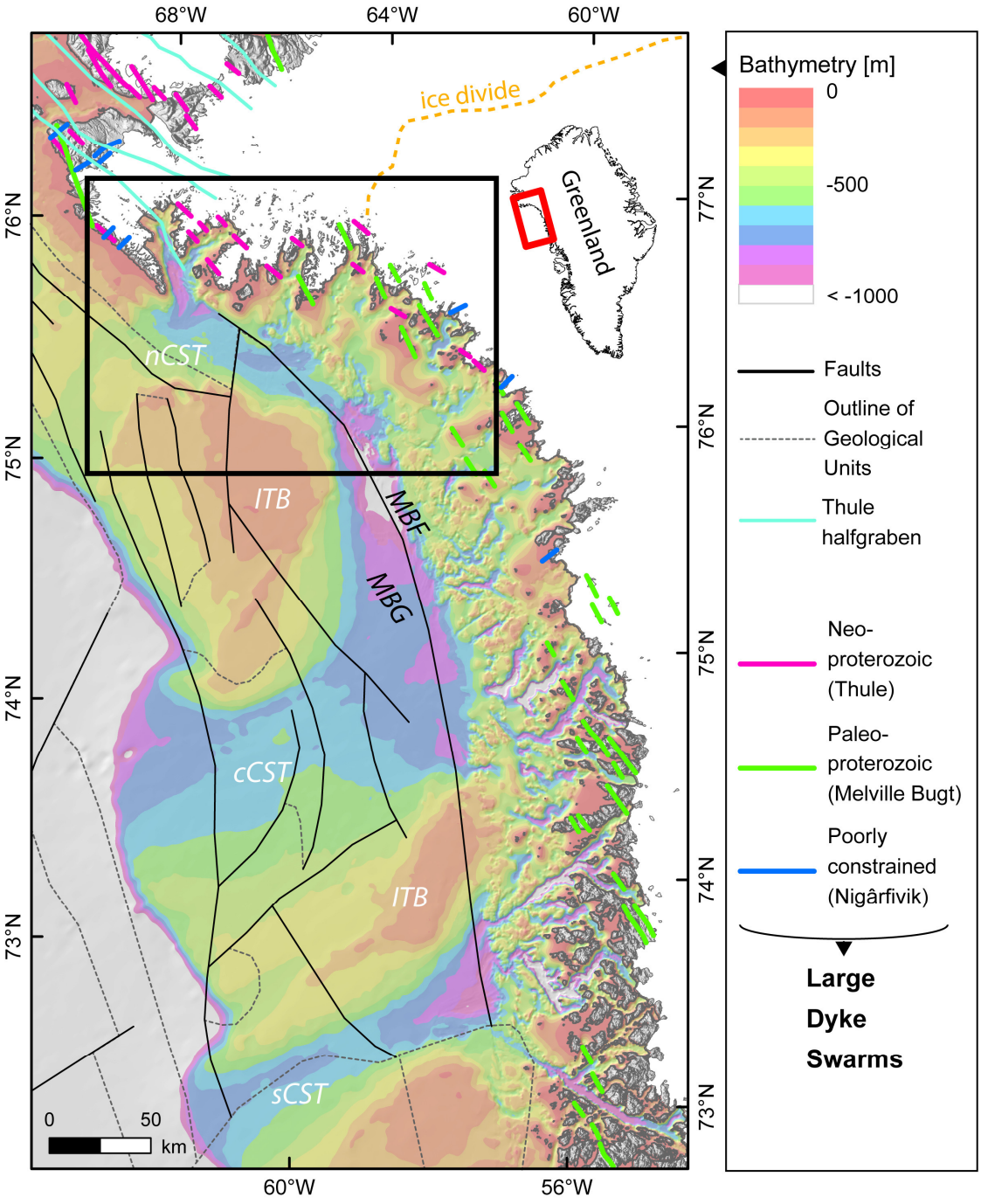
68°W
64°W
60°W
76°N
75°N
74°N
73°N
77°N
76°N
75°N
74°N
73°N
60°W
56°W
ice divide
Greenland
nCST
ITB
MBF
MBG
cCST
ITB
sCST
0
50
km
Bathymetry [m]
0
-500
< -1000
Faults
Outline of Geological Units
Thule halfgraben
Neo-proterozoic (Thule)
Paleo-proterozoic (Melville Bugt)
Poorly constrained (Nigârfivik)
Large Dyke Swarms

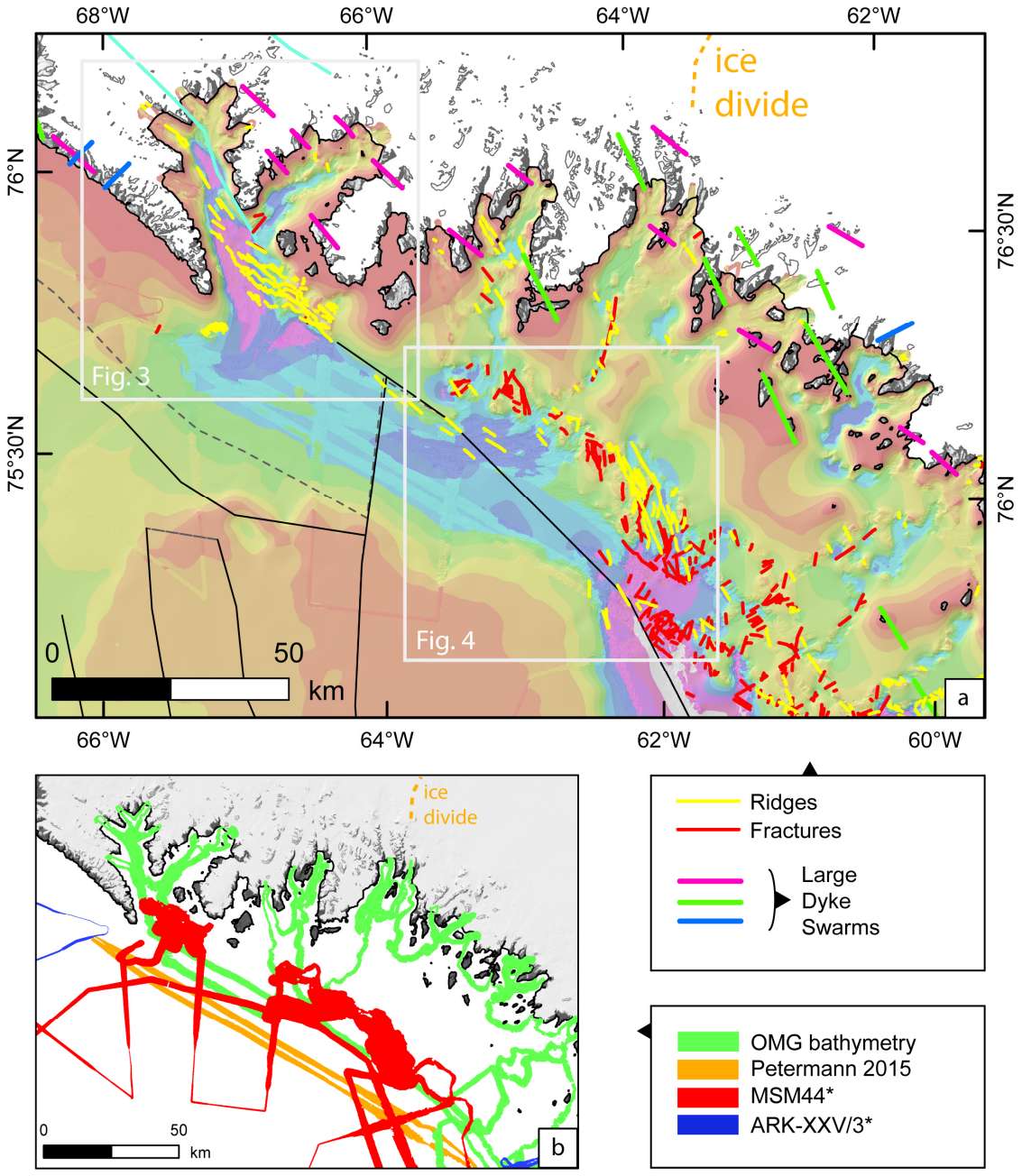

*Figure 6.2: Zoom to study area. Thin lines on the high-resolution bathymetry data indicate ridges (yellow) and fractures (red). Note the parallel and subparallel trend to dyke swarms. White boxes show location of Figs. 6.3 and 4. Fig. 6.2b: Coverage of high-resolution bathymetry compiled for this study. The different cruises and datasets are colour coded. * indicates part of compilation from Slabon et al. (2016). White spaces in the background indicate area filled with bathymetry data from BedMachine v3 (Morlighem et al., 2017). Background topography is from GIMP (Howat et al., 2014).*

6.2. Material and methods

The high-resolution digital bathymetric model used for this compilation is from Slabon et al. (2016) complemented by datasets from NASA OMG-Mission (2016) and *RV Oden* "Petermann expedition" in summer 2015 (Department of Geological Sciences, Stockholm University) (Fig. 6.2b). The new dataset is gridded to 10 m resolution, partly artificial, as the datasets from Stockholm University and OMG are of 25 m resolution. As background bathymetry and topography, the new BedMachine v3 compilation from Morlighem et al. (2017) and the Greenland Ice Mapping Project digital elevation model (GIMP DEM, 90 m grid) from Howat et al. (2014) are used. In addition, during expedition MSM44, a hull-mounted Parasound P70 sediment echosounder system collected simultaneously data from the sub bottom (Dorschel et al., 2015).

All geographical analysis of geomorphological structures and glacial landforms was conducted using ESRI ArcMap. Main map projection is based on EPSG 3413, NSIDC Polar Stereographic North. Geologic background information is given by NRCAN Map 2159A (Harrison et al., 2011) and NRCAN Map 2022 (Buchan and Ernst, 2004), used to compare the identified landforms to larger geological structures. Glacial landforms as well as prominent geomorphological structures have been visually identified and manually digitized (Figs. 6.2a, 6.3c, 6.4e).

6.3. Results and interpretation

After deglaciation, the ice sheets left glacial landforms of both erosional and depositional character behind. Therefore, the seafloor morphology shows significant differences from primary sedimentary structures and steep ridges in the west to crystalline basement structures with significant fractures and steep ridges in the east. Depending on their orientation to former ice and meltwater pathways, the ridges partially acted as obstacles that channelled or blocked the corresponding flow towards the CSTs. Fractures in the crystalline part obviously aided as pathways.

The obstacles in form of steep sub-parallel elongated ridges are 40-150 m high, 200-1500 m wide, and 2.5-25 km long and occur in water depths from 50 to 800 m. They trend mainly in NW and WNW direction with a shallow, seaward dipping gradient of 5-20° and a steeper landward dipping gradient of 20-60°. The ridges occur both in the sedimentary part but also as part of the crystalline basement. In places, they can be traced over long distances (>50 km) where they occasionally appear and disappear within the sedimentary units (Figs. 6.2a, 6.3c). In plan view, the ridges are linear to slightly sinuous. Their orientations are generally parallel to the faults and dykes in Melville Bay (Fig. 6.1). In both

parts of the study area (Figs. 6.3a, 6.3c, 6.4a, 6.4e), the ridges are glacially overprinted. In the sedimentary part, characteristic crag-and-tails have been observed that extend into mega-scale glacial lineations (MSGL) (Slabon et al., 2016) (Figs. 6.3c, 6.4e). They are composed of a sedimentary tail and a rocky crag-head that developed at the steep, partly buried ridges. On the crystalline bedrock, however, abraded and quarried Roche moutonnées-type landforms predominate (Figs. 6.3c, 6.4e). Both landforms indicate former ice-stream and subglacial meltwater pathways. Their down-stream tails and quarried backsides provide information on flow-directions of ice and meltwater in the past. In the northwest part of the study area (Fig. 6.3c), these landforms show a clear southward orientation, thus, indicating ice streaming with subglacial meltwater flow from the modern coastline towards the northern CST confined by the topography along the fjords.

In the eastern part of the study area (Figs. 6.4a, 6.4e), the landforms indicate a less defined path of ice streams with subglacial meltwater flows. There, west of the shallow bedrock (Figs. 6.4a, 6.4e), the glacial landforms mark a clear westward transition into the northern CST. In the north of it, we see landforms bending south and westward around the shallow bedrock ridges to merge with those in the northern CST. In the east of the shallow bedrock, we see a southward trend of the landforms. There, the landforms indicate a meandering path of ice-streams and meltwater flows around the steep ridges into the overdeepened basin of the central CST. Adjacent to this overdeepened basin, landforms are oriented northwest towards the northern CST, whereas others inside the basin are oriented south-eastwards to the central CST. Those landform orientations generally coincide with channel orientations.

In the northwest, where the steep ridges (Figs. 6.2a, 6.3c) are oblique to former ice and meltwater pathways, channels or elongated potholes on their up-ice sides and associated glacial landforms indicate that the ridges partly blocked the flow paths of meltwater. These channels are u- and partly v-shaped, 50-150 m deep, 500-1000 m wide, up to 20 km long and parallel to the steep ridges. Their long profiles rise from the overdeepened part in the west to the shallow part in the east. The channel outlets coincide with the boundaries of crag-and-tails, thus, they discharge into the wide northern CST of Melville Bay.

Whereas east of the shallow bedrock (Figs. 6.4a, 6.4e), the ridges tend to be parallel to sub-parallel to the southward ice-streaming direction, thus, channelling ice and meltwater further southwards into the central CST. There, only one wide and less confined major channel occurs. This channel is 8-10 km wide, 600-950 m deep and ~30 km long and seems to continue in the unmapped northern part. It trends SE-wards, parallel to the steep ridges, and at their termination, it turns SW-wards into the

overdeepened basin of the central CST. Along the channel are several minor ridges that produce small basins in between (Figs. 6.4d, 6.4e, 6.4f). Within those basins are stratified sedimentary deposits of varying thickness (Fig. 6.4f). The deepest part of the channel is east of the steep ridges. There, we suggest a more confined flow in a partly u-shaped sub-channel that is ~2 km wide and 200 m deep. North of the shallow bedrock in the eastern part of the study area, we see u-shaped channels eroded into it, (Fig. 6.4e). They are 2-3.5 km wide, 200-300 m deep, oriented southwest towards the northern CST but also southeast towards the central CST. They are dendritic and partly meandering around the shallow bedrock highs, and seem to continue northward in the unmapped area.

In addition to the channels that are confined by steep ridges and shallow bedrock highs, the flow path of ice and meltwater was likely also influenced by fractures in crystalline basement. The outcropping bedrock in Melville Bay is highly incised by fractures and elongated depressions (Figs. 6.3c, 6.4e). Fractures are most common in the eastern part of the study area, especially in the overdeepened section of the CST (Fig. 6.4e). The fractures are 10-40 m deep, 1-7 km long, and 150-500 m wide. They are linear to slightly sinuous and occur in a wide depth range of 270-880 m below sea level. The orientations of the fractures are parallel and sub-parallel to Baffin Bay faults (Harrison et al., 2011) striking N, NW, W and NE .

Figure 6.3: High-resolution bathymetry in the northwest part of the study area. Note the steep ridges across the deep fjords. Background is from BedMachine v3 (Morlighem et al., 2017) and GIMP (Howat et al., 2014). Dashed white lines indicate cross profiles shown in Fig. 6.3b. Fig. 6.3b: Profiles of cross sections indicated in Fig. 6.3a. Note the different x-axis of lines a-a', C-C' and D-D'. Fig. 6.3c: Black arrows indicate the location of landforms oriented towards the northern CST. Thin coloured lines indicate identified ridges and fractures (this study) as well as mega-scale glacial lineations (MSGL) and crag-and-tails from Slabon et al. (2016)(*), with minor modifications from this study. Thick pink and blue lines on land indicate dyke swarm orientations from Buchan and Ernst (2004).

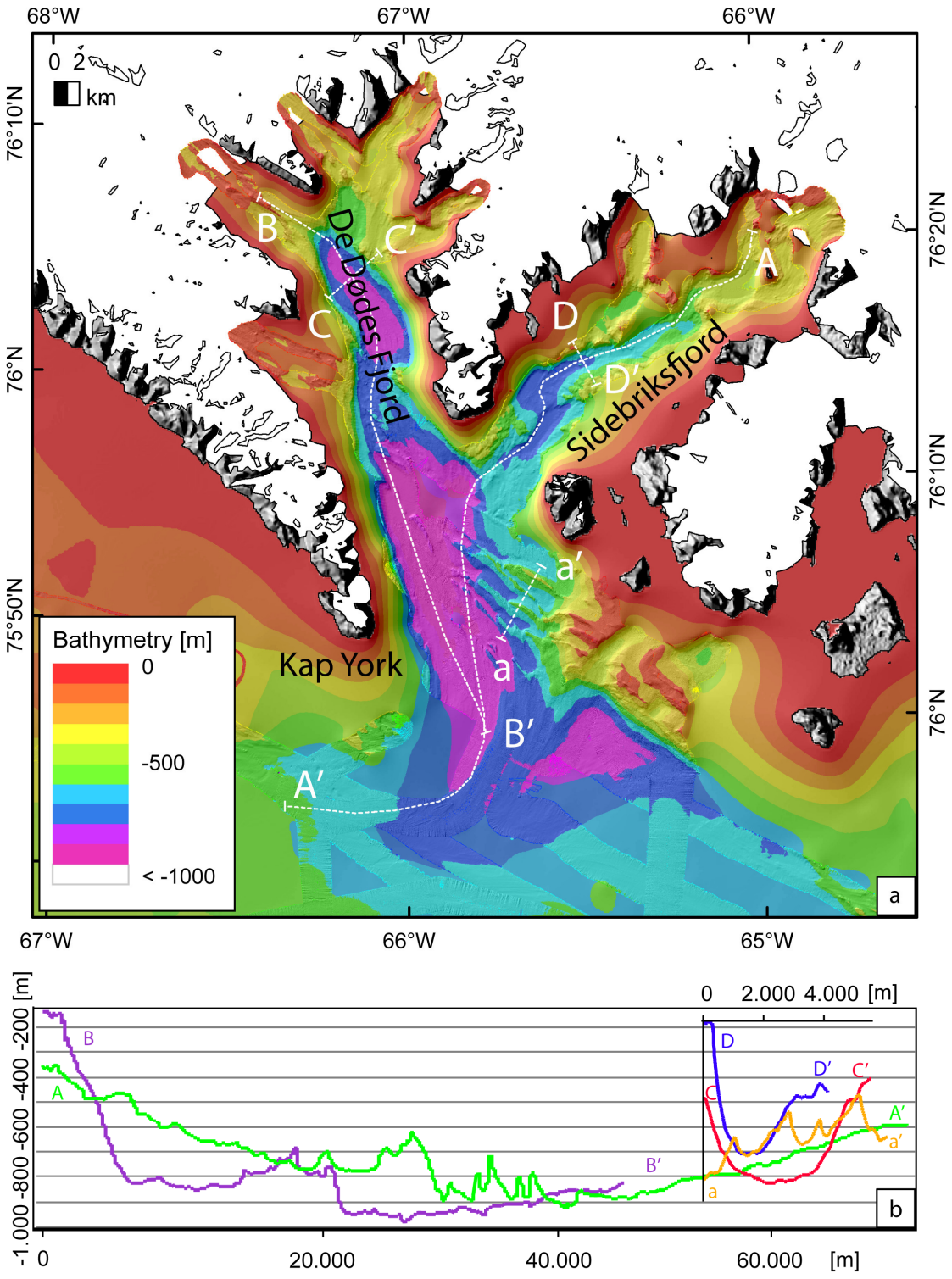
68°W
67°W
66°W
0 2
km
76°10'N
76°N
75°50'N
76°20'N
76°10'N
76°N
De Dødes Fjord
Sidebriksfjord
Kap York
A
B
C
C′
D
D′
a
a′
A′
B′
Bathymetry [m]
0
-500
< -1000
a
67°W
66°W
65°W
[m]
-200
-400
-600
-800
-1.000
0
20.000
40.000
60.000
[m]
0
2.000
4.000
[m]
b

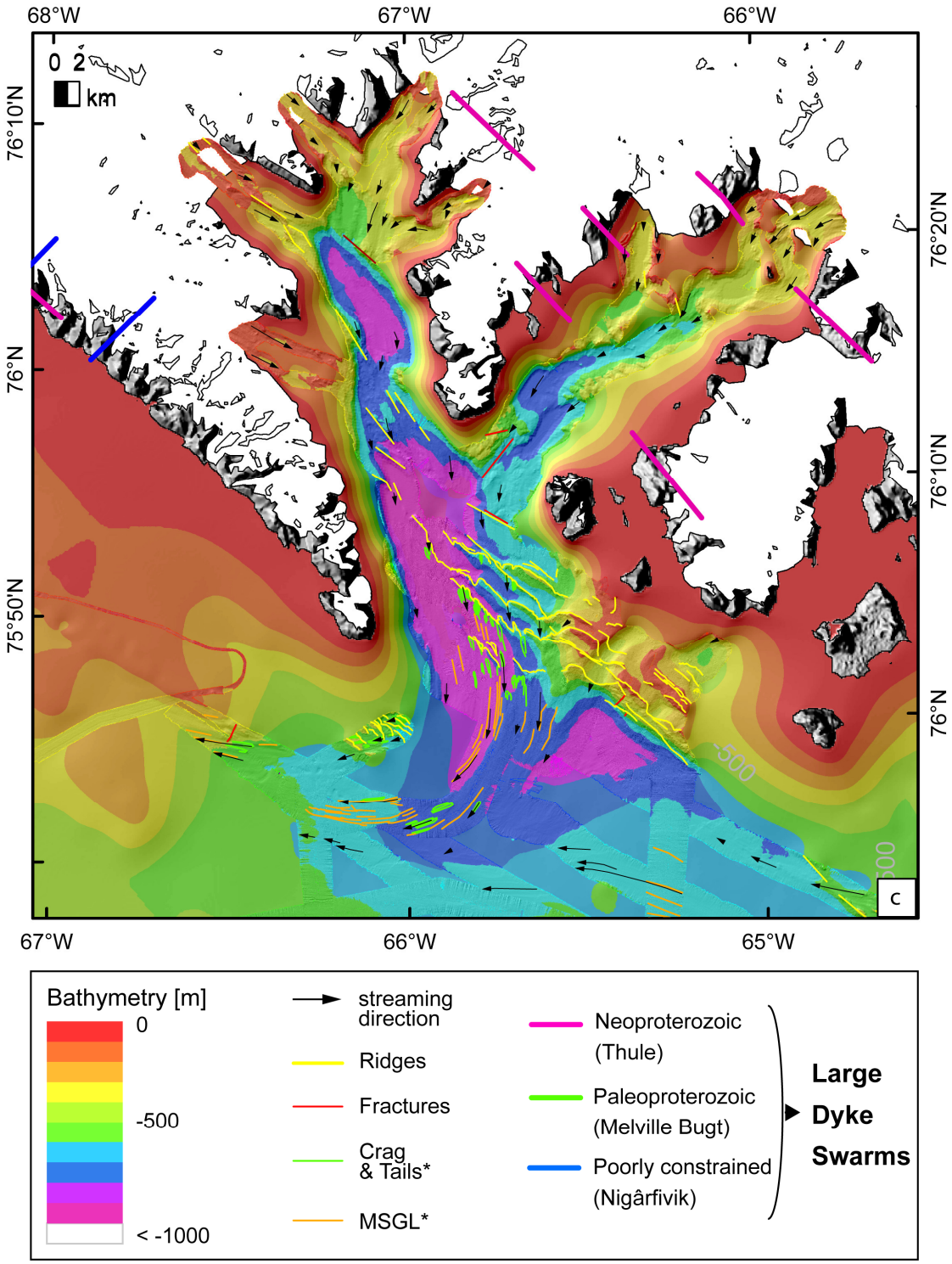
68°W
67°W
66°W
0 2
km
76°10'N
76°N
75°50'N
76°20'N
76°10'N
76°N
-500
-1000
c
67°W
66°W
65°W
Bathymetry [m]
0
-500
< -1000
streaming direction
Ridges
Fractures
Crag & Tails*
MSGL*
Neoproterozoic (Thule)
Paleoproterozoic (Melville Bugt)
Poorly constrained (Nigârfivik)
Large Dyke Swarms

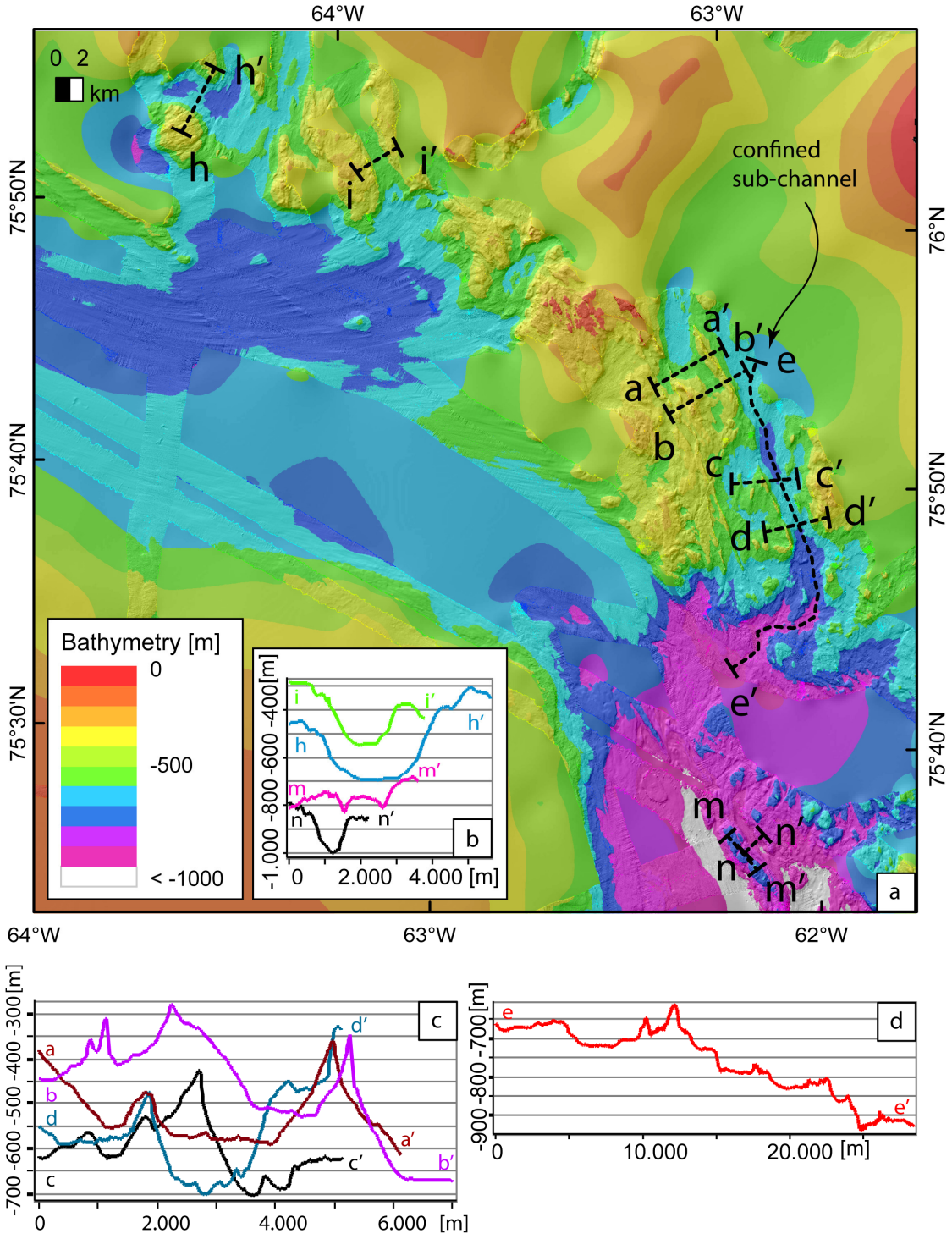
64°W
63°W
62°W
75°50'N
75°40'N
75°30'N
76°N
0 2
km
confined
sub-channel
Bathymetry [m]
0
-500
< -1000
-1.000 -800 -600 -400[m]
0 2.000 4.000 [m]
b
a
-700 -600 -500 -400 -300[m]
0 2.000 4.000 6.000 [m]
c
-900 -800 -700[m]
0 10.000 20.000 [m]
d

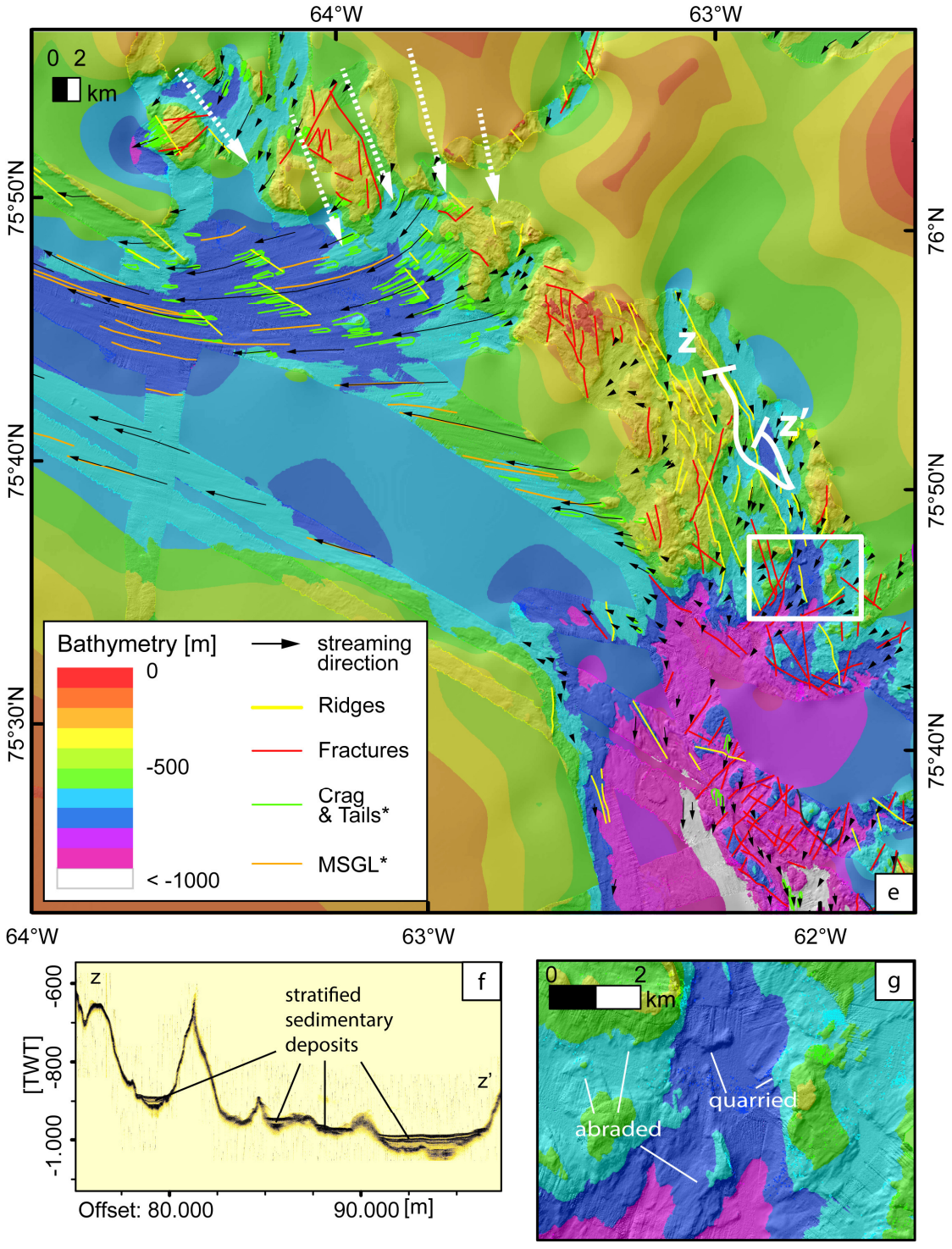
64°W
63°W
0 2
km
75°50'N
75°40'N
75°30'N
76°N
75°50'N
75°40'N
z
z'
Bathymetry [m]
0
-500
< -1000
streaming direction
Ridges
Fractures
Crag & Tails*
MSGL*
e
64°W
63°W
62°W
f
z
z'
stratified sedimentary deposits
[TWT]
-600
-800
-1.000
Offset: 80.000
90.000 [m]
g
0 2
km
abraded
quarried

Figure 6.4: High-resolution bathymetry in the eastern part of the study area. Note the shallow bedrock in the centre and the steep ridges east of it. Background is from Morlighem et al. (2017). Black dashed lines indicate cross profiles shown in Figs. 6.4b-6.4d. Fig. 6.4b: Profile of cross sections indicated in Fig. 6.4a showing u-shaped channels but also fractures (m-m') in the overdeepened basin of the CST. Fig. 6.4c: Profile of cross sections indicated in Fig. 6.4a showing the steep ridges east of the shallow bedrock and the u-shaped channel. Fig. 6.4d: Profile of cross section indicated in Fig. 6.4a showing the long profile of the channel next to the steep ridges. Note the steep ridges along the channel path. Fig. 6.4e: Identified ridges and fractures (this study) as well as mega-scale glacial lineations and crag-and-tails from Slabon et al. (2016)(*), with minor modifications from this study. Black arrows indicate location and direction of landforms oriented towards the CSTs. Note the different orientation between landforms east and west of the shallow bedrock. Dashed white lines indicate inferred former ice streaming direction in the northwest part, oblique to the glacial landforms. The white box indicates the location of Fig. 6.4g. White solid line indicates sub-bottom profile shown in Fig. 6.4f. Fig. 6.4f: Sub-bottom profile across the steep, highly reflective ridges reveals stratified sediments of varying thickness within most of the basins. TWT = two-way travel time in seconds. Offset shows distance in meters to start of line. Fig. 6.4g: Zoom to the white box indicated in Fig. 6.4e. Note the abraded and quarried glacial landforms next to the steep ridges.

6.4. Discussion

6.4.1 Ridges act as obstacles to ice and meltwater

The ridges are prominent obstacles in the study area. In the northwest, they are almost perpendicular to the flow of ice and water. There, the ridges (Figs. 6.3a, 6.3c) resemble ribbed moraines (e.g. Dunlop and Clark, 2006; Stokes et al., 2008). Morlighem et al. (2017) proposed that the same ridges, identified in 150 m resolution are moraines that may originate from the little ice age. However, more detailed, higher resolution bathymetry data show that the ridges are in size much larger than typical ribbed moraines (Hättestrand, 1997, and references therein). Ribbed moraines commonly have a steeper ice-distal slope and are often drumlinized (Hättestrand, 1997, and references therein). The ridges in Melville Bay show similarly drumlinization, but their ice-distal slope is much shallower than their ice-proximal slope. Thus, the orientation of these ridges is opposite to normal ribbed moraines. Furthermore, the ridges strike remarkably parallel to faults and tectonic blocks in Baffin Bay (Fig. 6.1). Therefore, we suggest that these landforms are not of glacigenic origin, although they are partly glacially overprinted. Similar ridges are described from Disko Bay in central West Greenland and are interpreted as simple bedrock highs developed by the throw at adjacent faults (Hogan et al., 2012; Streuff et al., 2017). We, thus, suggest that the steep ridges of Melville Bay may be of similar origin. However, due to their fault-parallel orientation, the ridges (Figs. 6.2a, 6.3c, 6.4e) are likely part of the steeply dipping grabens and halfgrabens (Figs. 6.1) that developed during rifting, prior to opening of the Baffin Bay (Chalmers et al., 1999; Dawes, 2006; Whittaker et al., 1997).

Furthermore, they likely belong to the Thule halfgraben system with its compression and inversion structures stretching across Nares Strait, north of Baffin Bay (Neben et al., 2006; Whittaker et al., 1997). In this regard, the ridges might be related to the steeply dipping Thule or Melville Bay dyke swarms and their associated basic sills (Dawes, 2006; Denyszyn et al., 2006; Harrison et al., 2011) that strike parallel and sub-parallel to the ridges. Ridges of similar height, extent and orientation can be also identified onshore cutting the Thule Supergroup, e.g. in the Dundas region (Dawes, 1997) or on small Islands in northern Melville Bay (Dawes, 2006). Similar ridges have been also identified in seismic data from offshore central west Greenland where they are interpreted as dykes and sills (Chalmers et al., 1999) and in magnetic data from Nares Strait (Oakey and Damaske, 2004). Some of them are equally eroded. The heads of some of the crag-and-tails (Figs. 6.2a, 6.3c, 6.4e), already identified by Slabon et al. (2016), are aligned parallel to the ridges near Kap York (Fig. 6.3c) and seem to be a continuation of these. The extension of the Thule Supergroup into the Kap York region (Dawes, 1997; Harrison et al., 2011) further supports the dyke-origin of the ridges and in reverse indicates a further offshore continuation of the

formation into northern Melville Bay as previously proposed. The ridges in the eastern part of the study area (Fig. 6.4e) were likely generated similar to those in the northwest (Fig. 6.3c). Their WNW to NW orientation indicates a relation to the Melville Bugt dyke swarms (Fig. 6.1). However, their different overprinted appearance compared to those ridges of the northwest part of the study area, as well as their different orientation, not only indicates ice streaming from a different direction but also likely indicates a change in bedrock lithology. This change in bedrock lithology might reflect a turned tectonic block of the halfgraben system. Furthermore, the significant fractures in the bedrock area may be similarly dykes, as proposed by Dawes (2006).

6.4.2 Meltwater pathways defined by ice and morphology

Glacial landforms oblique to the steep ridges in the northwest of the study area (Fig. 6.2a, 6.3c) indicate that ice was streaming across them during glacials. However, we see small channels or elongated potholes on the land-facing sides of the ridges that indicate that the ridges partly confined subglacial meltwater flow. Depending on pressure from the overlying ice sheet, meltwater is not restricted to follow the slope and may have created the partly overdeepened channels (Alley et al., 2003). This is likely due to less permeable rock compared to sedimentary rock. Similar meltwater-eroded channels have been identified in front of basalt scarps in Disko Bay (Hogan et al., 2016) but also in front of bedrock highs in other glaciated regions, e.g. Amundsen Sea Embayment, Antarctica (Smith et al., 2009). In Melville Bay, the ice likely covered the ridges, while it capped subglacial meltwater under high pressure streaming upwards in the channels (Fig. 6.5) and further seaward into the northern CST. Thus, ice, in combination with sediment-laden meltwater streaming through narrow passages under the ice, likely formed the crag-and-tails oblique to the ridges. The crag-heads are part of the steep ridges and their tails are sediments deposited in their shadows. Crag-and-tails, thus, indicate general flow path of the ice and meltwater. Furthermore, as meltwater generally transports high sediment loads that help erode the bedrock (Shreve, 1972), these sediments can settle in the depressions if the energy is too low to keep the sediments in suspension.

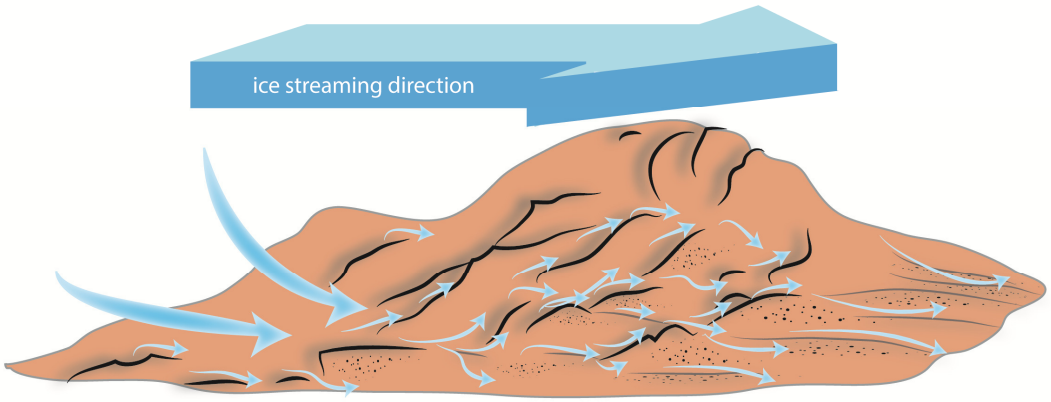

Figure 6.5: Sketch (not to scale) of subglacial meltwater flow (blue small arrows) along and across the ridges in northern Melville Bay creating potholes and crag-and-tails. Sediment-laden meltwater is capped by the ice, thus, under pressure able to stream upwards along the cavities in front of the ridges. Sedimentary tails are indicated by dotted texture.

In the east of the study area (Fig. 6.4e), meltwater flow was likely similar confined by ice and bedrock morphology, as indicated by the glacial landforms along and across the ridges, as well as along the channel pathway. There, the inclination of the shallow bedrock and the steep ridges partly blocked the westward flow of the meltwater, resulting in a broad southward flow direction towards the central CST. This southward flow was especially confined in the deep and narrow channel east of the shallow bedrock (Figs. 6.4e, 6.4g). Furthermore, several of the shallow fractures we observe in this area are inclined parallel to the ridges (Fig. 6.3b), thus, aiding the flow to the south into the overdeepening and even further. We suggest that ice capped similarly the shallow bedrock and the steep ridges as in the NW study area. Meltwater could drain below through narrow cavities and channels that built between the ridges and that are partly eroded into the basement. The glacial landforms furthermore indicate meltwater flow between the small basins along the channel, similar to suggestions for channels and basins confined by small ridges in Pine Island Bay, Antarctica (Nitsche et al., 2013). Similarly, in Melville Bay, varying sediment infill and stratification (Fig. 6.4f) indicate that some of the basins were not always occupied by meltwater and, thus, likely have been occasionally blocked by the capping ice.

The channels northwest of the shallow bedrock are less confined, as shown by their plan view that reveals a smooth and more meandering path of ice and meltwater towards the northern CST (Fig. 6.4e). They resemble those channels identified in Marguerite Bay, Antarctic Peninsula (Anderson and Fretwell, 2008). Basins and channels oblique to the

streaming direction that is inferred by glacial landforms (Fig. 6.4e) indicate that at relatively earlier times, ice streamed also south-eastwards in this part of Melville Bay (Fig. 6.6a). This is furthermore consistent with glacial landforms and channels identified in the overdeepening of the central CST. There, the glacial landforms direct from the northern CST southwards into it and even further southwards (Figs. 6.4e, 6.6a). Unfortunately, all those channels are eroded into bedrock and absolute age dating is difficult. However, cross-cutting sedimentary glacial landforms (crag-and-tails and MSGL) (Figs. 6.4e) oriented westwards across the shallow bedrock and in the sedimentary part of the northern CST indicate that this was not always the case. At times with abundant meltwater, ice and meltwater could pass this bedrock barrier more easily, thus, cross cutting the basement ridges and fractures (Fig. 6.6b). This indicates that ice must have overflown the shallow bedrock and the steep ridges to stream further westwards, which occurred likely in combination with higher meltwater fluxes. Therefore, the seafloor morphology of Melville Bay has not only an impact on meltwater flow but may have also partly influenced ice-stream orientation across the inner continental shelf. This is likely due to channelling of the sediment-laden meltwater that is an efficient lubricant for ice streaming (Anandakrishnan et al., 1998; Studinger et al., 2001; Weertman, 1972).

6.4.3 Change in orientation of ice streaming

The sedimentary glacial landforms in the northern CST are youngest (Fig. 6.4e), likely showing the imprint from the last deglaciation, as the major ice-streams in the CST are expected to have been active during the last glacial maximum (LGM) (Slabon et al., 2016). The glacial landforms in this part of Melville Bay indicate that the last occupied ice stream direction was westwards, across the shallow bedrock and into the northern CST (Fig. 6.6b), whereas the imprints on the crystalline basement oriented southwards (Fig. 6.6a) are likely older. We, therefore, suggest that during LGM, the ice sheet in the northern part of Melville Bay drained into the northern CST instead of the central CST as previously expected from sedimentary glacial landforms further to the south (Slabon et al., 2016). However, those ice streams further to the south may still have influenced ice streaming in the central CST and subsequent creation of those glacial landforms, as earlier proposed. Nevertheless, the glacial landforms surrounding the shallow bedrock indicate a migration from the ice divide from west to east during retreat, accompanied by an ice-stream reorganization. We suggest that the northern part of the southward-oriented ice stream retreated earlier and merged with the westward-trending ice stream, likely during subsequent re-advance (Figs. 6.6a, 6.6b). Nevertheless, it may be still possible that the ice streams occupying northern and central CST were active simultaneously as proposed by Slabon et al. (2016), but likely with a slight shift of the individual ice streams.

The ice-stream switching is likely the result of both, topographic steering of the ice stream due to the influence of the steep ridges on meltwater pathways, but also likely a reorganization of the ice divide in the hinterland during retreat and re-advance. However, we do not know exactly when this ice divide migration occurred, but, from the relatively young sedimentary glacial landforms in both troughs (Slabon et al., 2016), we suggest a reorientation during the last glacial instead of between individual glacial stages. Ice divide migration, however, is a mechanism triggered by change of ice and snow accumulation and ablation as well as a change in drainage pathways. A modern ice divide is located directly north of the eastern part of the study area (Figs. 6.1, 6.2a) at the direct extension of the shallow bedrock that divides the northern and central CST. It is responsible for a southward stream as part of the northwest Greenland Ice Sheet and a separate northwestward stream in the Thule region (Zwally and Giovinetto, 2011; Zwally et al., 2012). It is likely that the same ice divide was responsible for the change in ice stream orientation during the LGM, and later reoriented to its current position. Migrating ice divides with associated ice-stream switching are common and have been similarly identified from glacial landforms formed by the Laurentide Ice Sheet that covered North America during past glacials (e.g. Jansson et al., 2002; Krabbendam et al., 2016).

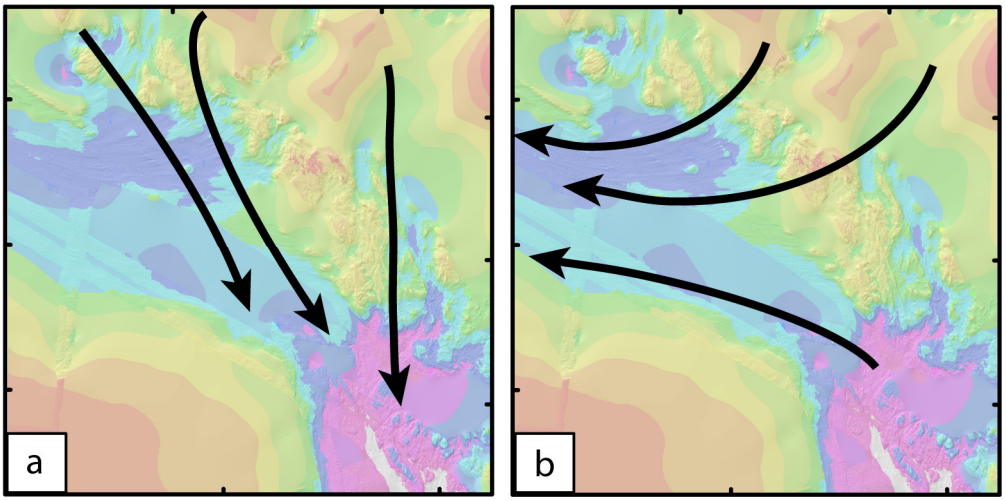

Figure 6.6: Ice-stream reorganization. Location is similar to that of Fig. 6.4. Ice and meltwater flow was first oriented southwards (black arrows) into the central CST as indicated by glacial landforms imprinted on bedrock as well as channel orientations. A reorganization during retreat and re-advance likely channelled the ice westwards (black arrows) into the northern CST as indicated by younger sedimentary glacial landforms.

6.5. Conclusion

Mapping of glacial landforms and geomorphological features in high-resolution bathymetry data from northern Melville Bay, Northeast Baffin Bay, indicates strong paleo-subglacial activity. Steep, glacially overprinted ridges had an impact on ice and meltwater.

- The steep ridges in Melville Bay stand in relation to large Paleoproterozoic and Neoproterozoic dyke swarm systems. They have been partly eroded by ice and sediment-laden subglacial meltwater.
- The ridges may indicate a further continuation of the Thule Supergroup into northern Baffin Bay.
- They partly influenced and steered subglacial meltwater, thus may have impacted on ice-stream orientation and reorganization.
- For a small part of Melville Bay, glacial landforms eroded into bedrock indicate former ice-stream orientation into the central cross-shelf trough. Sedimentary glacial landforms indicate westward re-orientation.
- This ice-stream reorganization between the northern and central cross-shelf trough likely occurred during retreat and subsequent re-advance.

Acknowledgements

We thank NASA JPL for providing OMG bathymetry data. We thank crew and scientists of *RV Maria S. Merian* expedition MSM44 and *RV Polarstern* expedition ARK-XXV/3 for their help during the cruise. Thanks to the German Science Foundation (DFG) for providing ship time on *RV Maria S. Merian*.

7. Conclusion

The aim of this thesis was to understand and reconstruct the Greenland Ice Sheet dynamics by analysing glacial landforms identified in new bathymetry data from Melville Bay, northeast Baffin Bay. To summarize my research, as presented in the previous chapters 4-6, I will relate my findings to the research questions raised in chapter 1.3. Figure 7.1 gives and overview of the glacial landforms and geological structures used for reconstruction of the paleo-ice sheet extent and dynamics.

Paleo-ice sheet extent to the shelf edge

Glacial landforms on the outer continental shelf and at the shelf break of northwest Greenland indicate that ice-streams fully occupied the cross-shelf troughs of Melville Bay, northeast Baffin Bay (Fig. 7.1). Age dating in this part of Baffin Bay was difficult. Hence, no direct ages are available. However, linking the landforms to those in the adjacent cross-shelf troughs in central West Greenland gives a relative age that dates to the LGM. Nevertheless, an older glaciation responsible for the glacial landforms cannot be ruled out until further evidence is given.

Elongated depressions overprinted by glacial landforms on the seaward flanks of the inter-trough banks infer small glacial troughs eroded by minor ice-streams. Ice domes that probably developed on these banks may have fed them and likely channelled the ice streams of the cross-shelf troughs around the banks.

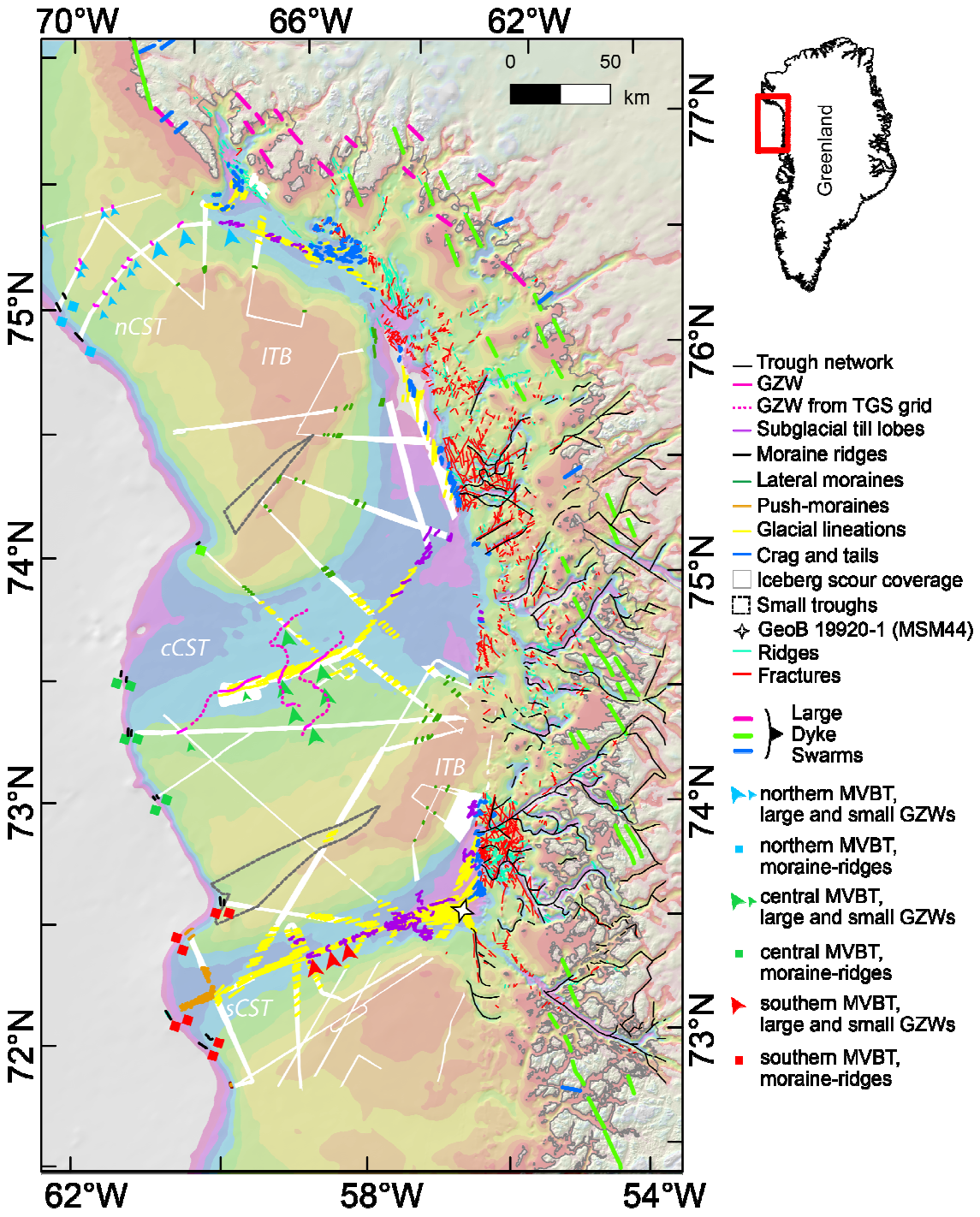

Figure 7.1: Overview of glacial landforms in Melville Bay identified within the different studies of this thesis. Note the glacial landforms indicating a stabilization on the shelf edge and on the mid-shelf. A trough network characterizes the inner continental shelf and extends subglacially under the modern GIS. Steep ridges and fractures on the inner continental shelf influenced ice-sheet dynamics. ITB: Inter-trough bank; nCST: northern Cross-shelf trough; cCST: central CST; sCST: southern CST

Ice-sheet dynamics

Large GZWs and smaller subglacial till-lobes occur on the mid- and outer shelf in the three cross-shelf troughs of Melville Bay indicating stagnation of the ice sheet (Fig. 7.1). They have been identified within the narrow swaths of the high-resolution bathymetry data and on associated sub-bottom profiler data. Superimposed are mega-scale glacial lineations that are related to the crag-and-tails on the inner continental shelf. They indicate the orientation of fast streaming ice within the cross-shelf troughs. Moraines on the outer shelf and at the shelf edge indicate the maximum ice-sheet extent and repeated re-advances to it. Lateral moraines line the lateral margin of the paleo-ice streams. Chaotic iceberg scours on the shallow banks and on the shallower parts of the troughs obscure smaller landforms.

Ice-stream retreat from the shelf edge to its current position varied between the three individual cross-shelf troughs in Melville Bay. The number, dimensions, and locations of the recessional wedges within GZW-complexes give insight in the retreat dynamics after the LGM. The GZW-complexes are complemented by additional glacial landforms like moraines and MSGL that give the maximum extent and flow directions of the ice sheet. A number of GZWs in the northern cross-shelf trough indicates that at this location, the ice-stream retreat was slow, continuous, and stepwise on the outer shelf. Moraines and MSGL on the central and southern cross-shelf trough indicate that retreat was more episodic. In particular, ice-streams in the South repeatedly re-advanced to the shelf edge followed by a fast retreat to a mid-shelf position. Mid-shelf stabilizations occurred in all three troughs as indicated by the presence of large GZW-complexes. The analogy to mid-shelf stabilizations from central West Greenland indicate a stabilization of the ice-stream margin during the YD. MSGL and recessional subglacial till lobes on the mid-to inner shelf indicate episodic to slow final ice-stream retreat towards the crystalline basement near the coast with re-advancing ice-stream lobes.

Timing of ice-sheet dynamics

Absolute age dating of Quaternary sediments is difficult in Melville Bay due to lack of calcareous or organic material in the sediment cores. This may be a result of carbonate dissolution, high input of clastic material or reduced foraminiferal abundances as suggested similar for central and southern Baffin Bay. From relative age dating by relation to glacial landforms in adjacent glacial troughs in central West Greenland, a LGM age for the outer shelf stabilizations and a YD age for the mid-shelf stabilizations were concluded but need further evidence to proof. So far, only one sediment core (GeoB 19920-1; Fig. 7.1) from the inner continental shelf contained dateable material. An AMS radiocarbon dating from the lower section of this core indicates a final ice-stream retreat across the

inner shelf of the southern cross-shelf trough before at least 8.41 ka BP (uncalibrated age 7925 radiocarbon years). This age is in good agreement with datings from previous onshore studies.

Trough network in eastern Melville Bay

In eastern Melville Bay, at the transition between crystalline bedrock and sedimentary sequences on the inner continental shelf of northwest Greenland, systematic surveys with local full coverage were conducted. They indicate a network of submerged glacial troughs or fjords with overdeepenings that are lined with glacial landforms. The troughs are linked to the large cross-shelf troughs of Melville Bay (Fig. 7.1). The data show that the trough network continues further towards the modern glacial fjords and extends under the modern GIS. Thus, a fjord network extending from the cross-shelf troughs towards deep under the modern ice-sheet characterizes the bedrock morphology. It represents a former ice-sheet margin on the inner continental shelf of Greenland.

The network of overdeepened troughs that crosses the crystalline bedrock of Melville Bay likely hosted supercooled paleo-subglacial meltwater at the bed. The overdeepenings furthermore indicate that the ice-sheet margin stabilized in this area either once or repeatedly during past glacial cycles. However, neither exposure dating techniques nor AMS radiocarbon dating can be applied here, making a verification of the age of the troughs difficult.

Many troughs in Melville Bay developed along fractures that relate to major faults in Baffin Bay. The fractures were likely widened and deepened by ice streams draining along them. Erosional glacial landforms along and across the troughs are indicative of the streaming ice. By analogy to similar glaciated bedrock regions, the fractures are suggested to have been previously occupied by rivers draining across the preglacially uplifted bedrock. Variations of the troughs are related to changes in bedrock morphology, e.g. troughs incised in outcropping flood basalts in the south of Melville Bay differ to those in Archaean and reworked Paleo-Proterozoic crystalline bedrock north of it.

The trough network on the inner continental shelf of Greenland extends sub-glacially below the modern Greenland Ice Sheet. The same glacial processes likely form the network under the modern GIS as they did during past glacial advances across the present-day seafloor. As already proposed for the modern GIS, advance of warm Atlantic water to the base of marine terminating glaciers may have also accelerated their retreat in the past. The deep troughs likely acted as pathway of the warm Atlantic waters to the GIS margin accelerating the ice-sheet retreat since the LGM.

Steep ridges in northern Melville Bay

In northern Melville Bay, glacial landforms are mainly expressed in outcropping crystalline bedrock. These outcrops occurred in the northwest Melville Bay near the coast but also at the transition between the northern and central cross-shelf trough of Melville Bay. Most significant glacial landforms in northern Melville Bay are crag-and-tails that developed at steep bedrock ridges (Fig. 7.1). They tend to converge into MSGLs. The ridges that we think are related to large Proterozoic volcanic dyke swarms intruding the lower sedimentary sequences of the Thule Supergroup form the erosional crag-heads. The depositional sedimentary tails form in the down-ice direction of the ice stream. Smaller glacial landforms were eroded in the crystalline bedrock. They show abraded and quarried down-ice sides, indicating past ice-stream orientations.

The glacial landforms along and across the steep ridges in northern Melville Bay indicate that the ridges to some extend had an impact on ice and meltwater orientation. Ice capping the steep ridges allowed meltwater to flow beneath. Ridges inclined oblique to the ice-stream orientation show potholes on their ice-facing sides. The potholes indicate the influence of the ridges on meltwater by occasional blocking the flow and confining its path through narrow cavities. Ridges inclined along the streaming direction aided the meltwater flow that acts as lubricant for the streaming ice.

These landforms influenced southward streaming of the ice and meltwater east of the steep ridges in the northeast Melville Bay as indicated by erosional glacial landforms and channels extending southwards into the central cross-shelf trough. Depositional glacial landforms indicate a westward flow of the ice-streams into the northern cross-shelf trough. This indicates an ice-stream reorganization with westward re-orientation streaming across the steep ridges, likely at times with abundant meltwater, e.g. during retreat with subsequent re-advance.

Thus, by including erosional glacial landforms into the investigation, it was possible to re-analyse the transition between the northern and central cross-shelf troughs. This area was studied before and addressed in the first manuscript. There, based on depositional glacial landforms only, it was suggested that the ice streams operated simultaneously, being channelled around the inter-trough bank. The re-analysis indicates that at least in this part of Melville Bay, simultaneous streaming was less likely. Instead, an ice-stream reorganization with re-orientation into the norther cross-shelf trough is suggested. Nevertheless, this re-organization does not exclude overall ice-stream activity in the central cross-shelf trough, as a shift of the individual ice streams is possible.

8. Outlook

The new acquired bathymetric data from Melville Bay, northeast Baffin Bay, increase our understanding of the northwest Greenland ice sheet dynamics, as seen in the previous chapters. However, this study rose more questions regarding the timing of glacial dynamics and the influence of bedrock on glacial processes in Melville Bay.

Further analysis on the paleo-ice sheet extent

The processing and analysis of the bathymetric data for this thesis laid the foundation for further research. An additional research cruise, expedition MSM66 with *RV Maria S. Merian*, was conducted in summer 2017, surveying northern Baffin Bay (No. 1, Fig. 8.1). Based on the findings of this thesis, the glacial landforms near the shelf edge of Melville Bay were surveyed more extensively. The new data provide information on the distribution of ice marginal landforms in Melville Bay and may thus give further insight into the composition, distribution and the complexity of the moraines and GZWs at the shelf edge. Furthermore, although this task remains difficult in Melville Bay due to lack of dateable calcareous or organic material, dating of glacial landforms is needed in order to understand the timing of the ice-stream retreat since the LGM. In addition, the bathymetric datasets acquired for this study are included in the BedMachine v.3 compilation (Morlighem et al., 2017) (Fig. 8.1), thus, aiding new research of the coast of Greenland and improving the base for future ice-sheet modelling studies.

In summer 2012, a shallow coring program was conducted with the scientific drilling vessel *Joides Resolution* during expedition 344S on the inter-trough bank in northern Melville Bay (No. 2, Fig. 8.1). This program was a joint venture of different companies of the oil industry. This joint venture has also mapped large parts of the continental shelf with 3D seismic data to understand the stratigraphy of Melville Bay for oil and gas exploration. Once publically available, the outcome of this program may further enhance the knowledge of the glacial development of northwest Greenland.

Based on additional seismic data from Melville Bay, Batchelor and Dowdeswell (2016) suggest that the depressions on the inter-trough banks are the result of lateral shear-moraines deposited on the side of the banks. As the outer parts of the lateral moraines shown there are slightly truncated, the elongated depression might be the result of both, shear-moraine deposition and simultaneous erosion by a small ice-stream fed by an ice dome on the bank. To resolve the remaining uncertainties, additional bathymetric surveys combined with sub-bottom and shallow seismic data orthogonal to the elongated

depressions should be recorded and analysed (No. 3, Fig. 8.1). If the findings reveal further MSGL, they may have hosted small ice streams, whereas if the elongated landforms turn out as simple multi-keeled iceberg scours, they are of different origin.

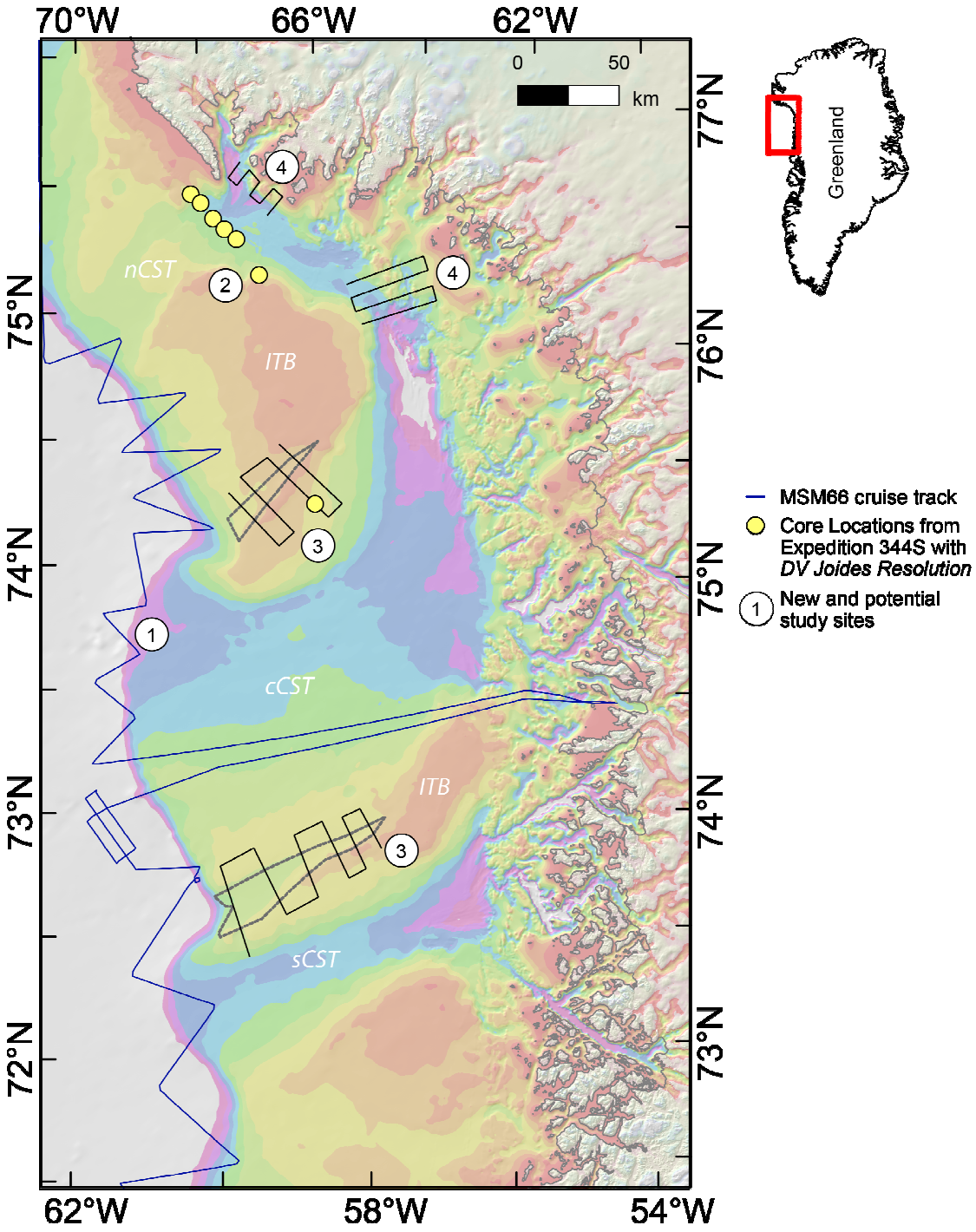

Figure 8.1: Map of new and potential study sites. Background is BedMachine v.3 (Morlighem et al., 2017). Numbers 1-4 indicate new and potential study sites.

Additional bedrock analysis

The relation between troughs and fractures in crystalline bedrock raises the question, if the large glacial cross-shelf troughs and their size are also related to the tectonic arrangement of Baffin Bay. Closely spaced seismic data with focus on glacial erosional and depositional structures bordering the faults of Melville Bay may solve this question. However, before conducting further seismic surveys in Melville Bay, a collaboration with the oil industry that has already seismically surveyed vast parts of Baffin Bay in their individual licensing areas, might be beneficial.

In chapter 6, it was suggested that the steep ridges in northern Melville Bay might be Proterozoic volcanic dyke swarms that developed along faults and fractures. Anomalies in magnetometer surveys orthogonal across the ridges as well as drilling into them could give more insight into their composition (No. 4, Fig. 8.1), as previously done onshore.

Thus, due to lack of additional data, further research is required to understand all aspects and the timing of the Greenland ice-sheet dynamics in Melville Bay.

References

Alley, R.B., Lawson, D.E., Larson, G.J., Evenson, E.B., Baker, G.S., 2003. Stabilizing feedbacks in glacier-bed erosion. Nature 424, 758-760. doi: 10.1038/nature01839

Altenbernd, T., Jokat, W., Heyde, I., Damm, V., 2014. A crustal model for northern Melville Bay, Baffin Bay. Journal of Geophysical Ressearch: Solid Earth 119, 8610-8632. doi: 10.1002/2014JB011559

Altenbernd, T., Jokat, W., Heyde, I., Damm, V., 2015. Geophysical evidence for the extent of crustal types and the type of margin along a profile in the northeastern Baffin Bay. J. Geophys. Res. 120, 7337-7360. doi: 10.1002/2015JB012307

Anandakrishnan, S., Blankenship, D.D., Alley, R.B., Stoffa, P.L., 1998. Influence of subglacial geology on the position of a West Antarctic ice stream from seismic observations. Nature 394, 62-65. doi: 10.1038/27889

Anandakrishnan, S., Catania, G.A., Alley, R.B., Horgan, H.J., 2007. Discovery of Till Deposition at the Grounding Line of Whillans Ice Stream. Science 315, 1835-1838. doi: 10.1126/science.1138393

Anderson, J.B., Fretwell, L.O., 2008. Geomorphology of the onset area of a paleo-ice stream, Marguerite Bay, Antarctic Peninsula. Earth Surface Processes and Landforms 33, 503-512. doi: 10.1002/esp.1662

ArcticNet, 2016. ArcticNet Amundsen Multibeam Data. Ocean Mapping Group, University of New Brunswick Canada.

Arndt, J.E., Jokat, W., Dorschel, B., 2017. The last glaciation and deglaciation of the Northeast Greenland continental shelf revealed by hydro-acoustic data. Quaternary Science Reviews 160, 45-56. doi: 10.1016/j.quascirev.2017.01.018

Arndt, J.E., Jokat, W., Dorschel, B., Myklebust, R., Dowdeswell, J.A., Evans, J., 2015. A new bathymetry of the Northeast Greenland continental shelf: Constraints on glacial and other processes. Geochemistry, Geophysics, Geosystems 16, 3733-3753. doi: 10.1002/2015GC005931

Bamber, J.L., Griggs, J.A., Hurkmans, W.L., Dowdeswell, J.A., Gogineni, P., Howat, I., Mouginot, J., Paden, J., Palmer, S., Rignot, E., Steinhage, D., 2013. A new bed elevation dataset for Greenland. The Cryosphere 7, 499-510. doi: 10.5194/tc-7-499-2013

Batchelor, C.L., Dowdeswell, J.A., 2014. The physiography of High Arctic cross-shelf troughs. Quaternary Science Reviews 92, 68-96. doi: 10.1016/j.quascirev.2013.05.025

Batchelor, C.L., Dowdeswell, J.A., 2015. Ice-sheet grounding-zone wedges (GZWs) on high-latitude continental margins. Mar. Geol. 363, 65-92. doi: 10.1016/j.margeo.2015.02.001

Batchelor, C.L., Dowdeswell, J.A., 2016. Lateral shear-moraines and lateral marginal-moraines of palaeo-ice streams. Quaternary Science Reviews 151, 1-26. doi: 10.1016/j.quascirev.2016.08.020

Benn, D.I., Evans, D.J.A., 2010. Glaciers and glaciation. isbn: 978 0 340 905791

Bennett, M.R., 2001. The morphology, structural evolution and significance of push moraines. Earth-Science Reviews 53, 197-236. doi: 10.1016/S0012-8252(00)00039-8

Bennett, M.R., 2003. Ice streams as the arteries of an ice sheet: their mechanics, stability and significance. Earth-Science Reviews 61, 309-339. doi: 10.1016/S0012-8252(02)00130-7

Bennett, M.R., Glasser, N.F., 2009. Glacial Geology: Ice Sheets and Landforms, second ed. Wiley-Blackwell. isbn: 978-0-470-51690-4

Bennike, O., Björck, S., 2002. Chronology of the last recession of the Greenland Ice Sheet. Journal of Quaternary Science 17, 211-219. doi: 10.1002/jqs.670

Bingham, R.G., King, E.C., Smith, A.M., Pritchard, H.D., 2010. Glacial geomorphology: Towards a convergence of glaciology and geomorphology. Progress in Physical Geography 34, 327-355. doi: 10.1177/0309133309360631

Bonow, J.M., 2005. Re-exposed basement landforms in the Disko region, West Greenland — disregarded data for estimation of glacial erosion and uplift modelling. Geomorphology 72, 106-127. doi: 10.1016/j.geomorph.2005.05.006

Bonow, J.M., Japsen, P., Lidmar-Bergström, K., Chalmers, J.A., Pedersen, A.K., 2006a. Cenozoic uplift of Nuussuaq and Disko, West Greenland—elevated erosion surfaces as uplift markers of a passive margin. Geomorphology 80, 325-337. doi: 10.1016/j.geomorph.2006.03.006

Bonow, J.M., Lidmar-Bergström, K., Japsen, P., 2006b. Palaeosurfaces in central West Greenland as reference for identification of tectonic movements and estimation of erosion. Global and Planetary Change 50, 161-183. doi: 10.1016/j.gloplacha.2005.12.011

Bonow, J.M., Lidmar-Bergström, K., Japsen, P., Chalmers, J.A., Green, P.F., 2007. Elevated erosion surfaces in central West Greenland and southern Norway: their significance in integrated studies of passive margin development. Norwegian Journal of Geology 87, 197-206.

Box, J.E., Fettweis, X., Stroeve, J.C., Tedesco, M., Hall, D.K., Steffen, K., 2012. Greenland ice sheet albedo feedback: thermodynamics and atmospheric drivers. The Cryosphere 6, 821-839. doi: 10.5194/tc-6-821-2012

Buchan, K.L., Ernst, R.E., 2004. Diabase dyke swarms and related units in Canada and adjacent regions; Map 2022A, scale 1:5 000 000. Geological Survey of Canada.

Burrough, P.A., McDonell, R.A., 1998. Principles of Geographical Information Systems. Oxford University Press, New York.

Cazenave, A., Remy, F., 2011. Sea level and climate: measurements and causes of changes. Wiley Interdisciplinary Reviews: Climate Change 2, 647-662. doi: 10.1002/wcc.139

Chalmers, J.A., Pulvertaft, T.C.R., 2001. Development of the continental margins of the Labrador Sea: a review. Geological Society Special Publication 187, 77-105.

Chalmers, J.A., Pulvertaft, T.C.R., Marcussen, C., Pedersen, A.K., 1999. New insight into the structure of the Nuussuaq Basin, central West Greenland. Mar. Petrol. Geol. 16, 197-224. doi: 10.1016/S0264-8172(98)00077-4

Chauché, N., Hubbard, A., Gascard, J.-C., Box, J.E., Bates, R., Koppes, M., Sole, A., Christoffersen, P., Patton, H., 2014. Ice–ocean interaction and calving front morphology at two west Greenland tidewater outlet glaciers. The Cryosphere 8, 1457-1468.

Chen, C.-T., Millero, F.J., 1977. Speed of sound in seawater at high pressures. Journal of the Acoustical Society of America 62, 1129-1135.

Clark, C.D., 1993. Mega-scale glacial lineations and cross-cutting ice-flow landforms. Earth Surface Processes and Landforms 18, 1-29. doi: 10.1002/esp.3290180102

Clark, P.U., Dyke, A.S., Shakun, J.D., Carlson, A.E., Clark, J., Wohlfarth, B., Mitrovica, J.X., Hostetler, S.W., McCabe, A.M., 2009. The Last Glacial Maximum. Science 325, 710-714. doi: 10.1126/science.1172873

Clark, P.U., Mix, A.C., 2002. Ice sheets and sea level of the Last Glacial Maximum. Quaternary Science Reviews 21, 1-7.

Clark, P.U., Pisias, N.G., Stocker, T.F., Weaver, A.J., 2002. The role of the thermohaline circulation in abrupt climate change. Nature 415, 863-869.

Damm, V., 2010. The expedition of the Research Vessel "Polarstern" to the Arctic in 2010 (ARK-XXV/3). Reports on Polar and Marine Research 621, 234. doi: hdl:10013/epic.36297

Dawes, P.R., 1997. The Proterozoic Thule Supergroup, Greenland and Canada: history, lithostratigraphy and development. Geology of Greenland Survey Bulletin 174, 150.

Dawes, P.R., 2006. Explanatory notes to the Geological map of Greenland, 1:500 000, Thule, Sheet 5. Geological Survey of Denmark and Greenland Map Series 2.

Dawes, P.R., Christie, R.L., 1991. Geomorphic regions, in: Trettin, H.P. (Ed.), Geology of the Innuitian Orogen and Arctic Platform of Canada and Greenland. Geological Survey of Canada, Ottawa, pp. 29-56.

Dawes, P.R., Rex, D.C., 1986. Proterozoic basaltic magmatic periods in North-West Greenland: evidence from K/Ar ages, Rapport Grønlands Geologiske Undersøgelse, 130, pp. 24-31.

de Jong, C.D., Lachapelle, G.S., S., Elema, I.A., 2002. Hydrography. Delft University Press. isbn: 90-407-2359-1

Denyszyn, S.W., Halls, H.C., Davis, D.W., 2006. A Paleomagnetic, Geochemical and U-Pb Geochronological Comparison of the Thule (Greenland) and Devon Island (Canada) Dyke Swarms and Its Relevance to the Nares Strait Problem. Polarforschung 74, 63-75. doi: 10013/epic.29925.d001

Domack, E., Amblàs, D., Gilbert, R., Brachfeld, S., Camerlenghi, A., Rebesco, M., Canals, M., Urgeles, R., 2006. Subglacial morphology and glacial evolution of the Palmer deep outlet system, Antarctic Peninsula. Geomorphology 75, 125-142. doi: 10.1016/j.geomorph.2004.06.013

Dorschel, B., Afanasyeva, V., Bender, M., Dreutter, S., Eisermann, H., Gebhardt, A.C., Hansen, K., Hebbeln, D., Jackson, R., Jeltsch-Thömmes, A., Jensen, L., Kolling, H., Le Duc, C., Lenz, K.-F., Lübben, B., Madaj, L., Martínez Mendez, G., Meyer-Schack, B., Schade, T., Siccha, M., Slabon, P., Wangner, D.J., 2015. Short Cruise Report MARIA S. MERIAN – MSM44, in: Ozeanographie, D.-S.f., Bremen, M.Z.f.M.U.d.U. (Eds.), MARIA S. MERIAN-Berichte, p. 148.

Dorschel, B., Afanasyeva, V., Bender, M., Dreutter, S., Eisermann, H., Gebhardt, A.C., Hansen, K., Hebbeln, D., Jackson, R., Jeltsch-Thömmes, A., Jensen, L., Kolling, H., Le Duc, C., Lenz, K.-F., Lübben, B., Madaj, L., Martínez Mendez, G., Meyer-Schack, B., Schade, T., Siccha, M., Slabon, P., Wangner, D.J., 2016. BAFFEAST Past Greenland Ice Sheet dynamics, Palaeoceanography and Plankton Ecology in the Northeast Baffin Bay - Cruise No. MSM44 - June 30 - July 30, 2015 - Nuuk (Greenland) - Nuuk (Greenland). , MARIA S. MERIAN-Berichte. DFG-Senatskommission für Ozeanographie, p. 51. doi: 10.2312/cr_msm44

Dowdeswell, J.A., Canals, M., Jakobsson, M., Todd, B.J., Dowdeswell, E.K., Hogan, K.A., (Eds), 2016. Atlas of Submarine Glacial landforms: Modern, Quaternary and Ancient. Geological Society, London, Memoirs.

Dowdeswell, J.A., Fugelli, E.M.G., 2012. The seismic architecture and geometry of grounding-zone wedges formed at the marine margins of past ice sheets. Geological Society of America Bulletin 124, 1750-1761. doi: 10.1130/b30628.1

Dowdeswell, J.A., Hogan, K.A., Ó Cofaigh, C., Fugelli, E.M.G., Evans, J., Noormets, R., 2014. Late Quaternary ice flow in a West Greenland fjord and cross-shelf trough system: submarine landforms from Rink Isbrae to Uummannaq shelf and slope. Quaternary Science Reviews 92, 292-309. doi: 10.1016/j.quascirev.2013.09.007

Dowdeswell, J.A., Ottesen, D., Evans, J., Ó Cofaigh, C., Anderson, J.B., 2008. Submarine glacial landforms and rates of ice-stream collapse. Geology 36, 819-822. doi: 10.1130/G24808A.1

Dunlop, P., Clark, C.D., 2006. The morphological characteristics of ribbed moraine. Quaternary Science Reviews 25, 1668-1691. doi: 10.1016/j.quascirev.2006.01.002

Dyke, A.S., Andrews, J.T., Clark, P.U., England, J.H., Miller, G.H., Shaw, J., Veillette, J.J., 2002. The Laurentide and Innuitian ice sheets during the Last Glacial Maximum. Quaternary Science Reviews 21, 9-31. doi: 10.1016/s0277-3791(01)00095-6

Dyke, A.S., Hooper, J., Savelle, J.M., 1996. A history of sea ice in the Canadian Arctic Archipelago based on postglacial remains of the bowhead whale (Balaena mysticetus). Arctic 49, 235-255.

Ehlers, J., Gibbard, P.L., 2007. The extent and chronology of Cenozoic Global Glaciation. Quaternary International 164–165, 6-20. doi: 10.1016/j.quaint.2006.10.008

Enderlin, E.M., Howat, I.M., Jeong, S., Noh, M.J., Angelen, J.H., Broeke, M.R., 2014. An improved mass budget for the Greenland ice sheet. Geophysical Research Letters 41, 866-872. doi: 10.1002/2013GL059010

Engelhardt, H., Kamb, B., 1997. Basal hydraulic system of a West Antarctic ice stream: constraints from borehole observations. Journal of Glaciology 43 (144), 207-230.

England, J., 1987. Glaciation and the evolution of the Canadian high arctic landscape. Geology 15, 419-424. doi: 10.1130/0091-7613(1987)15<419:gateot>2.0.co;2

England, J.H., Atkinson, N., Bednarski, J., Dyke, A.S., Hodgson, D.A., Ó Cofaigh, C., 2006. The Innuitian Ice Sheet: configuration, dynamics and chronology. Quaternary Science Reviews 25, 689-703. doi: 10.1016/j.quascirev.2005.08.007

Evans, J., Pudsey, C.J., Ó Cofaigh, C., Morris, P., Domack, E.W., 2005. Late Quaternary glacial history, flow dynamics and sedimentation along the eastern margin of the Antarctic Peninsula Ice Sheet. Quaternary Science Reviews 24, 741-774. doi: 10.1016/j.quascirev.2004.10.007

Fenty, I., Willis, J.K., Khazendar, A., Dinardo, S., Forsberg, R., Fukumori, I., Holland, D., Jakobsson, M., Moller, D., Morison, J., Münchow, A., Rignot, E., Schodlok, M.P., Thompson, A.F., Tinto, K., Rutherford, M., Trenholm, N., 2016. Oceans Melting Greenland: Early Results from NASA's Ocean-Ice Mission in Greenland Oceanography 29.

Freire, F., Gyllencreutz, R., Greenwood, S.L., Mayer, L., Egilsson, A., Thorsteinsson, T., Jakobsson, M., 2015. High resolution mapping of offshore and onshore glaciogenic features in metamorphic bedrock terrain, Melville Bay, northwestern Greenland. Geomorphology 250, 29-40. doi: 10.1016/j.geomorph.2015.08.011

Fretwell, P., Pritchard, H.D., Vaughan, D.G., Bamber, J.L., Barrand, N.E., Bell, R., Bianchi, C., Bingham, R.G., Blankenship, D.D., Casassa, G., Catania, G., Callens, D., Conway, H., Cook, A.J., Corr, H.F.J., Damaske, D., Damm, V., Ferraccioli, F., Forsberg, R., Fujita, S., Furukawa, T., Gogineni, P., Griggs, J.A., Hamilton, G., Hindmarsh, R.C.A., Holmlund, P., Holt, J.W., Jacobel, R.W., Jenkins, A., Jokat, W., Jordan, T., King, E.C., Krabill, W., Riger-Kusk, M., Tinto, K., Langley, K.A., Leitchenkov, G., Luyendyk, B.P., Matsuoka, K., Nixdorf, U., Nogi, Y., Nost, O.A., Popov, S.V., Rignot, E., Rippin, D., Riviera, A., Ross, N., Siegert, M.J., Shibuya, K., Smith, A.M., Steinhage, D., Studinger, M., Sun, B., Thomas, R.H., Tabacco, I., Welch, B., Young, D.A., Xiangbin, C., Zirizzotti, A., 2013. Bedmap2: Improved ice bed, surface and thickness datasets for Antarctica. The Cryosphere 7, 375-393. doi: doi:10.5194/tc-7-375-2013

Funder, S., Feyling-Hanssen, R.W., Houmark-Nielsen, M., Kelly, M., Kronborg, C., Landvik, J., Mejdahl, V., Mörner, N.-A., Petersen, K.S., Sejrup, H.-P., Sorby, L., 1989. The Baffin Bay Region during the Last Interglaciation: Evidence from Northwest Greenland. Géographie physique et Quaternaire 43, No. 3, 255-262.

Funder, S., Hansen, L., 1996. The Greenland ice sheet - a model for its culmination and decay during and after the last glacial maximum. Bulletin of the Geological Society of Denmark 42, 137-152.

Funder, S., Jennings, A., Kelly, M., 2004. Middle and late quaternary glacial limits in Greenland, in: Ehlers, J., Gibbard, P.L. (Eds.), Developments in Quaternary Sciences. Elsevier, Amsterdam, pp. 425-430. doi: 10.1016/S1571-0866(04)80210-0

Funder, S., Kjeldsen, K.K., Kjær, K.H., Ó Cofaigh, C., 2011. The Greenland Ice Sheet During the Past 300,000 Years: A Review, in: Ehlers, J., Gibbard, P.L., Hughes, P.D. (Eds.), Quaternary Glaciations - Extent and Chronology A Closer Look, pp. 699-713. 978-0-444-53447-7

Funder, S., Weidick, A., 1991. Holocene boreal molluscs in Greenland - palaeoceanographic implications. Palaeogeography, Palaeoclimatology, Palaeoecology 85, 123-135. doi: 10.1016/0031-0182(91)90029-Q

Glasser, N.F., Bennett, M.R., 2004. Glacial erosional landforms: origins and significance for palaeoglaciology. Progress in Physical Geography 28, 43-75. doi: 10.1191/0309133304pp401ra

Glasser, N.F., Ghiglione, M.C., 2009. Structural, tectonic and glaciological controls on the evolution of fjord landscapes. Geomorphology 105, 291-302. doi: 10.1016/j.geomorph.2008.10.007

Glasser, N.F., Warren, C.R., 1990. Medium Scale Landforms of Glacial Erosion in South Greenland; Process and Form. Geografiska Annaler. Series A, Physical Geography 72, 211-215. doi: 10.2307/521149

Graham, A.G.C., Larter, R.D., Gohl, K., Hillenbrand, C.-D., Smith, J.A., Kuhn, G., 2009. Bedform signature of a West Antarctic palaeo-ice stream reveals a multi-temporal record of flow and substrate control. Quaternary Science Reviews 28, 2774-2793. doi: 10.1016/j.quascirev.2009.07.003

Graham, A.G.C., Nitsche, F.O., Larter, R.D., 2011. An improved bathymetry compilation for the Bellingshausen Sea, Antarctica, to inform ice-sheet and ocean models. The Cryosphere 5, 95-106. doi: 10.5194/tc-5-95-2011

Gregersen, U., Hopper, J.R., Knutz, P.C., 2013. Basin seismic stratigraphy and aspects of prospectivity in the NE Baffin Bay, Northwest Greenland. Mar. Petrol. Geol. 46, 1-18. doi: 10.1016/j.marpetgeo.2013.05.013

Groh, A., Ewert, H., Fritsche, M., Rülke, A., Rosenau, R., Scheinert, M., Dietrich, R., 2014. Assessing the Current Evolution of the Greenland Ice Sheet by Means of Satellite and Ground-Based Observations. Surveys in Geophysics 35, 1459-1480. doi: 10.1007/s10712-014-9287-x

Gyllencreutz, R., Freire, F., Greenwood, S.L., Mayer, L.A., Jakobsson, M., 2016. Glacial landforms in a hard bedrock terrain, Melville Bay, northwestern Greenland. Geological Society, London, Memoirs 46, 201-202.

Harrison, J.C., Brent, T.A., Oakey, G.N., 2006. Bedrock Geology of the Nares Strait Region of Arctic Canada and Greenland, with explanatory text and GIS content. Geological Suvey of Canada Open File 5278, 60. doi: 10.4095/222524

Harrison, J.C., St-Onge, M.R., Petrov, O., Strelnikov, S., Lopatin, B., Wilson, F., Tella, S., Paul, D., Lynds, T., Shokalsky, S., Hults, C., Bergmann, S., Jepsen, H.F., Solli, A., 2008. Geological map of the Arctic. Geological Survey of Canada.

Harrison, J.C., St-Onge, M.R., Petrov, O.V., Strelnikov, S.I., Lopatin, B.G., Wilson, F.H., Tella, S., Paul, D., Lynds, T., Shokalsky, S.P., Hults, C.K., Bergman, S., Jepsen, H.F., Solli, A., 2011. Geological map of the Arctic, Map 2159A, scale 1:5 000 000. Geological Survey of Canada.

Hättestrand, C., 1997. Ribbed moraines in Sweden — distribution pattern and palaeoglaciological implications. Sedimentary Geology 111, 41-56. doi: 10.1016/S0037-0738(97)00005-5

Heezen, B.C., Tharp, M., Ewing, M., 1959. The Floors of the Oceans: I. The North Atlantic. Geological Society of America, Special Papers 65.

Hofmann, J.C., Knutz, P.C., Nielsen, T., Kuijpers, A., 2016. Seismic architecture and evolution of the Disko Bay trough-mouth fan, central West Greenland margin. Quaternary Science Reviews. doi: 10.1016/j.quascirev.2016.05.019

Hogan, K.A., Cofaigh, C.Ó., Jennings, A.E., Dowdeswell, J.A., Hiemstra, J.F., 2016. Deglaciation of a major palaeo-ice stream in Disko Trough, West Greenland. Quaternary Science Reviews 147, 5-26. doi: 10.1016/j.quascirev.2016.01.018

Hogan, K.A., Dowdeswell, J.A., Ó Cofaigh, C., 2012. Glacimarine sedimentary processes and depositional environments in an embayment fed by West Greenland ice streams. Mar. Geol. 311-314, 1-16. doi: 10.1016/j.margeo.2012.04.006

Holland, D.M., Thomas, R.H., de Young, B., Ribergaard, M.H., Lyberth, B., 2008. Acceleration of Jakobshavn Isbræ triggered by warm subsurface ocean waters. Nature Geoscience 1, 659-664. doi: 10.1038/ngeo316

Horgan, H.J., Anandakrishnan, S., 2006. Static grounding lines and dynamic ice streams: Evidence from the Siple Coast, West Antarctica. Geophysical Research Letters 33. doi: 10.1029/2006GL027091

Howat, I.M., Negrete, A., Smith, B.E., 2014. The Greenland Ice Mapping Project (GIMP) land classification and surface elevation data sets. The Cryosphere 8, 1509-1518. doi: 10.5194/tc-8-1509-2014

IPCC, 2013. Climate Change 2013: The Physical Science Basis. Contribution of Working Group I to the Fifth Assessment Report of the Intergovernmental Panel on Climate Change, in: Stocker, T.F., Qin, D., Plattner, G.-K., Tignor, M.M.B., Allen, S.K., Boschung, J., Nauels, A., Xia, Y., Bex, V., Midgley, P.M. (Eds.), Cambridge, United Kingdom and New York, NY, USA, p. 1535.

Jakobsson, M., Anderson, J.B., Nitsche, F.O., Gyllencreutz, R., Kirshner, A.E., Kirchner, N., O'Regan, M., Mohammad, R., Eriksson, B., 2012a. Ice sheet retreat dynamics inferred from glacial morphology of the central Pine Island Bay Trough, West Antarctica. Quaternary Science Reviews. doi: 10.1016/j.quascirev.2011.12.017

Jakobsson, M., Andreassen, K., Bjarnadóttir, L.R., Dove, D., Dowdeswell, J.A., England, J.H., Funder, S., Hogan, K., Ingólfsson, Ó., Jennings, A., Krog-Larsen, N., Kirchner, N., Landvik, J.Y., Mayer, L., Mikkelsen, N., Möller, P., Niessen, F., Nilsson, J., O'Regan, M., Polyak, L., Nørgaard-Pedersen, N., Stein, R., 2014. Arctic Ocean glacial history. Quaternary Science Reviews 92, 40-67. doi: 10.1016/j.quascirev.2013.07.033

Jakobsson, M., Gyllencreutz, R., Mayer, L.A., Dowdeswell, J.A., Canals, M., Todd, B.J., Dowdeswell, E.K., Hogan, K.A., Larter, R.D., 2016. Mapping submarine glacial landforms using acoustic methods. Geological Society, London, Memoirs 46, 17-40. doi: 10.1144/m46.182

Jakobsson, M., Mayer, L.A., Coakley, B., Dowdeswell, J.A., Forbes, S., Fridman, B., Hodnesdal, H., Noormets, R., Pedersen, R., Rebesco, M., Schenke, H.-W., Zarayskaya, Y., Accettella, D., Armstrong, A., Anderson, R.M., Bienhoff, P., Camerlenghi, A., Church, I., Edwards, M., Gardner, J.V., Hall, J.K., Hell, B., Hestvik, O.B., Kristoffersen, Y., Marcussen, C., Mohammad, R., Mosher, D., Nghiem, S.V., Pedrosa, M.T., Travaglini, P.G., Weatherall, P., 2012b. The International Bathymetric Chart of the Arctic Ocean (IBCAO) Version 3.0. Geophysical Research Letters 39. doi: 10.1029/2012GL052219

Jansen, E., Fronval, T., Rack, F., Channell, J.E.T., 2000. Pliocene-Pleistocene ice rafting history and cyclicity in the Nordic Seas during the last 3.5 Myr. Paleoceanography 15, 709-721. doi: 10.1029/1999PA000435

Jansson, K.N., Kleman, J., Marchant, D.R., 2002. The succession of ice-flow patterns in north-central Quebec-Labrador, Canada. Quaternary Science Reviews 21, 503-523.

Japsen, P., Bonow, J.M., Green, P.F., Chalmers, J.A., Lidmar-Bergström, K., 2006. Elevated, passive continental margins: Long-term highs or Neogene uplifts? New evidence from West Greenland. EPSL 248, 330-339. doi: 10.1016/j.epsl.2006.05.036

Jennings, A.E., Andrews, J.T., Ó Cofaigh, C., Onge, G.S., Sheldon, C., Belt, S.T., Cabedo-Sanz, P., Hillaire-Marcel, C., 2017a. Ocean forcing of Ice Sheet retreat in central west Greenland from LGM to the early Holocene. EPSL 472, 1-13. doi: 10.1016/j.epsl.2017.05.007

Jennings, A.E., Andrews, J.T., Ó Cofaigh, C., St-Onge, G., Belt, S.T., Cabedo-Sanz, P., Pearce, C., Hillaire-Marcel, C., Campbell, D.C., 2017b. Baffin Bay paleoenvironments in the LGM and HS1: Resolving the ice-shelf question. Mar. Geol. doi: 10.1016/j.margeo.2017.09.002

Jennings, A.E., Sheldon, C., Cronin, T.M., Francus, P., Stoner, J., Andrews, J., 2011. The Holocene History of Nares Strait: Transition from Glacial Bay to Arctic-Atlantic Throughflow. Oceanography 24, 26-41.

Jennings, A.E., Walton, M.E., Ó Cofaigh, C., Kilfeather, A., Andrews, J.T., Ortiz, J.D., De Vernal, A., Dowdeswell, J.A., 2014. Paleoenvironments during Younger Dryas-Early Holocene retreat of the Greenland Ice Sheet from outer Disko Trough, central west Greenland. Journal of Quaternary Science 29, 27-40. doi: 10.1002/jqs.2652

Joughin, I., Abdalati, W., Fahnestock, M., 2004. Large fluctuations in speed on Greenland's Jakobshavn Isbræ glacier. Nature 432, 608-610. doi: 10.1038/nature03130

Joughin, I., Smith, B.E., Howat, I.M., Scambos, T., Moon, T., 2010. Greenland flow variability from ice-sheet-wide velocity mapping. Journal of Glaciology 56, 415-430. doi: 10.3189/002214310792447734

Kalsbeek, F., 1986. The tectonic framework of the Precambrian shield of Greenland. A review of new isotopic evidence, in: Kalsbeek, F., Watt, W.S. (Eds.), Developments in Greenland geology, Rapport Grønlands Geologiske Undersøgelse, 128, pp. 55–64.

Kaufman, D.S., Ager, T.A., Anderson, N.J., Anderson, P.M., Andrews, J.T., Bartlein, P.J., Brubaker, L.B., Coats, L.L., Cwynari, L.C., Duvall, M.L., Dyke, A.S., Edwards, M.E., Eisner, W.R., Gajewski, K., Geirsdóttir, A., Hu, F.S., Jennings, A.E., Kaplan, M.R., Kerwin, M.W., Lozhkin, A.V., MacDonald, G.M., Miller, G.H., Mock, C.J., Oswald, W.W., Otto-Bliesner, B.L., Porinchu, D.F., Rühland, K., Smol, J.P., Steig, E.J., Wolfe, B.B., 2004. Holocene thermal maximum in the western Arctic (0–180°W). Quaternary Science Reviews 23, 529-560. doi: 10.1016/j.quascirev.2003.09.007

Kelley, S.E., Briner, J.P., Young, N.E., 2013. Rapid ice retreat in Disko Bugt supported by 10Be dating of the last recession of the western Greenland Ice Sheet. Quaternary Science Reviews 82, 13-22. doi: 10.1016/j.quascirev.2013.09.018

Khan, S.A., Aschwanden, A., Bjørk, A.A., Wahr, J., Kjeldsen, K.K., Kjær, K.H., 2015. Greenland ice sheet mass balance: a review. Reports on Progress in Physics 78. doi: 10.1088/0034-4885/78/4/046801

King, E.C., Hindmarsh, R.C.A., Stokes, C.R., 2009. Formation of mega-scale glacial lineations observed beneath a West Antarctic ice stream. nature Geoscience 2, 585-588. doi: 10.1038/NGEO581

Kjær, K.H., Khan, S.A., Korsgaard, N.J., Wahr, J., Bamber, J.L., Hurkmans, R., van den Broeke, M.R., Timm, L.H., Kjeldsen, K.K., Bjørk, A.A., Larsen, N.K., Jørgensen, L.T., Færch-Jensen, A.,

Willerslev, E., 2012. Aerial Photographs Reveal Late–20th-Century Dynamic Ice Loss in Northwestern Greenland. Science 337, 569-573. doi: 10.1126/science.1220614

Klages, J.P., Kuhn, G., Graham, A.G.C., Hillenbrand, C.D., Smith, J.A., Nitsche, F.O., Larter, R.D., Gohl, K., 2015. Palaeo-ice stream pathways and retreat style in the easternmost Amundsen Sea Embayment, West Antarctica, revealed by combined multibeam bathymetric and seismic data. Geomorphology 245, 207-222. doi: 10.1016/j.geomorph.2015.05.020

Kleman, J., 1994. Preservation of landforms under ice sheets and ice caps. Geomorphology 9, 19-32. doi: 10.1016/0169-555X(94)90028-0

Kleman, J., Borgström, I., 1996. Reconstruction of paleo-ice sheets: the use of geomorphological data. Earth Surface Processes and Landforms 21, 893-909. doi: 10.1002/(SICI)1096-9837(199610)21:10<893::AID-ESP620>3.0.CO;2-U

Knudsen, K.L., Stabell, B., Seidenkrantz, M.-S., Eiríksson, J., Blake, W., Jr., 2008. Deglacial and Holocene conditions in northernmost Baffin Bay: sediments, foraminifera, diatoms and stable isotopes. Boreas 37, 346-376. doi: 10.1111/j.1502-3885.2008.00035.x

Knutz, P.C., Hopper, J.R., Gregersen, U., Nielsen, T., Japsen, P., 2015. A contourite drift system on the Baffin Bay–West Greenland margin linking Pliocene Arctic warming to poleward ocean circulation. Geology 43, 907-910. doi: 10.1130/g36927.1

Krabbendam, M., Bradwell, T., 2014. Quaternary evolution of glaciated gneiss terrains: pre-glacial weathering vs. glacial erosion. Quaternary Science Reviews 95, 20-42. doi: 10.1016/j.quascirev.2014.03.013

Krabbendam, M., Eyles, N., Putkinen, N., Bradwell, T., Arbelaez-Moreno, L., 2016. Streamlined hard beds formed by palaeo-ice streams: A review. Sedimentary Geology 338, 24-50. doi: 10.1016/j.sedgeo.2015.12.007

Krabbendam, M., Glasser, N.F., 2011. Glacial erosion and bedrock properties in NW Scotland: Abrasion and plucking, hardness and joint spacing. Geomorphology 130, 374-383. doi: 10.1016/j.geomorph.2011.04.022

Lane, T.P., Roberts, D.H., Rea, B.R., Ó Cofaigh, C., Vieli, A., 2015. Controls on bedrock bedform development beneath the Uummannaq Ice Stream onset zone, West Greenland. Geomorphology 231, 301-313. doi: 10.1016/j.geomorph.2014.12.019

Larter, R.D., Graham, A.G.C., Gohl, K., Kuhn, G., Hillenbrand, C.-D., Smith, J.A., Deen, T.J., Livermore, R.A., Schenke, H.-W., 2009. Subglacial bedforms reveal complex basal regime in a zone of paleo-ice stream convergence, Amundsen Sea Embayment, West Antarctica. Geology 37, 411-414. doi: 10.1130/G25505A.1

Lavoie, C., Domack, E.W., Pettit, E.C., Scambos, T.A., Larter, R.D., Schenke, H.W., Yoo, K.C., Gutt, J., Wellner, J., Canals, M., Anderson, J.B., Amblas, D., 2015. Configuration of the Northern Antarctic Peninsula Ice Sheet at LGM based on a new synthesis of seabed imagery. The Cryosphere 9, 613-629. doi: 10.5194/tc-9-613-2015

Levac, E., De Vernal, A., Blake, W., Jr., 2001. Sea-surface conditions in northernmost Baffin Bay during the Holocene: palynological evidence. Journal of Quaternary Science 16, 353-363. doi: 10.1002/jqs.614

Leventer, A., Domack, E., Dunbar, R., Pike, J., Brachfeld, S., Stickley, C., Maddison, E., Manley, P., McClennen, C., 2006. Marine sediment record from the East Antarctic margin reveals dynamics of ice sheet recession. GSA Today 16, No. 12, 4-10. doi: 10.1130/GSAT01612A.1

Løken, O.H., Hodgson, D.A., 1971. On the Submarine Geomorphology Along the East Coast of Baffin Island. Canadian Journal of Earth Sciences 8, 185-195. doi: 10.1139/e71-020

Long, A.J., Roberts, D.H., 2003. Late Weichselian deglacial history of Disko Bugt, West Greenland, and the dynamics of the Jakobshavns Isbrae ice stream. Boreas 32, 208-226. doi: 10.1111/j.1502-3885.2003.tb01438.x

Lurton, X., 2004. An Introduction to Underwater Acoustics: Principles and Applications. Springer-Verlag, Praxis Publishing. isbn: 3-540-42967-0

Lynch-Stieglitz, J., Curry, W.B., Slowey, N., 1999. Weaker Gulf Stream in the Florida Straits during the Last Glacial Maximum. Nature 402, 644-648.

Margold, M., Stokes, C.R., Clark, C.D., 2015. Ice streams in the Laurentide Ice Sheet: Identification, characteristics and comparison to modern ice sheets. Earth-Science Reviews 143, 117-146. doi: 10.1016/j.earscirev.2015.01.011

McNeely, R., Dyke, A.S., Southon, J.R., 2006. Canadian marine reservoir ages, preliminary data assessment, Open File 5049. Geological Survey Canada, 3.

Moore, T.C., 2005. The Younger Dryas: From whence the fresh water? Paleoceanography 20, PA4021. doi: 10.1029/2005pa001170

Morlighem, M., Rignot, E., Mouginot, J., Seroussi, H., Larour, E., 2014a. Deeply incised submarine glacial valleys beneath the Greenland ice sheet. Nature Geosci 7, 418-422. doi: 10.1038/ngeo2167

Morlighem, M., Rignot, E., Mouginot, J., Seroussi, H., Larour, E., 2014b. High-resolution ice-thickness mapping in South Greenland. doi: 10.3189/2014AoG67A088

Morlighem, M., Rignot, E., Willis, J.K., 2016. Improving Bed Topography Mapping of Greenland Glaciers Using NASA's Oceans Melting Greenland (OMG) Data. Oceanography 29. doi: 10.5670/oceanog.2016.99

Morlighem, M., Williams, C.N., Rignot, E., An, L., Arndt, J.E., Bamber, J.L., Catania, G., Chauché, N., Dowdeswell, J.A., Dorschel, B., Fenty, I., Hogan, K., Howat, I., Hubbard, A., Jakobsson, M., Jordan, T.M., Kjeldsen, K.K., Millan, R., Mayer, L., Mouginot, J., Noël, B.P.Y., Ó Cofaigh, C., Palmer, S., Rysgaard, S., Seroussi, H., Siegert, M.J., Slabon, P., Straneo, F., van den Broeke, M.R., Weinrebe, W., Wood, M., Zinglersen, K.B., 2017. BedMachine v3: Complete bed topography and ocean bathymetry mapping of Greenland from multi-beam echo sounding combined with mass conservation. Geophysical Research Letters 44, 11051-11061. doi: 10.1002/2017GL074954

Mörner, N.-A., Funder, S., 1990. C-14 dating of samples collected during the NORDQUA 86 expedition, and notes on the marine reservoir effect. - Appendix. In Funder, S. (ed.), Late Quaternary stratigraphy and glaciology in the Thule area, Northwest Greenland. - Meddelelser om Grønland. Geoscience 22, 57-63.

Neben, S., Damm, V., Brent, T., Tessensohn, F., 2006. New Multi-Channel Seismic Reflection Data from Northwater Bay, Nares Strait: Indications for Pull-Apart Tectonics. Polarforschung 74, 77-96.

Nesje, A., Whillans, I.M., 1994. Erosion of Sognefjord, Norway. Geomorphology 9, 33-45. doi: 10.1016/0169-555X(94)90029-9

Newton, A.M.W., Knutz, P.C., Huuse, M., Gannon, P., Brocklehurst, S.H., Clausen, O.R., Gong, Y., 2017. Ice stream reorganization and glacial retreat on the northwest Greenland shelf. Geophysical Research Letters, n/a-n/a. doi: 10.1002/2017GL073690

Nghiem, S.V., Hall, D.K., Mote, T.L., Tedesco, M., Albert, M.R., Keegan, K., Shuman, C.A., DiGirolamo, N.E., Neumann, G., 2012. The extreme melt across the Greenland ice sheet in 2012. Geophysical Research Letters 39. doi: 10.1029/2012GL053611

Nielsen, T., Kuijpers, A., 2013. Only 5 southern Greenland shelf edge glaciations since the early Pliocene. Scientific Reports 3, 1875. doi: 10.1038/srep01875

Nielsen, T.F.D., 1990. Melville Bugt dyke swarm: a major 1645 Ma alkaline magmatic event in West Greenland, in: Parker, A.J., Rickwood, P.C., Tucker, D.H. (Eds.), Mafic dykes and emplacement mechanisms. A.A. Balkema, Rotterdam, pp. 497-505.

Nitsche, F.O., Gohl, K., Larter, R.D., Hillenbrand, C.D., Kuhn, G., Smith, J.A., Jacobs, S., Anderson, J.B., Jakobsson, M., 2013. Paleo ice flow and subglacial meltwater dynamics in Pine Island Bay, West Antarctica. The Cryosphere 7, 249-262. doi: 10.5194/tc-7-249-2013

NOAA, N.O.a.A.A., 2016. Bathymetric Data Viewer, 2.5.2 ed.

O'Leary, D.W., Friedman, J.D., Pohn, H.A., 1976. Lineament, linear, lineation: Some proposed new standards for old terms. GSA Bulletin 87, 1463-1469. doi: 10.1130/0016-7606(1976)87<1463:LLLSPN>2.0.CO;2

Ó Cofaigh, C., Andrews, J.T., Jennings, A.E., Dowdeswell, J.A., Hogan, K.A., Kilfeather, A.A., Sheldon, C., 2013a. Glacimarine lithofacies, provenance and depositional processes on a West Greenland trough-mouth fan. Journal of Quaternary Science 28, 13-26. doi: 10.1002/jqs.2569

Ó Cofaigh, C., Dowdeswell, J.A., Evans, J., Larter, R.D., 2008. Geological constraints on Antarctic palaeo-ice-stream retreat. Earth Surface Processes and Landforms 33, 513-525. doi: 10.1002/esp.1669

Ó Cofaigh, C., Dowdeswell, J.A., Jennings, A.E., Hogan, K.A., Kilfeather, A., Hiemstra, J.F., Noormets, R., Evans, J., McCarthy, D.J., Andrews, J.T., Lloyd, J.M., Moros, M., 2013b. An extensive and dynamic ice sheet on the West Greenland shelf during the last glacial cycle. Geology 41, 219-222. doi: 10.1130/G33759.1

Ó Cofaigh, C., Evans, D.J.A., Smith, I.R., 2010. Large-scale reorganization and sedimentation of terrestrial ice streams during late Wisconsinan Laurentide Ice Sheet deglaciation. GSA Bulletin 122, 743-756. doi: 10.1130/B26476.1

Ó Cofaigh, C., Pudsey, C.J., Dowdeswell, J.A., Morris, P., 2002. Evolution of subglacial bedforms along a paleo-ice stream, Antarctic Peninsula continental shelf. Geophysical Research Letters 29, 41-44. doi: 10.1029/2001gl014488

Oakey, G.N., Chalmers, J.A., 2012. A new model for the Paleogene motion of Greenland relative to North America: Plate reconstructions of the Davis Strait and Nares Strait regions between Canada and Greenland. J. Geophys. Res. 117. doi: 10.1029/2011JB008942

Oakey, G.N., Damaske, D., 2004. Continuity of Basement Structures and Dyke Swarms in the Kane Basin Region of Central Nares Strait Constrained by Aeromagnetic Data. Polarforschung 74 (1-3), 51-62.

OMG-Mission, 2016. Bathymetry (sea floor depth) data from the ship-based bathymetry survey, 0.1 ed. OMG SDS, CA, USA. doi: 10.5067/OMGEV-BTYSS

Ottesen, D., Dowdeswell, J.A., Landvik, J.Y., Mienert, J., 2007. Dynamics of the Late Weichselian ice sheet on Svalbard inferred from high-resolution sea-floor morphology. Boreas 36, 286-306. doi: 10.1080/03009480701210378

Ottesen, D., Dowdeswell, J.A., Rise, L., 2005. Submarine landforms and the reconstruction of fast-flowing ice streams within a large Quaternary ice sheet: The 2500-km-long Norwegian-Svalbard margin (57°–80°N). GSA Bulletin 117, 1-18. doi: doi: 10.1130/B25577.1

Ottesen, D., Stokes, C.R., Rise, L., Olsen, L., 2008. Ice-sheet dynamics and ice streaming along the coastal parts of northern Norway. Quaternary Science Reviews 27, 922-940. doi: 10.1016/j.quascirev.2008.01.014

Pieńkowski, A.J., England, J.H., Furze, M.F.A., MacLean, B., Blasco, S., 2013. The late Quaternary environmental evolution of marine Arctic Canada: Barrow Strait to Lancaster Sound. Quaternary Science Reviews. doi: 10.1016/j.quascirev.2013.09.025

Reimer, P.J., Bard, E., Bayliss, A., Beck, J.W., Blackwell, P.G., C., B.R., Buck, C.E., Cheng, H., Edwards, R.L., Friedrich, M., Grootes, P.M., Guilderson, T.P., Haflidason, H., Hajdas, I., Hatté, C., Heaton, T.J., Hogg, A.G., Hughen, K.A., Kaiser, K.F., Kromer, B., Manning, S.W., Niu, M., Reimer, R.W., Richards, D.A., Scott, E.M., Southon, J.R., Staff, R., Turney, C.S.M., van der Plicht, J., 2013. IntCal13 and Marine13 Radiocarbon Age Calibration Curves 0–50,000 Years cal BP. Radiocarbon 55, No 4, 1869-1887. doi: 10.2458/azu_js_rc.55.16947

Renssen, H., Seppäb, H., Crosta, X., Goosse, H., Roche, D.M., 2012. Global characterization of the Holocene Thermal Maximum. Quaternary Science Reviews 48, 7-19. doi: 10.1016/j.quascirev.2012.05.022

Rignot, E., Fenty, I., Menemenlis, D., Xu, Y., 2012. Spreading of warm ocean waters around Greenland as a possible cause for glacier acceleration. Annals of Glaciology 53 (60), 257-266. doi: 10.3189/2012AoG60A136

Rignot, E., Fenty, I., Xu, Y., Cai, C., Kemp, C., 2015. Undercutting of marine-terminating glaciers in West Greenland. Geophysical Research Letters 42, 5909-5917. doi: 10.1002/2015GL064236

Rignot, E., Fenty, I., Xu, Y., Cai, C., Velicogna, I., Cofaigh, C.Ó., Dowdeswell, J.A., Weinrebe, W., Catania, G., Duncan, D., 2016. Bathymetry data reveal glaciers vulnerable to ice-ocean interaction in Uummannaq and Vaigat glacial fjords, west Greenland. Geophysical Research Letters 43, 2667-2674. doi: 10.1002/2016GL067832

Rignot, E., Kanagaratnam, P., 2006. Changes in the Velocity Structure of the Greenland Ice Sheet. Science 311, 986-990. doi: 10.1126/science.1121381

Rignot, E., Koppes, M., Velicogna, I., 2010. Rapid submarine melting of the calving faces of West Greenland glaciers. Nature Geosci 3, 187-191. doi: 10.1038/ngeo765

Rignot, E., Velicogna, I., van den Broeke, M.R., Monaghan, A., Lenaerts, J.T.M., 2011. Acceleration of the contribution of the Greenland and Antarctic ice sheets to sea level rise. Geophysical Research Letters 38, 1-5. doi: 10.1029/2011GL046583

Rinterknecht, V., Jomelli, V., VBrunstein, D., Favier, V., Masson-Delmotte, V., Bourlès, D., Leanni, L., Schläppy, R., 2014. Unstable ice stream in Greenland during the Younger Dryas cold event. Geology 42, 759–762. doi: 10.1130/G35929.1

Roberts, D.H., Long, A.J., Schnabel, C., Davies, B.J., Xu, S., Simpson, M.J.R., Huybrechts, P., 2009. Ice sheet extent and early deglacial history of the southwestern sector of the Greenland Ice Sheet. Quaternary Science Reviews 28, 2760-2773. doi: 10.1016/j.quascirev.2009.07.002

Roberts, D.H., Rea, B.R., Lane, T.P., Schnabel, C., Rodés, A., 2013. New constraints on Greenland ice sheet dynamics during the last glacial cycle: Evidence from the Uummannaq ice stream system. J. Geophys. Res. 118, 519-541. doi: 10.1002/jgrf.20032

Rydningen, T.A., Vorren, T.O., Laberg, J.S., Kolstad, V., 2013. The marine-based NW Fennoscandian ice sheet: glacial and deglacial dynamics as reconstructed from submarine landforms. Quaternary Science Reviews 68, 126-141. doi: 10.1016/j.quascirev.2013.02.013

Schoof, C., 2010. Ice-sheet acceleration driven by melt supply variability. Nature 468, 803-806. doi: 10.1038/nature09618

Seidenkrantz, M.-S., Ebbesen, H., Aagaard-Sørensen, S., Moros, M., Lloyd, J.M., Olsen, J., Knudsen, M.F., Kuijpers, A., 2013. Early Holocene large-scale meltwater discharge from Greenland documented by foraminifera and sediment parameters. Palaeogeography, Palaeoclimatology, Palaeoecology 391, Part A, 71-81. doi: 10.1016/j.palaeo.2012.04.006

Shaw, R., 1997. Variations in sub-tropical deep weathering profiles over the Kowloon Granite, Hong Kong. Journal of the Geological Society 154, 1077-1085. doi: 10.1144/gsjgs.154.6.1077

Sheldon, C., Jennings, A., Andrews, J.T., Ó Cofaigh, C., Hogan, K., Dowdeswell, J.A., Seidenkrantz, M.-S., 2016. Ice stream retreat following the LGM and onset of the west Greenland current in Uummannaq Trough, west Greenland. Quaternary Science Reviews 147, 27-46. doi: 10.1016/j.quascirev.2016.01.019

Shipp, S.S., Wellner, J.S., Anderson, J.B., 2002. Retreat signature of a polar ice stream: sub-glacial geomorphic features and sediments from the Ross Sea, Antarctica, in: Dowdeswell, J.A., Ó Cofaigh, C. (Eds.), Glacier-Influences Sedimentation on High Latitude Continental Margins. The Geologial Society of London, Special Publications, London, pp. 277-304.

Shreve, R.L., 1972. Movement of Water in Glaciers. Journal of Glaciology 11 (62), 205-214.

Simpson, M.J.R., Milne, G.A., Huybrechts, P., Long, A.J., 2009. Calibrating a glaciological model of the Greenland ice sheet from the Last Glacial Maximum to present-day using field observations of relative sea level and ice extent. Quaternary Science Reviews 28, 1631-1657. doi: 10.1016/j.quascirev.2009.03.004

Slabon, P., Dorschel, B., Jokat, W., Myklebust, R., Hebbeln, D., Gebhardt, C., 2016. Greenland ice sheet retreat history in the northeast Baffin Bay based on high-resolution bathymetry. Quaternary Science Reviews 154, 182-198. doi: 10.1016/j.quascirev.2016.10.022

Smith, J.A., Hillenbrand, C.-D., Larter, R.D., Graham, A.G.C., Kuhn, G., 2009. The sediment infill of subglacial meltwater channels on the West Antarctic continental shelf. Quat. Res. 71, 190-200. doi: doi:10.1016/j.yqres.2008.11.005

Smith, W.H.F., Sandwell, D.T., 1997. Global sea floor topography from satellite altimetry and ship depth soundings. Science 277, 1956–1962.

Sommerhoff, G., 1979. Submarine glazial übertiefte Täler vor Südgrönland. Eiszeitalter und Gegenwart 29, 201-213.

Spagnolo, M., Clark, C.D., Ely, J.C., Stokes, C.R., Anderson, J.B., Andreassen, K., Graham, A.G.C., King, E.C., 2014. Size, shape and spatial arrangement of mega-scale glacial lineations from a large and diverse dataset. Earth Surface Processes and Landforms 39, 1432-1448. doi: 10.1002/esp.3532

Steenfelt, A., Thomassen, B., Lind, M., Kyed, J., 1998. Karrat 97: reconnaissance mineral exploration in central West Greenland. Geology of Greenland Survey Bulletin 180, 73-80.

Stokes, C.R., Clark, C.D., 2001. Palaeo-ice streams. Quaternary Science Reviews 20, 1437-1457. doi: 10.1016/S0277-3791(01)00003-8

Stokes, C.R., Lian, O.B., Tulaczyk, S., Clark, C.D., 2008. Superimposition of ribbed moraines on a palaeo-ice-stream bed: implications for ice stream dynamics and shutdown. Earth Surface Processes and Landforms 33, 593-609. doi: 10.1002/esp.1671

Stokes, C.R., Spagnolo, M., Clark, C.D., 2011. The composition and internal structure of drumlins: Complexity, commonality, and implications for a unifying theory of their formation. Earth-Science Reviews 107, 398-422. doi: 10.1016/j.earscirev.2011.05.001

Stokes, C.R., Spagnolo, M., Clark, C.D., Ó Cofaigh, C., Lian, O.B., Dunstone, R.B., 2013. Formation of mega-scale glacial lineations on the Dubawnt Lake Ice Stream bed: 1. size, shape and spacing from a large remote sensing dataset. Quaternary Science Reviews 77, 190-209. doi: 10.1016/j.quascirev.2013.06.003

Storey, M., Duncan, R.A., Pedersen, A.K., Larsen, L.M., Larsen, H.C., 1998. 40Ar/39Ar geochronology of the West Greenland Tertiary volcanic province. EPSL 160, 569-586. doi: 10.1016/S0012-821X(98)00112-5

Streuff, K., Ó Cofaigh, C., Hogan, K., Jennings, A., Lloyd, J.M., Noormets, R., Nielsen, T., Kuijpers, A., Dowdeswell, J.A., Weinrebe, W., 2017. Seafloor geomorphology and glacimarine sedimentation associated with fast-flowing ice sheet outlet glaciers in Disko Bay, West Greenland. Quaternary Science Reviews 169, 206-230. doi: 10.1016/j.quascirev.2017.05.021

Studinger, M., Bell, R.E., Blankenship, D.D., Finn, C.A., Arko, R.A., Morse, D.L., Joughin, I., 2001. Subglacial sediments: A regional geological template for ice flow in West Antarctica. Geophysical Research Letters 28, 3493-3496. doi: 10.1029/2000GL011788

Stuiver, M., Reimer, P.J., 1993. Extended 14C data-base and revised calib. 3.0 14C age calibration program. Radiocarbon 35, 215-230.

Suckro, S.K., Gohl, K., Funck, T., Heyde, I., Ehrhardt, A., Schreckenberger, B., Gerlings, J., Damm, V., Jokat, W., 2012. The crustal structure of southern Baffin Bay: implications from a seismic refraction experiment. Geophysical Journal International 190, 37-58. doi: 10.1111/j.1365-246X.2012.05477.x

Tang, C.C.L., Ross, C.K., Yao, T., Petrie, B., DeTracey, B.M., Dunlap, E., 2004. The circulation, water masses and sea-ice of Baffin Bay. Progress in Oceanography 63, 183-228. doi: 10.1016/j.pocean.2004.09.005

Tedesco, M., Fettweis, X., Mote, T., Wahr, J., Alexander, P., Box, J.E., Wouters, B., 2013. Evidence and analysis of 2012 Greenland records from spaceborne observations, a regional climate model and reanalysis data. The Cryosphere 7, 615-630. doi: 10.5194/tc-7-615-2013

Thomas, R., Frederick, E., Krabill, W., Manizade, S., Martin, C., 2009. Recent changes on Greenland outlet glaciers. Journal of Glaciology 55, 147-162. doi: 10.3189/002214309788608958

van Kreveld, S.A., Sarnthein, M., Erlenkeuser, H., Grootes, P.M., Jung, S.J.A., Nadeau, M.J., Pflaumann, U., Voelkel, A., 2000. Potential links between surging ice sheets; circulation changes and the Dansgaard-Oeschger cycles in the Irminger Sea 60-18 kyr. Paleoceanography 15, 425-442. doi: 10.1029/1999PA000464

Vasskog, K., Langebroek, P.M., Andrews, J.T., Nilsen, J.E.Ø., Nesje, A., 2015. The Greenland Ice Sheet during the last glacial cycle: Current ice loss and contribution to sea-level rise from a palaeoclimatic perspective. Earth-Science Reviews 150, 46-67.

Weatherall, P., Marks, K.M., Jakobsson, M., Schmitt, T., Tani, S., Arndt, J.E., Rovere, M., Chayes, D., Ferrini, V., Wigley, R., 2015. A new digital bathymetric model of the world's oceans. Earth and Space Science 2, 331-345. doi: 10.1002/2015EA000107

Weertman, J., 1972. General theory of water flow at the base of a glacier or ice sheet. Reviews of Geophysics 10, 287-333. doi: 10.1029/RG010i001p00287

Weidick, A., Bennike, O., 2007. Quaternary glaciation history and glaciology of Jakobshavn Isbrae and the Disko Bugt region, West Greenland: a review. Geological Survey of Denmark and Greenland Bulletin 14.

Weidick, A., Kelly, M., Bennike, O., 2004. Late Quaternary development of the southern sector of the Greenland Ice Sheet, with particular reference to the Qassimiut lobe. Boreas 33, 284-299. doi: 10.1080/03009480410001947

Wellner, J.S., Lowe, A.L., Shipp, S.S., Anderson, J.B., 2001. Distribution of glacial geomorphic features on the Antarctic continental shelf and correlation with substrate: implications for ice behaviour. Journal of Glaciology 47, No. 158, 397-411.

Whittaker, R.C., Hamann, N.E., Pulvertaft, T.C.R., 1997. A New Frontier Province Offshore Northwest Greenland: Structure, Basin Development, and Petroleum Potential of the Melville Bay Area. AAPG Bulletin 81, No. 6, 978-996.

Xu, Y., Rignot, E., Fenty, I., Menemenlis, D., Flexas, M.M., 2013. Subaqueous melting of Store Glacier, west Greenland from three-dimensional, high-resolution numerical modeling and ocean observations. Geophysical Research Letters 40, 4648-4653. doi: 10.1002/grl.50825

Zwally, H.J., Giovinetto, M.B., 2011. Overview and Assessment of Antarctic Ice-Sheet Mass Balance Estimates: 1992–2009. Surveys in Geophysics 32, 351-376. doi: 10.1007/s10712-011-9123-5

Zwally, H.J., Giovinetto, M.B., Beckley, M.A., Saba, J.L., 2012. Antarctic and Greenland Drainage Systems.

Danksagung

Vielen lieben Dank allen, die mich auf diesem Weg begleitet haben!

- Wilfried Jokat möchte ich für die Ermöglichung meiner Promotion, der Begutachtung der Dissertation und der guten Betreuung danken. Danke für deine Unterstützung und dafür, dass ich auch einfach erstmal machen durfte!
- Gerhard Bohrmann danke ich für die Begutachtung dieser Doktorarbeit und die netten Gespräche auf dem Weg dorthin.
- Boris, Jan und Katharina danke ich für jegliche Korrekturen rund um diese Arbeit.
- Ein riesengroßer Dank geht vor allem an Boris Dorschel, für die vielen arbeitsintensiven Stunden und die gute Betreuung! Dafür, dass du mich auch ab und an ins kalte Wasser geschmissen und trotzdem immer unterstützt hast. Danke auch insbesondere für die großartige, wenn auch anstrengende, Merian-Fahrt in die Baffin Bay mit Fahrtleiter-Feeling.
- Meinem Büro-Mitbewohner Jan-Erik Arndt danke ich dafür, dass er mir immer wieder mit Rat und Tat zur Seite stand - und ganz besonders für die gute Stimmung in unserer kleinen Bathy-Villa.
- Meinen wunderbaren Kollegen und Freunden vom mittäglichen Hexenzirkel danke ich für die stets unterhaltsame Mittagspause und den Hoppelmädels danke ich obendrein für die vielen schönen Jahre mit Pferde-lastigem Abendprogramm!
- Den Bewohnern des Bathy-Häußchens danke ich für viele nette Unterhaltungen. Danke auch an Hans-Werner Schenke und Boris Dorschel für die Ermöglichung meiner zahlreichen Forschungsexpeditionen und der vorangegangenen Bachelor- und Master-Abschlussarbeiten.
- Ich danke ganz besonders meiner Familie und meinen Freunden, die mich immer in Gedanken auf meinem Weg, insbesondere auf den vielen Expeditionen zu Wasser und an Land, begleitet haben. Danke, dass es euch gibt!
- Dankschön Nils! Für deine Unterstützung, ständiges Pendeln und deine Geduld. Schön, dass du für mich da bist!

Curriculum Vitae

Patricia Slabon

Date of birth: 10.04.1989
Place of birth: Hamburg, Germany
Nationality: German

Affiliation

Alfred Wegener Institute Helmholtz Centre for Polar and Marine Research
Van-Ronzelen-Str. 2, 27568 Bremerhaven, Germany
phone: +49 471 4831 1226
email: patricia.slabon@awi.de

Education and Employments

Since 1.12.2014	Research associate in the bathymetry-group at the Department of Geophysics, Alfred Wegener Institute Helmholtz Centre for Polar and Marine Research (AWI), Bremerhaven; and Ph.D. candidate at University of Bremen
1.10.2011 – July 2014	Master of Science Geomatics, specialization Hydrography, HafenCity University Hamburg, Germany
1.10.2008 – 30.9.2011	Bachelor of Science Geomatics, HafenCity University Hamburg, Germany
July 2008	Abitur, Hamburg, Germany

Scientific Publications as first author

Slabon, P., Dorschel, B., Jokat, W., Myklebust, R., Hebbeln, D. and Gebhardt, C. (2016) *Greenland ice sheet retreat history in the northeast Baffin Bay based on high-resolution bathymetry*, Quaternary Science Reviews, 154 , pp. 182-198 . doi:10.1016/j.quascirev.2016.10.022

Slabon, P., Dorschel, B., Jokat, W., Freire F. (accepted, 2017) *Bedrock morphology reveals drainage network in northeast Baffin Bay,* Geomorphology

Slabon, P., Dorschel, B., Jokat, W., Freire F. (in review, 2017) Influence of bedrock morphology on ice and meltwater orientation in northern Baffin Bay, Geomorphology

Scientific Publications as co-author

Morlighem, M., Williams, C. N., Rignot, E., An, L., Arndt, J. E., Bamber, J. L., Catania, G., Chauché, N., Dowdeswell, J. A., Dorschel, B., Fenty, I., Hogan, K., Howat, I., Hubbard, A., Jakobsson, M., Jordan, T. M., Kjeldsen, K. K., Millan, R., Mayer, L., Mouginot, J., Noël, B. P. Y., Ó Cofaigh, C., Palmer, S., Rysgaard, S., Seroussi, H., Siegert, M. J., **Slabon, P.**, Straneo, F., van den Broeke, M. R., Weinrebe, W., Wood, M., Zinglersen, K. B. (2017) *BedMachine v3: Complete bed topography and ocean bathymetry mapping of Greenland from multi-beam echo sounding combined with mass conservation*, Geophysical Research Letters, doi:10.1002/2017GL074954

Conference Contributions

Slabon, P., Dorschel, B., Jokat, W., Myklebust, R., Hebbeln, D. and Gebhardt, C. (2017) Glacial landforms identified in high-resolution bathymetry indicate past Greenland ice sheet dynamics in Melville Bay, northeast Baffin Bay, Talk, EGU General Assembly, Vienna, April 2017

Dorschel, B., Arndt, J. E., **Slabon, P.** and Jensen, L. (2016) *Ocean mapping activities at the Alfred Wegener Institute* , Poster, Forum for Future Ocean Floor Mapping, Monaco, June 2016

Slabon, P., Dorschel, B. and Gebhardt, C. (2015) *Greenland Ice Sheet Development in the Northeast Baffin Bay Derived From Geo-Morphology Analysis*, Poster, Joint Assembly, Montréal, Canada, May 2015.

Scheduled for December 2017:
Slabon, P., Dorschel, B., Jokat, W., Freire F. *Bedrock morphology reveals drainage network in the northeast Baffin Bay,* Poster, AGU Fall Meeting, New Orleans, December 2017

Research Expeditions

with operation of the multibeam and sub-bottom echosounder installed on board

30.06. - 30.07.2015	MSM44 with Maria S. Merian, Baffin Bay
20.02. - 29.03.2014	SO-231 with RV SONNE, Mozambique Channel
16.04. - 29.05.2013	ANT-XXIX/5 with RV POLARSTERN, Falkland Plateau Revision of the “Hypack - Survival Guide”
03.08. - 07.10.2011	ARK-XXVI/3 with RV POLARSTERN, Central Artic Ocean Revision of the “Hypack - Survival Guide”
10.05. - 20.05.2011	ANT-XXVII/4 with RV POLARSTERN, transit Gran Canaria – Bremerhaven And HYPACK training provided by Joe Burnett from Hypack Inc. Revision of the “Hypack - Survival Guide””
31.07. - 10.10.2010	ARK-XXV/3 with RV POLARSTERN, Baffin Bay
Scheduled for 2018:	
19.01. - 14.03 2018	PS111 with RV Polarstern to the Antarctic

Patricia Slabon